R&D 6154 MS 02
84 M 0358

CONFERENCE PROGRAMME

AD-A212 293

DAJA 45-88-M-0358

FOURTH OXFORD INTERNATIONAL CONFERENCE ON

THE MECHANICAL PROPERTIES
OF MATERIALS AT HIGH
RATES OF STRAIN

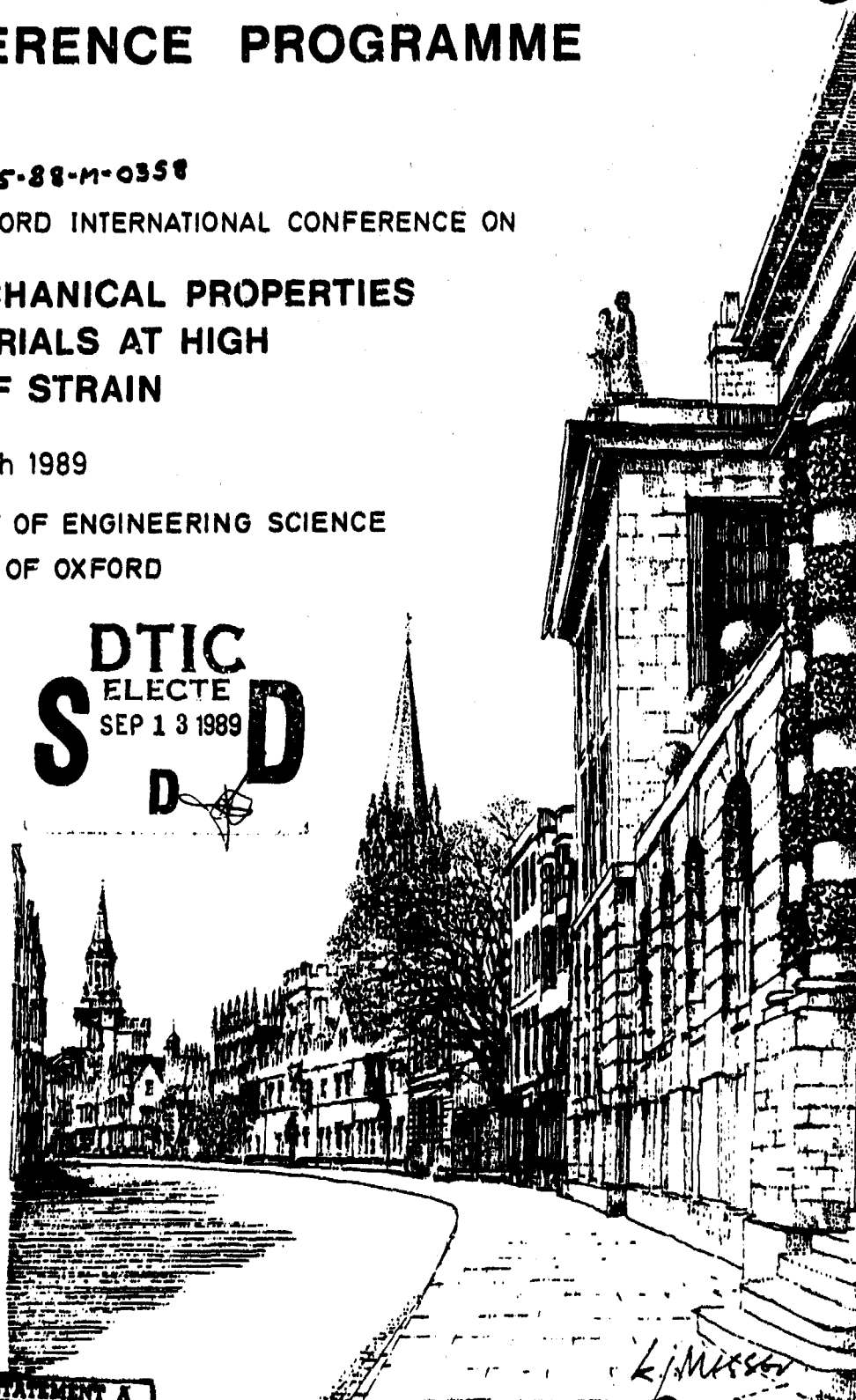19-22 March 1989

DEPARTMENT OF ENGINEERING SCIENCE
UNIVERSITY OF OXFORD

DTIC
ELECTE
SEP 1 3 1989
S D

89 9 13 099

REPRODUCTION QUALITY NOTICE

This document is the best quality available. The copy furnished to DTIC contained pages that may have the following quality problems:

- Pages smaller or larger than normal.

- Pages with background color or light colored printing.

- Pages with small type or poor printing; and or

- Pages with continuous tone material or color photographs.

Due to various output media available these conditions may or may not cause poor legibility in the microfiche or hardcopy output you receive.

☐ If this block is checked, the copy furnished to DTIC contained pages with color printing, that when reproduced in Black and White, may change detail of the original copy.

FOURTH OXFORD INTERNATIONAL CONFERENCE

ON

The Mechanical Properties of Materials

at High Rates of Strain

SPONSORED BY

United States Army

European Research Office

HOSTED BY

Department of Engineering Science

University of Oxford

with the support of

The Institute of Physics, Materials and Testing Group

and

The Institution of Mechanical Engineers, Engineering Sciences Division

CONFERENCE ADMINISTRATION BY

Continuing Professional Development Unit

Department of External Studies, University of Oxford

/

-2-

C O N T E N T S

Contributed Papers

2

Pages 4 + 5
Omitted

A MAP FOR IMPACT INDUCED DUCTILE FAILURE

Ian M. Fyfe

University of Washington, Seattle, WA 98195 U.S.A.

Because ductile failure is the nucleation, growth and coalesence of voids or microcracks, the paper focuses on developing a failure map in which experimental data and theories related to plastic instabilites and failure can be presented in terms of void nucleation concepts.

For failure maps in general the choice of variables is not obvious, but depends to a large extent on why the map is being used in the first place. Some useful guidelines have been presented by Ashby (1977), for use in earlier failure map construction, where the emphasis was on creating fracture maps showing the boundaries between different mechanisms of fracture. In the area of high strain rate behavior Lindholm (1974), in a review of dynamic testing methods, was more concerned with constitutive modeling, and so used effective stress and effective strain, with each curve, designated by a constant temperature strain rate parameter. However, void growth and spallation strongly suggest that failure maps for impact loading should also include the mean stress variations. The variables used in this paper are those which describe nucleation, but also cover the high strain rate conditions associated with shear bands and spallation. A case is made for using a normalized mean stress, effective plastic strain and temperature.

With this choice of variables it is possible to include results from three experimental configurations. Considered are the high mean stress case associated with the plate impact test, the intermediate condition of simple tension, and the zero mean case which results from the torsion configuration.

As one of the main objectives of impact testing is to determine the strain rate sensitivity of the process, and the influence of the different micromechanic mechanisms, both dynamic and quasi-static data is used. Use is also made of models developed from both a microscopic and a macroscopic viewpoint. Although, this paper deals mainly with the macro-level of damage initiation as characterized by localization and the loss of structural integrity.

With nucleation occurring at second phase particles or other inclusions, the process then depends on particle size. For this reason it has been determined that nucleation can occur almost immediately after yield, and can continue throughout the deformation process. However, at some stage of this deformation it has been observed that a proliferation point is reached where the nucleation increases dramatically, and it might be expected that this proliferation occurs when the macroscopic condition of localization and necking occurs. This possibility is discussed in relation to the two materials used in this study.

It will be shown that the Hill (1952) theory for localized necking in a thin sheet is quite compatible with plastic instabilities under high strain rate loading conditions, and that the formation of instabilities is essentially independent of the mean stress. In contrast ductile failure was found to be highly dependent on the mean stress, and the dislocation based nucleation model of Goods and Brown (1979) was also found to be

[6]

applicable under both quasi-static and the high strain rate loading conditions. These results suggest that plastic instabilities may not be triggered by void nucleation, even though ductile failure is in many instances dependent on this mechanism, at least in the final phase of the failure process. These results as they apply to VAR 4340 steel are presented in Figure 1.
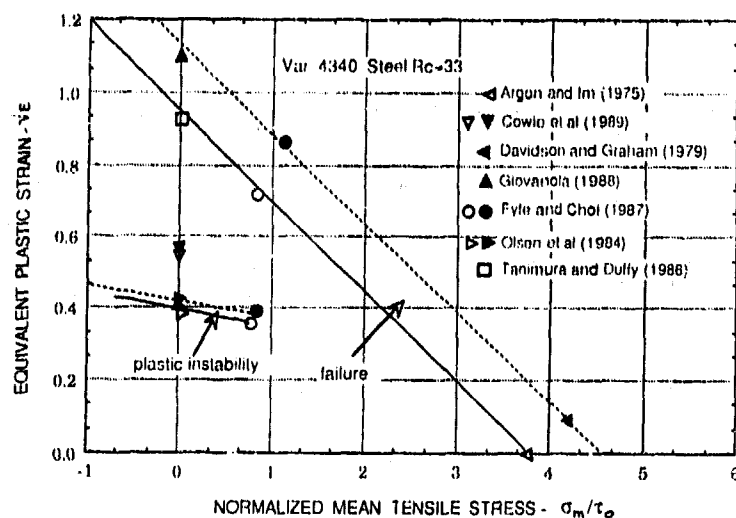
Figure 1 Effective plastic strain as a function of normalized tensile stress dynamic (- -●- - -) and static (—○—) loading conditions

REFERENCES

Ashby M F 1977 *Advances in Research on the Strength and Fracture of Materials* ed D M R Taplin (New York: Pergamon) pp 1-14
Goods S H and Brown L M 1979 Acta Met. **27** 1
Hill R 1952 J. Mech. Phys. Solids **1** 19
Lindholm U S 1974 *Mechanical Properties at High Rates of Strain* (Inst. Phys. Conf. Ser. 21) pp 3-21

Evolution of Thermo-Visco-Plastic Shearing

Y L Bai

Institute Of Mechanics, Chinese Academy of Sciences,
Beijing, China 100080

ABSTRACT

This paper reviews the recent advances in the study of evolution of shear
deformation into localized band-like structure in thermo-visco-plastic
materials. Particularly, the progress made in the impact laboratory of
the Institute of Mechanics is summarized. All the experimental observa-
tions and analytical and numerical results show that the evolution of
shear from homogeneous field into so-called adiabatic shear band is a
multi-stage process. The band-like structure is asymptotically stable.
So, to some extend, no matter how the disturbances or microscopical
structures are, the eventual features of the shear bands look roughly
alike in nature, although complicated details do exist in early and
intermediate stages.

In dealing with the concerned problem, a well-posed model and appropri-
ately simplified governing equations are the necessity. A one-dimen-
sional model of simple shear was reviewed. Furthermore, scaling is of
most significance in the analysis, since various time and length scales
are involved in various stages in the evolution. It was pointed out
that the effective Prandtl number appears to be the key dimensionless
parameter in approximations, which describe various stages of the shear
evolution. In particular, the implications of quasi-static and adiabatic
approximations are discussed.

Instability criteria resulting from linear perturbation analysis provide
helpful information about the ending of uniform shearing and growth rate
of disturbances at early stage. However, instability is not the synonym
of localization. Therefore, the concept and implication of localization
are reviewed.

Experiments show that a number of very fine shear bands appear, when
instability has just occured, although macroscopic uniform shearing seems
to remain. Following this, a localized shear zone emerges and develops
in the centre of testpiece. Afterwards, it drastically predominates the
whole field of the shear deformation. Finally, a fairly steady shear
band forms. Numerical simulations were carried out with different kinds
of disturbances in thermo-visco-plastic material and revealed all these
details of the process very clearly. In order to understand the under-
lying mechanism, which governs the transition to predominating shear band,
analytical interpretation was provided. It seems that the band-like

structure results from the balance of the input plastic work rate and
the heat diffusion. This mechanism can support a quasi-steady shear band
in the thermo-visco-plastic material as well. A close form quasi-steady
solution and an estimation of the shear band width are given. A variety
of observations appears to be in fairly good agreement with the suggested
prediction.

It is well known that the so-called adiabatic shear bands usually serve
as precusor to fracture. But how the eventual shear fracture forms and
why the eventual fracture surface is almost always parallel to shear
force remain unclear. It is reported that the cumulation of microdamage,
which accompanies evolution of shear deformation, plays crucially
important role in the formation of the shear fracture. Optical and TEM
observations reveal some microscopic details of the two processes -
shear localization and shear fracture. Perhaps, crystallographic slip on
dominate slip system within grains should be responsible for the formation
of microscopic shear bands. Whereas, large strains in localized shear
zone and the stress concentrations resulting from dislocation pile ups
at grain boundaries and phase boundaries initiate microcracks.

It is suggested that the theory concerning shear band induced fracture
is badly wanted, especially in engineering practice. So far, to the
author's knowledge, there is nearly no such a kind of theories available.
Consideration of the cumulation of microdamage and its variation with
the shear band evolution may be of crucial importance. The patterns of
shear bands under combined stresses also interest engineers in industries.
It is hoped that more practical models and theories can be developed
for this case. Finally, the role of material transformations, such as
phase transformation, vanishing strain hardening, etc., in the fully
developed shear band, needs to be clarified.

[9]

EXPERIMENTAL METHODS OF MATERIAL CHARACTERIZATION

J.L. LATAILLADE

Laboratoire de Mécanique Physique, Unité de Recherche Associée au CNRS n° 867
351 Cours de la Libération, 33405 TALENCE Cedex - France

Summary

The operating conditions - more and more severe - of the mechanical structures, as well as the security rules being increasingly constraining - especially in nuclear industries explain the subtantial development of the experimental research is the field of high strain rate testing. During the fifteen past years the experimental methods and the related testing techniques for materials becoming more and more tough and strong have received a particular attention of the researchers. The general purpose remains, of course, the materials characterization by means of reduced scales configurations; but a new approach - due to the introduction of microcomputer and hence of the appearence of hybrid methods - are noticeable.

The experimental techniques based on the well known principle of the Hopkinson-Kolsky bare are the most popular. Some modifications and improvements are reported in this conference. They allow a better control of the loading paths and consequently a more appropriate modelization of the viscoplastic behaviour of materials such as metallic alloys or a finer approach of the damage processes of advanced materials. In order to extend the range of the strain rates people use methods based on the stress waves propagation. The techniques allow them to generate biaxial stresses, and the lagrangian analysis helped by high performance guages lead to a modern tool for the constitutive relationship at very high strain rates.

On an other hand, the increasing variety of structural advanced materials (composites, thermomechanical, ceramics, engineering polymers), or the new requirements from the civil engineering (concrete, rocks) have suggested new methods, made easier, owing to new instruments for the measurements, or the observation of phenomena.

From this point of view the optical methods (laser, high speed cinematography) become more and more employed, since they afford mechanical parameters of a great importance like strains, COD, stress intensity factors, etc ...

Because high strain rate testing generally involves adiabatic processes it can be interesting or necessary to measure the temperature history of sample, in order to set up a thermomechanical approach, and to appreciate its influence on the microstructural modifications : the best example is that one of the shear banding. Due to the very short rise times the only experimental methods is the infrared thermography.

The advancements of the physics, microelectronics opto electronics have led to new transducers very sensitive exhibiting very small response times : some of their applications are mentioned in this conference.

[10] / 11

THE DEVELOPMENT OF CONSTITUTIVE RELATIONSHIPS FOR MATERIAL BEHAVIOUR AT HIGH RATES OF STRAIN

J. Harding
Department of Engineering Science
University of Oxford
Oxford, U.K.

ABSTRACT

The increasing use of computer codes for modelling the mechanical response of engineering structures under impact loading has highlighted the need for appropriate forms of constitutive relation, or mechanical equation of state, capable of describing material behaviour over a wide range of strain rate and temperature. Attempts to derive such relationships have varied from, at one extreme, the purely empirical, effectively a curve fitting exercise to available experimental data for the given material to, at the other, the development of purely theoretical expressions based on the micromechanical processes governing plastic flow at the atomic level under the given loading conditions.

Ideally these two contrasting approaches should come together in a single constitutive relationship which both describes, with good accuracy, the actual macroscopic behaviour of the given material and can also be related to, and hence derived from, the physical processes which control plastic deformation. However, while this ultimate goal is still some way from being achieved it remains necessary to consider both approaches when seeking to obtain the most suitable form for the constitutive relation. As a result several semi-empirical expressions have been proposed, the functional form of which is based on theoretical considerations but involving empirical constants which cannot be related directly to precise physical processes and which have to be determined for the particular material being studied.

The present review is mainly concerned with this semi-empirical approach. Attempts to model material behaviour in terms of the micromechanisms of plastic flow will be the concern of a subsequent review by Klepaczko while a discussion of the use of computer codes in modelling the actual impact response of engineering structures will be the subject of the review by Corran in the parallel session.

Experimental results for the temperature and strain-rate dependence of the flow stress at different rates of strain are briefly reviewed for a variety of materials. Functional relationships between the stress, the temperature and the strain rate are presented and their theoretical basis is discussed. The problems involved in developing a full equation of state, which includes some measure of the extent of deformation, are considered in the light of the frequently observed dependence of the flow stress on the previous strain rate history and the need for some internal structure sensitive parameter is made clear. Two attempts at defining the structural state of the material in terms of such a parameter, either the rate-sensitivity of work-hardening (Klepaczko and Chiem, 1986) or the mechanical threshold stress (Follansbee et al. 1985) are described and compared. In neither case, however, has an explicit functional relationship yet been developed of a form suitable for use

in computer codes for the numerical modelling of the impact response of a structural component.

In practice, the specific constitutive relationships which, although less satisfactory on theoretical grounds, have been used in computer codes are, in general, of two types - either the empirical, for example Johnson and Cook (1983), or the semi-empirical, for example Zerilli and Armstrong (1987). The results obtained when these two materials models are used in the computer program EPIC2 to describe the structural response in the cylinder impact test are compared and the differences are seen to be small.   It is concluded that in this application the numerical solution is relatively insensitive to the details of the material model.   While refinements to the Zerilli-Armstrong model lead to a second order improvement in the agreement between the experimental results and the numerical analysis the corresponding form of the constitutive relation is of considerably greater complexity.

In general, therefore, the use of relatively simple semi-empirical constitutive relationships would seem to be adequate for the computer modelling of many impact problems.   However, in situations where the overall impact response of the given component may be critically determined by the deformation processes and complex internal microstructural states arising in very localised regions then the details of the material model may become much more important.   Thus in studying the critical conditions for the initiation of adiabatic shear in aluminium and steel Klepaczko (1988) found it necessary to use a "fully temperature coupled" form of constitutive relation which, in the case of steel, involved a total of fifteen different material constants.   In such circumstances it might prove more profitable, it is suggested, to pursue further the development of material models based on the concept of an internal structure sensitive parameter for which there is strong theoretical support.   A further problem arises, however, if the critical condition arises from a change in the controlling mode of deformation from, say, constant volume plasticity to the growth and coalescence of voids or the propagation of cracks, requiring in addition to the appropriate constitutive relation also the inclusion in the computer code of some form of failure criterion.   This, however, is outside the scope of the present review.

REFERENCES

Follansbee P S, Kocks U F and Regazzoni G 1985 Proc. DYMAT 85 J. de Physique C5 No.8 46 25-34
Johnson G R and Cook W H 1983 in Proc 7th. Int. Symposium on Ballistics, The Hague, The Netherlands, 541
Klepaczko J R and Chiem C Y 1986 J. Mech. Phys. Solids 34 29-54
Klepaczko J R, Lipinski P and Molinari A 1988 Proc IMPACT 87 (DGM Informationsgesellschafft mbh, Oberursel) 2 695-704
Zerilli F J and Armstrong R W 1987 J Appl. Phys. 61 No.5 1816-1825

Numerical Modelling of Dynamic Plasticity

R.S.J. Corran

Rolls-Royce plc
Derby, U.K.

This review addresses the modelling of dynamic plastic deformation in solids. It commences with a survey of the techniques employed in codes that are available either commercially or in the public domain. Lagrangian, Eulerian and Arbitrary Lagrangian Eulerian formulations are described to allow a discussion of the different methods of problem definition and how this influences the limitations to the modelling. It is found that the Lagrangian formulation is most useful in problems involving impact, since it maintains a clear distinction of boundaries, but has the disadvantage that the discretization, i.e. the finite element mesh or finite difference grid, may become very distorted leading to numerical difficulties. The Eulerian formulation avoids this problem but does not provide a clear model of boundaries between bodies or materials. The arbitrary Lagrangian Eulerian formulation is a method that has not been much used for solid mechanics problems, although it combines some of the advantages of the two methods.

Time-stepping through a solution can be achieved by either explicit or implicit methods. Explicit methods have the advantage that they involve no, or possibly limited, iteration and hence proceed through each time-step at minimal computational cost. However the length of each time-step must be kept very small to avoid instability in the procedure and maintain an accurate modelling. Implicit methods may take considerably larger time-steps, up to a thousand times longer, but involve iterations to achieve equilibrium and compatibility at each time-step. Although explicit methods are generally used for impact modelling in three dimensions because of their relative efficiency, implicit methods may be more appropriate for simpler problems.

Difficulties with the modelling of continua discussed are the control of hourglassing, the level of discretization and the importance of the constitutive model. Hourglassing is a deformation mode that involves zero strain energy for the finite difference or finite element in use, but it can grow in an unstable manner to dominate the observed behaviour. An example is discussed and methods of controlling the hourglassing are reviewed. It is found that the hourglassing can occur not only

[14]

on an element or zonal level, but in certain problems at a structural level. Unfortunately the hourglass modes of deformation may be modes that occur due to the dynamic problem being modelled. Hence it is necessary to control them without eliminating them completely.

An example of the effects of inadequate discretization is given showing how the provision of too few zones in a finite difference modelling leads to unrealistic impact behaviour in predicting the contact time between the missile and the target. Further the coarse discretization leads to more hourglassing and causes an unstable development of deformation away from the impact. This implies that although there may be little interest in studying the missile behaviour, as much care must be taken in its modelling as in the target.

A limitation of simple constitutive relations which do not include rate sensitivity is that any localization of the deformation is related to the discretization. Hence the width of any shear bands that may be identified during the modelling will be of one element's width in a simple finite element description. However if the rate sensitivity is included the governing equations show that the shear band will have a dimension related to the constitutive model. Although most codes do not have any method for modelling such a concentration of the deformation, a discussion of the various approaches to shearing is given, based on solutions to a more idealllsed one-dimensional problem. It is found that for a rate-sensitive constitutive model there is indeed a natural sizing of the shear band, a result that is apparent from both finite element studies and an analytical solution.

Although this review concentrates on limitations to the use of numerical modelling, it is concluded that with care successful modelling of dynamic plastic behaviour is possible. The major limitation at the present is in the modelling of failure, especially ductile failure. As studies of shear bands have shown, however, this is particularly difficult to model although it is, paradoxically, theoretically easier if a more complicated constitutive model is used. Nevertheless it is possible to use some form of damage mechanics to give useful estimates of ductile fracture without modelling localization. Finally an example of an impact problem of industrial relevance is shown in which rate sensitivity was found to be important although strain hardening was not modelled. In this case the object is to predict the final deformed shape after impact for which dynamic relaxation was used to damp out the residual velocities after all plastic deformation had ceased.

Discussion of Microstructural Effects and its Modeling
at High Rates of Strain

L.P.M.M. - U.A. CNRS N° 1215
Université de METZ, Ile du Saulcy, 57045 - METZ CEDEX 01, France.

J.R. Klepaczko

EXTENDED ABSTRACT

During last decades a vast experimental evidence has been accumulated
that metals deformed plastically at different conditions (strain rate,
temperature, pressure) undergo a complicated microstructural evolution.
Recently, microstructural aspects have been more frequently introduced
into constitutive modeling, however, the emerging picture is still not
complete. Such approach, based on materials science, is very promising in
formulation a framework for rational constitutive modeling with a possi-
bility of reliable extrapolations beyond experimental conditions for
which the constitutive parameters have been determined.

This discussion presents a consistent approach to microstructure evolution
via the constitutive formalism which have been constantly improved over
last few years, Klepaczko (1988a). The formalism presents a consistent
approach to the kinetics of plastic flow of metals and alloys with FCC,
BCC and HCP lattices. The rate-sensitive strain hardening, instantaneous
rate sensitivity and temperature are taken into consideration in terms of
evolution of microstructural state variables. The notion is assumed that
the current mechanical properties of a metal depend entirely on its
current microstructure, and any changes in microstructure result in
changes of mechanical properties. Consequently, the formalism has been
applied in which thermal activation analysis is employed for both the
kinetics of glide and kinetics of microstructural evolution, Klepaczko
(1974). Although the formalism is to some extend similar in its construc-
tion to that based on the mechanical threshold stress as a state varia-
ble, Follansbee and Kocks (1988), it is more general.

The formalism employed in this study as the background for discussion of
microstructural evolution is based on the stress partitioning at constant
structure. Thus, the flow stress in shear τ at constant structure is
given to a good approximation by

$$\tau(\overset{\circ}{\Gamma},T)_{STR} = \tau_\mu(\overset{\circ}{\Gamma},T)_{STR} + \tau^\star(\overset{\circ}{\Gamma},T)_{STR} \tag{1}$$

where τ_μ and $\tau^\star$ are respectively the internal and effective stress compo-
nents, $\overset{\circ}{\Gamma}$ and T are plastic shear strain rate and absolute temperature.
The kinetics of defect (dislocation) movements interrelates at constant
structure, characterized by j state variables s_j, the instantaneous va-
lue of effective stress $\tau^\star$. Whereas, the internal stress τ_μ must be also
rate and temperature dependent via dynamic recovery processes (relaxation
of long range internal stresses) occuring due to annihilation and rearran-

[16]

gement of strong obstacles to dislocation motion. Since the microstructure undergoes an evolution, and the state of microstructure is defined by s_j state variables, the state variable evolution is assumed in the form of a set of j differential equations of the first order, Klepaczko (1987, 1988b)

$$\frac{ds_j}{dr} = f_j [s_k , \dot{r}(r) , T(r)] , k = 1 \ldots j \tag{2}$$

Assuming that microstructure is characterized by five instantaneous quantities : ρ_i, ρ_m, $d(\rho)$, D and Δ, where ρ_i and ρ_m are the mean immobile and mobile dislocation densities, $d(\rho)$ is the subgrain diameter which evolues with ρ_i, D is the grain diameter and Δ is the mean distance between twins or microtwins, the internal and effective components of stress are directly related to those quantities. Evolutions of each of five introduced state variables are discussed in view of the papers submitted to this session.

In addition, an evolution of microstructure specific for shock wave loading and microinstabilities in the form of the adiabatic micro-shear bands are also taken into consideration. Finally, a general discussion and more specific conclusions are offered.

REFERENCES

Follansbee P S and Kocks U F 1988 Acta metall. 36 81
Klepaczko J R 1975 Mater. Sci. Engng. 18 121
Klepaczko J R 1987 Proc. Conf. IMPACT 87 (Bremen : DGM) 823
Klepaczko J R 1988a Proc. Int. Conf. DYMAT 88 (Les Ulis : les éditions de physique) C5-553
Klepaczko J R 1988b Proc. 8-th Risö Int. Symp. (Roskilde : Risö) 387

Overview of impact properties of monolithic ceramics

C RUIZ

Oxford University
Department of Engineering Science
Parks Road
Oxford OX1 3PJ

The generic term 'ceramics' embraces a large variety of materials that range from naturally occurring rocks to to-day's man-made ceramics, cermets, etc. This review is only concerned with ceramics of high tensile strength, low porosity and relatively free from defects, often called 'fine ceramics'.

The characterisation of the mechanical properties of ceramics, even under static loading, presents difficulties associated with their variability. Fracture toughness is often measured by means of indentation tests. These have come under considerable criticism. An alternative is offered by conventional tests using single edge notched beams (SEN), double cantilever beams (DCB) or double torsion specimens. In all these cases the way in which the initiation notch or crack is introduced has been shown to be important. Ceramics are prone to suffer a severe strength degradation as a result of the machining process and when the notch is produced by plunge grinding it might be asked whether the subsequent specimen behaviour is truly indicative of that of the undamaged bulk material. Low speed impact tests of the Izod and Charpy types have been interpreted in terms of K_{IC} assuming that static equilibrium is reached and considering inertial loading by applying the Duhamel integral method to the raw force- time data provided by the impact tester. This approach, while preferable to a simple static analysis, neglects the stress wave action which is important in determining the initial response of the specimen.

As the strain rate increases, the deterministic relationship that exists between stress level and crack size under static loading breaks down. Fracture then depends on the stress wave velocity and the stress pulse duration or stress rate. The mechanism consists in the formation of clusters of microcracks and their subsequent growth. Microcracking has also been shown to explain the behaviour of multi-phase ceramics under shock loading, where cracks are formed at the boundaries between phases with different mechanical impedance. Cracks may be formed normal to the direction of propagation of the shock or along that direction. A damage mechanics approach, adapted to the mathematical modelling of failure in conjunction with numerical analysis, is potentially valuable but is still incomplete.

Ceramics are used for armour plating, backed by a resilient support. Accurate predictive numerical analysis are not yet possible in the absence of well established failure criteria and well documented mechanical properties. A purely empirical approach is normally followed to obtain the ballistic efficiency of the ceramic. This depends on the HEL, the compressive strength, the density and the wave velocity but the overall

efficiency of the shield will also be a function of the mechanical impedances of the front layer and the backing, of the properties of the adhesive and of the impact itself. The mode of failure changes when the ceramic is unsupported.

Erosion and small particle impact are briefly mentioned. This review considers only the response of a ceramic to a single loading at room temperature. The variation of mechanical properties with temperature is a question of obvious interest about which very little has yet been done as is the effect of repeated impact on the residual strength. Secondary causes, such as machining damage are known to have an important effect on the scatter of properties as well as on the strength, so much so that they can even mask the effect of the primary loading. The resistance to impact is also impaired by the presence of an applied static load inducing tensile stresses. The conclusion is therefore that much still remains to be done to understand fully the behaviour of high strength ceramics and build up a bank of design data that will permit to exploit their potential with confidence.

Overview of impact of composites

Graham Dorey

Royal Aerospace Establishment, FARNBOROUGH, Hants GU14 6TD, UK

Composite materials usually comprise a matrix material such as polymer, metal or ceramic, and reinforcing particles or fibres such as carbon, glass, polymer or ceramic. By combining the properties of the constituents, with the correct interface conditions, compositie materials offer the designer many potential advantages over homogeneous materials, such as high strength and stiffness, low density, elastic anisotropy giving tailored deformations, preferred fracture mechanisms giving increased toughness and improved high temperature stability.

Many of the applications, where the designer would like to make use of these properties, involve some form of impact or shock loading, for example in aerospace and transport structures, in armour applications, in reciprocating machinery and in sports goods. It is important to know the response of the materials at different loading rates appropriate to the application.

Increasing the loading rate on a component or test specimen, to rates representative of impact loading, can cause changes in response and damage. These may be because of strain rate effects, which alter the behaviour of the material on a microstructural scale, producing effects such as increased failure stress or reduced fracture energy. Alternatively, the component or specimen may respond differently on a macrostructural scale, so that higher frequency modes are excited, or stress waves may not be able to travel far in the ti ᷄ available for the impact event and energy may be more concentrated in the region of the impact.

There are many different test methods for investigating impact phenomena in composite materials, with strain rates ranging from 10^{-4}/s (quasistatic) to 10^4/s. Dropweight or pendulum impact tests are useful for simulating low velocity impact (a few m/s) on carbon fibre composites (Dorey 1987, Epstein et al 1989). Gas guns may be used to achieve impact velocities of several 100 m/s (Dorey 1987, Beaumont et al 1989), and ballistics can achieve several 1000 m/s. High strain rates can be achieved by other means such as by Hopkinson bar techniques (Lankford et al 1989, Harding et al 1989) and laser induced shock (Gilath et al 1989).

In studying impact events it is necessary to monitor loads and damage occurring in very short times and this may be done using strain gauges (Harding et al 1989, Beaumont et al 1989), moire fringes for strain

(Epstein et al), high speed cameras to follow damage (Gilath et al 1989, Beaumont el at 1989) or crack meters (Lankford et al 1989).

The damage produced by impact loading can be similar to that produced by quasistatic loading, for instance where elastic deformation is dominant, or the shock loading may induce different failure modes. In composites, the damage pattern can be dominated by weak fracture paths, such as at fibre/matrix interfaces, responding to secondary stresses in the complex load field.

Modelling impact events, either physically (Beaumont el at 1989) or by computer techniques, is important for understanding and predicting behaviour. It also gives valuable clues in the development of improved materials. But modelling impact performance in compsites is complex and difficult. Sometimes, to get adequate prediciitions, it is necessary to simulate the event experimentally as closely as possible, as in the case of bird strike on aircraft structures. But full scale tests of this kind can be very expensive, and laboratory impact tests can be very useful if they are interpreted intelligently.

REFERENCES

Beaumont N and Penazzi L 1989 Fourth Oxford Conference on The
  mechanical properties of material at high rates of strain
Dorey G 1987 Proc 6th Int Conf on Composite Materials ICCM6 and
  2nd European Conf on Composite Materials ECCM2 ed FL Matthews,
  NCR Buskell, J M Hodgkinson and J Morton (London and New York:
  Elsevier Applies Science) pp 3.1-3.26
Epstein J S, Murakami H, Abdallah M and Deason V A 1989 Fourth
  Oxford Conference
Gilath I, Eliezer S, Gazit Y, Barnea N and Wagner H D 1989 Fourth
  Oxford Conference
Harding J, Li Y, Saka K and Taylor M E C 1989 Fourth Oxford
  Conference
Lankford J and Couque J 1989 Fourth Oxford Conference

[21]

Some Comments on the Modelling of Material Properties for Dynamic
Structural Plasticity

Norman Jones

Impact Research Centre, Department of Mechanical Engineering
The University of Liverpool, P.O. Box 147, Liverpool L69 3BX

ABSTRACT

This article focuses on the modelling of material properties for
structures subjected to large dynamic loads causing extensive material
inelastic flow. Many articles have been published on the behaviour of
simple structures subjected to large dynamic loads [1-5], and the
literature contains a rich coverage of the well-known rigid, perfectly
plastic model [6,7].

The simple rigid-plastic idealisation gives reliable predictions for some
impact problems, but it is not always adequate for the increasingly wide
range of practical problems which confront a designer. Nevertheless, in
Reference [8], several recent studies are examined which confirm that the
rigid, perfectly plastic model is an acceptable approximation for an
elastic, perfectly plastic material, provided the dynamic energy input is
much larger than the maximum wholly elastic strain energy capacity of the
structure, and that the pulse duration is short relative to the corres-
ponding natural period.

The influence of material strain rate sensitivity is important for some
materials and structural designs and, in these cases, should be incor-
porated in the model of a material. This phenomenon is fairly well
understood, and a considerable body of experimental data now exists.
However, the quest for more efficient and lighter structural designs,
coupled with greater environmental demands, often require estimates for
the failure of structural systems under severe dynamic loads. These
calculations require information on the failure modes of structures and
the strain rate sensitive properties of materials which undergo large
plastic strains up to rupture.

Section 2 of the paper discusses some recent experimental and theoretical
studies on the dynamic, inelastic failure of beams, and contrasts the
behaviour under uniform impulsive velocities and local impact loads. It
is observed that the failure of beams subjected to local impact loads and
uniform impulsive velocities is not well understood. Further experimental
data is necessary to identify more clearly and model properly the failure
modes, particularly for mild steel beams under local impact loads.

Some further observations on the dynamic, inelastic failure of structures
are given in Section 3 of the paper, while Section 4 discusses several
outstanding problems on the influence of material strain rate sensitivity.
It is noted that the strain rate sensitive characteristics of materials
are well understood for small strains, whereas structural crashworthiness

studies, and other practical applications, may involve large inelastic strains. A modification of the Cowper-Symonds constitutive law is proposed in order to model the observed decrease of strain rate sensitivity with increase in inelastic strain.

Finally, a simple model for the variation of rupture strain with strain rate is discussed in Section 5 and compared with some experimental data [9-13]. However, it is evident from the available experimental data that the influence of strain rate on the rupture elongation of metals is unclear. Further careful experimental tests are required to resolve these difficulties before the proposed equation or any other complex expressions [14] are employed in design and for numerical calculations.

It emerges clearly from this article that further experimental studies are required in order to develop reliable models for the material properties and structural behaviour under large dynamic loads.

REFERENCES

1. Johnson W 1972 Impact Strength of Materials (London: Arnold)
2. Jones N and Wierzbicki T (ed) 1983 Structural Crashworthiness (London: Butterworths)
3. Reid S R (Ed) 1985 Metal Forming and Impact Mechanics (Oxford: Pergamon)
4. Wierzbicki T and Jones N (ed) 1989 Structural Failure (New York: Wiley)
5. Jones N 1989 Applied Mechanics Reviews 42(4)
6. Symonds P S 1967 Brown Univ. Rep. BU/NSRDC/1-67
7. Jones N 1989 Structural Impact (Cambridge: CUP)
8. Jones N 1989 3rd Conf. on Applied Solid Mechs. (London: Elsevier)
9. Kawata K et al 1968 proc. IUTAM Behaviour of Dense Media Under High Dynamic Pressure (Paris: Dunod) pp 313-23
10. Harding J 1977 Metals Tech. Jan. 6-16
11. Davies R G and Magee C L 1975 Trans. ASME J. Eng. Materials and Tech. 97 151-5
12. Soroushian P and Choi K-B 1987 proc. ASCE. J. Struct. Eng. 113(4) 663-72
13. Regazzoni G and Montheillet F 1984 Mech. Properties at High Rates of Strain ed J Harding (London: Inst. of Physics) pp 63-70
14. Jones N 1989 Structural Failure ed. T Wierzbicki and N Jones (New York: Wiley) pp 133-159

Pages 24 thru 27
Omitted

A COMPARISON OF DYNAMIC R-CURVE METHODS

H J MacGillivray and C E Turner

Imperial College of Science and Technology

There is considerable current interest in quantifying the initiation and propagation of ductile cracks under high-rate dynamic loading. Several experimental R-curve techniques including the Chipperfield multi-specimen R-curve, the dynamic DC potential drop method and for steel at certain temperatures, the transition from ductile tearing to cleavage, are now available to allow measurements to be made with reasonable precision and repeatability. These relatively simple techniques will be described, their advantages and limitations discussed and compared with other methods requiring more elaborate equipment.

The results from a number of dynamic experimental programmes conducted at Imperial College on structural and pressure vessel steels will be presented. These data have been obtained mainly from tests with small 3-point bend specimens and usually as a by-product of other research aims. They show a consistent trend of increased initiation toughness and increased slope of the J R-curve for higher loading rates, and a decrease in these properties when lateral constraint is raised by means of side-grooves The limited results on specimens of varying absolute size give conflicting results. To further investigate this area, a series of tests is now in progress using specimens of two steels, BS 4360 50D and HY 130, for which the static properties have already been thoroughly explored.

A Modified "Moving Singular Element" Method for Fast Crack Propagation

Wei Jian, Liu yuanyong

Northwestern Polytechnical University
Xi'an, Shaanxi, China

Synopsis

There are a lot of Numerical Methods to Solve Dynamic Crack Propagation problems. The accuracy and efficieney of those methods are greatly based the simulating model of crack propagation and the basic variational equation for dynamic solution. In the past, the propagation models are "Nodal Force Release Method"[1] and "Moving Singular Element Method"[2]. The former is much rough in theory, so can't simulate the crack propagation accuratly but it is easy to perform and takes less CPU time of computation; The latter can express the crack running more accuratly, but it has some serious drawbacks:difficult to creat meshs and a large amount of running time. As to the variational equation, Nishioka etc. presented an "energy consistent variational statement" regarding for the crack propagation. But the results show that this variational eqution is not quite success, it is ambiguous in theory and results in an oscillation in actual computation.

In this paper, we will present a modified method of Ref[2] in which a new simulation of propagation and variational equation are used in order to combine the advantages of above two methods.

Basic Theory: In a cracked-body in which the crack moves at velocity v, we have the displacement and stress eigen-function near the crack tip as follows:

$$u_{xn} = \frac{4}{3\sqrt{2\pi}} \frac{Kn}{G} \frac{(1+S_2^4)}{4S_1 S_2 - (1+S_2^2)^2} (\frac{n}{2}+1)\left\{ r_1^{\frac{n}{2}}\cos(\frac{n}{2}\theta_1) - \frac{1}{2}q_{(n)}r_1^{\frac{n}{2}}\cos(\frac{n}{2}\theta_1) \right\}$$

$$u_{yn} = \frac{4}{3\sqrt{2\pi}} \frac{Kn}{G} \frac{(1+S_2^4)}{4S_1 S_2 - (1+S_2^2)^2} (\frac{n}{2}+1)\left\{ -S_1 r_1^{\frac{n}{2}}\sin(\frac{n}{2}\theta_1) + \frac{1}{2}q_{(n)}/S_2 r_2^{\frac{n}{2}}\sin(\frac{n}{2}\theta_1) \right\}$$

$$\dots\dots\dots(1)$$

Uxxn=......
Uyyn=......
Uxyn=......   (To be ignored)

where:

$$S_1^2 = 1-(V/C_L)^2, \quad S_2^2 = 1-(V/C_T)^2$$

$$q_{(n)} = \begin{cases} 4S_1 S_2/(1+S_2^4), & n=\text{odd} \\ 1+S_2^2, & n=\text{even} \end{cases}$$

when v=0, the equation (1) changes into the well-know williams-functions, which is deduced in the static condition.

From the oringal definition, the energy releae rate:

$$G = \lim_{\delta\to 0} \frac{1}{\delta}\int_0^\delta \sigma_{xx}(x) u_y(x-\delta)dx \qquad \dots\dots\dots(2)$$

If we use the propagation eigen-functions and williaims-functions as the basic displacement and stress function of singular elements---called propagating singular element and static singular element respectively. We can derive the different energy release rate Gs and Gd using (2):

$$G_s = \frac{(K_1^s)^2}{2G} \cdot F(1,1)$$

and

$$G_d = \frac{[K_1^p(V)]^2}{2G} \cdot F(S_1,S_2)$$

where:

$$F(1,1) = \begin{cases} 1-V & \text{(plane strain)} \\ \frac{1}{1+V} & \text{(plane stress)} \end{cases}$$

$$F(S_1,S_2) = \frac{S_1(1-S_2^4)}{4S_1 S_2 - (1+S_2^2)^2}$$

$$\dots\dots\dots(3)$$

In the meantime, from another expression of G:

$$G = \frac{1}{b}(\frac{dw}{da} - \frac{dv}{da} - \frac{dt}{da})$$

We can see that if the propagation singular element is replaced by the static singular element, there is only a little change in total energy release. Because the singular element only takes a little part in whole body, we can give an approximation:

$$Gd = Gs \qquad \dots\dots\dots(4)$$

Substitute (3) for (4), we get:

$$K_I^\circ(v) = \frac{F(1,1)}{F(S_1,S_2)} K_I^\wedge = \alpha(v) K_I^3 \qquad \dots\dots\dots(5)$$

Now, using (5), we can largly reduce the computing time. Because we need no longer to reproduce singular elements stiffness and mass matrices when v is varying, which take a lot of time to perform, and the programe is much simplified as well.

As to the variational equation, Because inany genetic time t_i , we can consider the crack is not propagating, So unlike [2], we can use a simple variational equation to a running crack:

$$\int_v (\sigma_{ij}\delta\epsilon_{xy} + \rho\ddot{u}i\delta ui)dv - \int_{S_q} \bar{T}i\delta uids - \int_z \bar{T}i\delta uids = 0 \qquad \dots\dots\dots(6)$$

Finally, we got:

$$K\cdot q + M\cdot\ddot{q} - Q = 0 \qquad \dots\dots\dots(7)$$

This eq. was solved by New mark-β time integration.

EXAMPLE: We first use a steel DCB specimen: K_{IQ} =7066N/mm$^{1.5}$ v=1000m/s, Δt=3μs, All the experiment data were got by J.F.Kalthoff [3]. Fig.1 shows the comparasion results of different variational eq. using propagation singular element. Fig.2 shows the comparasion of propagation singular element and static singular element under new variational eq.; the latter takes 25% less CPU time than former. Second, we use Hemilate-100 DCB specimen: K_{IQ} =73.36N/mm$^{1.5}$, v=295m/s, t=6μs, we got nearly the same result compared with the [2], while the time increment Δt is 30 times large then [2].

CONCLUSION:
This method is more accurate than "Nodal Force Release Method", and more efficient then "Moving Singular Element Method". And compared with the Experimental results, it shows a good consistence. The stability and convergency of this method is also attractive, especilly, it can be performed in such large increment of Δt.

References: (To be ignored)

Fig. 1

(K_{IQ}=7066 N/mm$^{1.5}$, V=1000 m/s)

Fig. 2

[30]
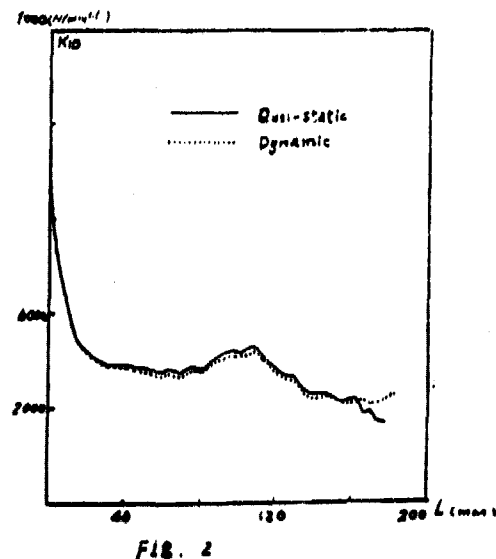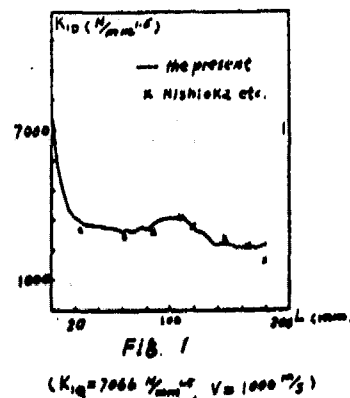
HEAT GENERATION DURING FRACTURE

By Akira KOBAYASHI,Professor,Dr.
   Nobuo OHTANI, Research Fellow,Dr.
   Michel GOROG, Research Student

Faculty of Engineering,Department of Materials Science,
The University of Tokyo,Hongo 7-3-1, Bunkyo-ku,Tokyo 113
Japan

In the present report,the validity on the estimation of dynamic energy release rate by generated heat is presented.
The specimen in interest is PMMA. Experiments are done under various pre-strain conditions in crack propagation,during which generated heat in the function of temperature rise is measured by thermistors and the crack velocity by velocity gages. A crack is initiated by an impact of a sharp edge on a notch in the specimen to realize the crack propagation.

Dynamic energy release rate G_{Id} for a finite width elastic body with fixed displacement is expressed as

$$G_{Id} = 1/2 \ f(\nu) \cdot E \cdot h \cdot \mathcal{E}_p^2 \qquad ---(1)$$

where $f(\nu) = 1/(1 - \nu)^2$ for plane stress

$$= 1 - \nu/(1 + \nu)(1 - 2\nu) \text{ for plane strain}$$

and E=Young's modulus, ν=Poisson's ratio,h=a distance between jaws for gripping,and $\mathcal{E}_p$=pre-strain. (Ref.1)

As for heat generation,assuming the one-dimensional heat conduction,generated heat can be expressed as

$$Q = \sqrt{2\pi e} \ \rho \cdot c \cdot y \cdot \triangle T_m \qquad ---(2)$$

where e=2.71828---, ρ=density,c=specific heat,and
$\triangle T_m$ = temperature rise. (Refs.2 & 3)

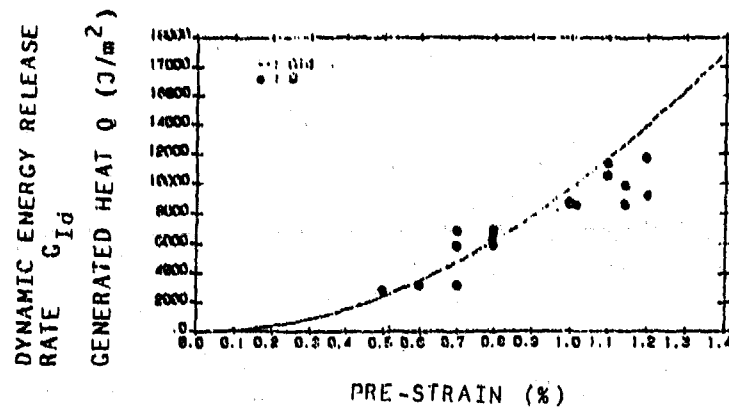Measurement of pre-strain and temperature rise in combination with Eqs.(1) and (2) leads to Fig.3

[31]

Fig.3 Dynamic Energy Release Rate/Generated Heat vs.Pre-Strain

Fig.2 Crack Propagation Velocity vs. Pre-Strain

    Further combination of Figs.2 and 3 presents a solid line
in Fig.4,in which previous experimental results through a caustic
method (Ref.4) are shown by solid circles.
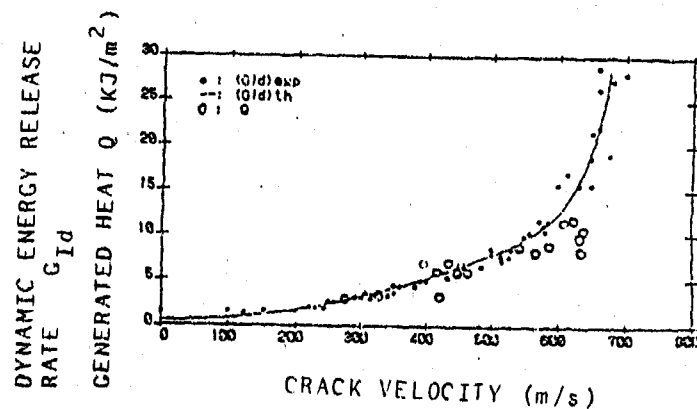

Fig.4 Dynamic Energy Release Rate/Generated Heat vs. Crack
       Velocity

    As seen from Fig.4,dynamic energy release rate and
generated heat are in good agreement until the crack velocity
reaches about 550 m/s,which is almost seventy percent of terminal
velocity. Therefore,the validity on estimation of dynamic energy
release rate by generated heat holds in the range mentioned above.
One reason of this deviation from 550 m/s is explained by fracto-
graphy of fractured surfaces,showing much microscopic crack
branching leading toward   much energy consumption.

[32]

THREE-DIMENSIONAL SEMI-INFINITE CRACKS SUBJECTED TO DYNAMIC LOADS

P. PINTADO[1] AND F.G. BENITEZ[2]

Escuela Superior de Ingenieros Industriales, Avda. Reina Mercedes, 41012 Sevilla, Spain

The boundary-integral equation method for elastostatics and elastodynamics is especially helpfull when the particular geometry of the problem being analyzed is, to some extent, acounted for by the fundamental Green's function used. In this paper, the three-dimensional solution for an impact point load acting in the interior of an unbounded, homogeneus, linearly-elastic, isotropic thick layer has been studied. This fundamental solution is used in connection with the boundary-integral equation method to obtain the stress and displacement fields in problems concerning semi-infinite through-cracks in plates subjected to dynamic loads. The technique proposed can be used for the analysis of other geometrical configurations such as presurized cracks and circular holes in plates of arbitrary thickness.

---

[1] Research Assistant
[2] Associate Professor

TENSILE INSTABILITIES AT HIGH STRAIN RATE: INERTIA AND MULTIAXIAL EFFECTS.

C.Fressengeas, A.Molinari
Laboratoire de Physique et Mecanique des Matériaux, U.A. C.N.R.S. 1215
Université de Metz, Ile du Saulcy, 57045- Metz Cedex, France.

High speed metallic jets are formed by the collapse of a conical or wedge-shaped liner under explosive loading. Typical velocities are 8km/s at the tip and 4km/s at the tail of the jet: consequently, the jots are submitted to an enormous stretching: their length can be multiplied 4 times in 100µs. However, beyond some standoff distance, the jets neck down, in a series of locations and soon break down into closely similar fragments. This is known to limit the jet penetration ability (BIRKHOFF et al, 1948). Such a phenomenon resembles the breakup of capillary liquid jets: therefore it has been suggested that surface tension is the destabilizing mechanism, and classical capillary instability theories have been applied to the metallic jets breakup (FRANKEL and WEIHS,1985). Yet, the perturbation growth issued by such models is too small by several orders of magnitude when it comes to compare the predicted breakup time with the observed data.

In this paper, the metallic jet breakup is rather viewed as a necking instability; it is shown that the necking instability analysis of a non linear viscoplastic material can provide perturbation growths large enough to account for the observed breakup time and fragments aspect. The driving mechanism is the geometric softening of the jet due to its section reduction; it renders the uniform stretching jet unable to sustain the axial force involved. In the meantime, stabilizing factors are at work, which delay the growth of non uniform perturbations: in addition to the damping of rate sensitivity, the axial and lateral inertia effects slow down the growth of long wavelength perturbations. As a matter of fact, the latter involve larger mass amounts. The multiaxial aspects of the stress field in the neck do so at the short wavelengths: the average axial stress applied to the neck cross section is larger at long wavelengths: consequently, for a given applied force, the section area is smaller, which means that the instability proceeds faster at long wavelengths. Between the two foregoing limiting cases, an optimum non zero finite wavelength is selected at each moment, for which the perturbation growth is maximum. This is indicative of multiple necking and of jet fragmentation.

Due to the stretching, the basic uniform plastic flow is time dependent. Therefore, the problem cannot be solved by using the classical simple eigenvalue formulation: the perturbation growth is not that of a simple exponential, and there is no single dominant wavelength. In this paper, we consider a "quasi-steady" uniform plastic flow: it is assumed that the time scale of perturbation growth is much smaller than the uniform stretching jet time scale. This is well verified in all the specific cases we investigated. Then it is shown that the problem can be addressed through a series of instantaneous eigenvalue problems. At each moment a different dominant wavelength and a different pertubation growth rate are found. The procedure provides

predictions for the breakup time and the fragments aspect ratio (length to maximum diameter); at breakup time (i.e. when the non uniform perturbed radius is zero), the instantaneous critical wavelength is indicative of the the fragments size.

The comparison with the available experimental data on copper jets (CHOU et al. 1977) suggests that both predictions are realistic, and that the models allows a consistent prediction of the jet breakup phenomenon. The compatibility with the observed data is achieved for material constants (reference stress, rate sensitivity) in agreement with the accepted experimental trend. Such controlling parameters of the jet breakup as lateral inertia and rate sensitivity are pointed out, and their influence discussed. It is shown that a large rate sensitivity yields longer fragments. Axial and lateral inertia effects are more complex: in highly dynamic cases, the fracture process is delayed at larger plastic deformations. The fragments are shorter than in less dynamic events however. Although it focused on metallic jets, such an analysis might have implications on similar processes, like polymer fibre spinning.

References:

BIRKHOFF, G., MACDOUGALL, D.P., PUGH, E.M. and TAYLOR, G.I.: 1948. Explosives with lined cavities. J.Appl.Phys. 19, 563-582.
CARLEONE, J., CHOU, P.C. and CICCARELLI, R.D.: 1977. Shaped charge jet stability and penetration calculations. BRL-CR-351 Report.
FRANKEL, I. and WEIHS, D.: 1985. Stability of a capillary jet with linearly increasing axial velocity (with application to shaped charges), J.Fluid.Mech., 155, 289-307.

[35]

DUCTILE FRACTURE OF METALS INVESTIGATED BY DYNAMIC TENSILE TESTS ON SMOOTH AND NOTCHED BARS

C. DUMONT, C. LEVAILLANT, M. ARMINJON, J.P. ANSART*, R. DORMEVAL*

Centre de Mise en Forme des Matériaux - Ecole des Mines de Paris
Sophia Antipolis - 06560 VALBONNE - FRANCE

* Service Métallurgie Commissariat à l'Energie Atomique
BP 12 - 91680 BRUYERES LE CHATEL - FRANCE

A cooperative research program has been developed on the dynamic tensile testing facility built by CEA. Results obtained on smooth bars up to 500 s^{-1} suggest that a linear strain rate dependency of stress can be used to represent the constitutive equation of various high purity metals or alloys (such as Copper, Tantalum or Copper-Tungsten), as :

$$\bar{\sigma} = \bar{\sigma}_o + \beta \dot{\bar{\epsilon}} \quad (1) \qquad \text{with} \qquad \bar{\sigma}_o = K \bar{\epsilon}^n \quad (2).$$

There remained a problem with dynamic tensile testing due to transient stages of heterogeneous strains caused by inertial effects. Recent numerical simulations using a one dimensional or a two dimensional finite element method show that inertial effects at 2000 s^{-1} are significant only at the very beginning of the test, but do not alter the validity of the linear stress-strain rate relationship assumed earlier.

In order to complete our investigation about mechanical behaviour of high purity copper at high strain rate, we performed dynamic and quasistatic tensile tests on notched bars, with three different notch radii. Our work deals with the variation of the maximum load value and of the intrinsic ductility as a function of strain rate or of the notch radius. The intrinsic ductility is characterized by the length relative variation of the notch part between the initial state and the fractured one. These experimental results are discussed on the basis of the two dimensional finite element simulation which takes into account inertia effects.

Our computation shows that whatever the strain rate, for a given geometry, a same relative variation of the minimum diameter leads to similar values of the equivalent strain or of the stress triaxiality. So, these parameters which are in direct relation to damage effects are not influenced by the test conditions and consequently by the inertia effects.

In all the cases (figure 1), the maximum load value increases when the notch radius decreases. This phenomenon is well-known for quasistatic test conditions and named "notch strengthening effect" : it increases with strain rate in dynamic conditions.
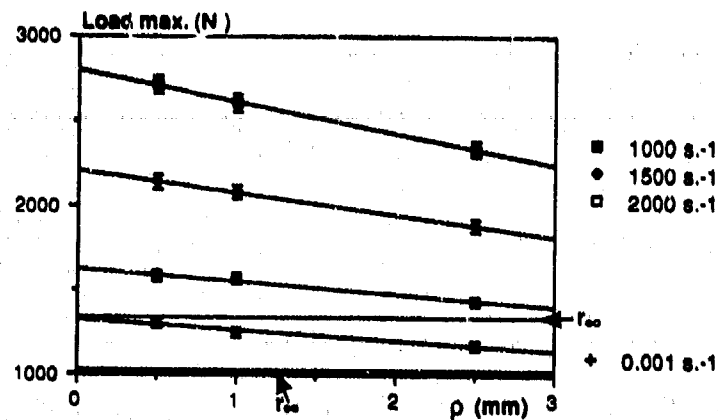
[36]

figure 1: Maximum load values as a function of notch radius at different strain rates

The numerical simulation leads also to an increase of the maximum load value with strain rate, which appears at the same macroscopic elongation or at the same relative variation of the minimum diameter whatever the dynamic strain rate. So, the equivalent strain being the same in the minimum cross section, we are in position to assume that the maximum load value increase is due to the linear strain rate behaviour of the high purity copper (equation 1). However, our computation does not show an increase of the notch strengthening effect with strain rate.

Whatever the strain rate, the intrinsic ductility increases when the notch radius decreases (figure 2). This result can be justified if we study the variation of the equivalent strain along the minimum cross section at the same relative variation of the minimum diameter. The lower the notch radius value, the higher the equivalent strain gradient, but the lower the mean equivalent strain.
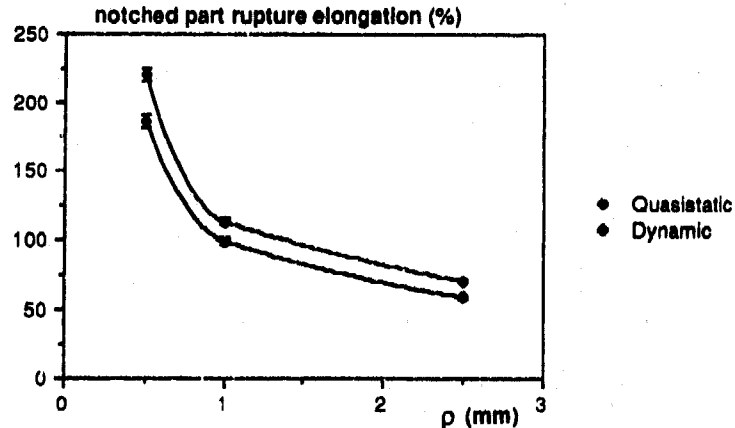

figure 2: The notch part rupture elongation as a function of notch radius
between quasistatic and dynamic strain rates

On the other hand, we are not able to explain simply with these computation results, the differences observed between quasistatic and dynamic strain rates : the mean equivalent strain decreases from the dynamic to the quasistatic strain rates.

Nevertheless, we may remark that the dynamic constitutive equation leads to higher strain rate sensitivity parameter m than in quasistatic conditions where m is particularly low ($m = 0.012$).

[37]

Deformation and Fracture of Polycarbonate at High Strain Rate

Fleck, N.A.[*], Wright, S.C.[*]

[*]Cambridge University Engineering Department,
Trumpington Street, Cambridge, CB2 1PZ

Results from high strain rate tension and torsion tests using Split Hopkinson Pressure Bars have been combined with data from the literature to determine the effects of temperature, strain rate and stress on the deformation and fracture of polycarbonate (PC). See Fig. 1.

An increase in strain rate results in a modest increase in yield stress. Decreasing temperatures result in increased yield and fracture stresses. For temperatures below $-60°C$ bond rotation is frozen, resulting in small fracture strains. Above $-60°C$ deformation is by sliding of backbone molecules and longer strains are achieved.

For temperatures in the range $-60°C$ to $140°C$ the response consists of three stages; I - non-linear viscoelasticity until yield, II - strain softening, III - strain hardening.

Shear bands develop in torsion and compression, and necking occurs in tension. Above $140°C$ the van der Waals bonds melt and the material behaves as a viscous liquid.

The Eyring Equation is shown to fit the available data for yield of PC for temperatures T in the range $0.6 < T/Tg < 1.0$, ($Tg = 145°C =$ glass transition temperature) and for strain rates between $10^{-4} s^{-1}$ and $5 \times 10^3 s^{-1}$. A summation of two Eyring terms is required for temperatures below 0.6 Tg. The model accounts for the different stress states associated with tension, shear and compression.

Strain to fracture for PC drops linearly with increasing ln (strain rate), with compression failure occuring at about 70% greater strain than tensile failure. Fracture is not by adiabatic softening, as orientation hardening stabilises the material.

In shear, fracture is by the formation of tensile microcracks which then coalesce by plastic collapse in shear. Compression failure is thought to be by a similar process. Tensile failure is by the propagation of one or two tensile cracks from pre-existing surface flaws, following sub critical flaw growth.
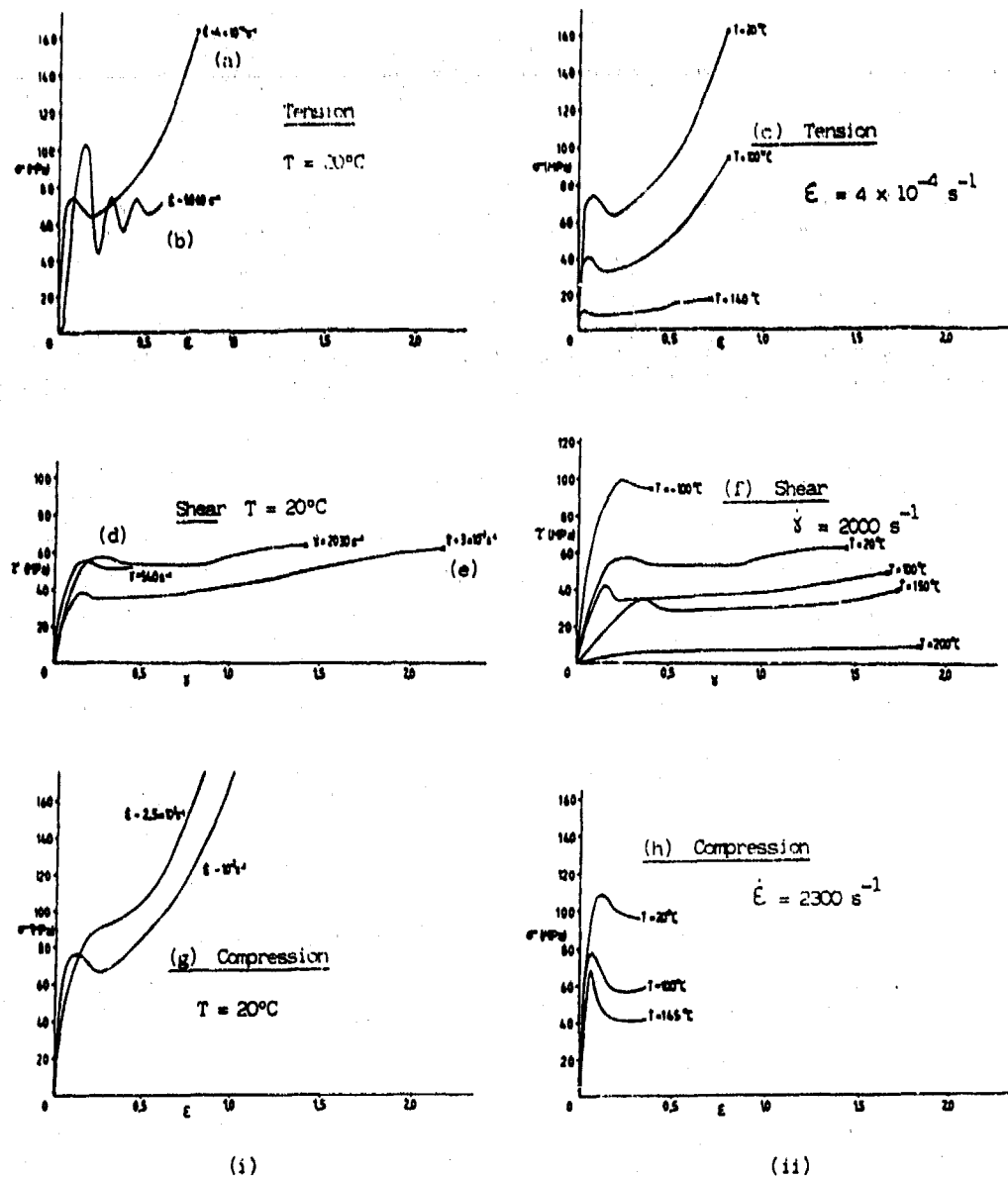
1

[38]

Fig. 1. Stress-strain response of PC. (i) Effect of strain rate; (ii) Effect of temperature. Sources: (a),(c) Vest, Amoedo and Lee (1987); (b),(d),(f) the authors; (g) Walley et al (1989); (h) Steer (1985); × at the end of a curve denotes fracture.

[39]

COMBINATION OF MICRO- AND MACROREPRESENTATIONS
IN THE MODEL OF DYNAMIC DEFORMATION
AND FRACTURE OF METALS

M.A.Merzhievsky
Lavrentyev Institute of Hydrodynamics
Siberian Division of the USSR Academy of Sciences
Novosibirsk 630090 USSR

In modelling dynamical strain and fracture of metals, the model of a Maxwell-like type visco-elastic body is used, in which the relation between the relaxation time of shear stresses τ and the medium state parameters is determined on the basis of dislocation representations of plastic deformation. When obtaining the τ relation, the experimental data are used on determining the dynamical yield limit as a function of strain rate. The model is supplemented by the temporal fracture criterion relating the life time with the load. The criterion generalizing the well-known approach suggested by S.N.Zhurkov,describes, in terms of dislocations, both "static" and "dynamic" branches of the experimentally observed dependence.

Testing of the proposed model and of the numerical methods is realized on the basis of some one-dimensional problems. The results are compared with the experimental data. The capabilities of the model and of the method are illustrated by the solutions of two-dimensional problems of high rate strain and fracture. A good qualitative and quantitative agreement between the predicted and experimental results has been established.

INFLUENCE OF LOADING RATE ON FRACTURE PROPERTIES OF HEAVY METALS

H. COUQUE and J. LANKFORD

Division of Engineering and Materials Sciences,
Southwest Research Institute,
6220 Culebra, P.O. Drawer 28510, San Antonio, TX 78284

Abstract - The applicability of dynamic fracture mechanics to the failure of heavy metal alloys subject to high velocity impact is a relatively unexplored area. This is principally due to the lack of knowledge of the effect of loading rate on deformation and fracture toughness. Recent progress, however has been made towards identifying the failure modes involved in impact loading rate in tungsten alloys [1]. As the loading rate increases, the fracture process changes from a ductile to a special, brittle type of failure. Specifically, the transition from ductile to brittle is associated with a decrease of fracture of the tungsten particles (W) and the nickel base matrix (M) and with an increase of cracking along tungsten/matrix (W/M) and tungsten/tungsten (W/W) interfaces [1,2]. Unfortunately, due to the high strain rate sensitivity of this material, identification of the micromechanical processes alone is insufficient to predict fracture toughness at ultra high loading rates.

The purpose of this investigation is to report fracture toughnesses measured over a wide range in loading rate; interpretation of these results is based on SEM observations of the fracture specimens and quantitative micromechanical modeling. A novel technique has been used to measure fracture toughness at dynamic loading rates $\dot{K}_1$ varying from 10^6 to 3.5×10^6 MPa$\sqrt{\text{m}}$ s^{-1} using small compact specimens [3]. The quasi-static toughness was evaluated using a standard compact specimen at a loading rate $\dot{K}_1$ of 1 MPa$\sqrt{\text{m}}$ s^{-1}. Micromechanical modeling was performed using simple fracture models for ductile and brittle fracture, following a procedure developed in a previous study of the effect of loading rate on fracture properties of a plain carbon steel [4]. Specifically the modeling is based on quantification of the micromechanical processes involved in ductile and brittle fracture, and measurement of tensile deformation properties at strain rates of 8×10^{-5} s^{-1} and 1.5×10^3 s^{-1}.

Decrease in toughness was observed with increasing loading rate and was correlated with increasing apparent embrittlement of the macroscopic fracture surfaces. The transition from ductile to brittle failure is associated with an increased frequency in the tungsten/tungsten separation. Good agreement was obtained between

[41]

SHEAR BANDING IN TITANIUM WITH CONTROLLED ELONGATIONS AT 10^6/SEC

K.P. Staudhammer* and A.J. Gray
Materials Science and Technology Division
Los Alamos National Laboratory, Los Alamos, New Mexico, USA
 *Currently on sabbatical leave at the Fraunhofer-Institut für
  angewandte Materialforschung, Bremen, FRG

Abstract

Over the past nearly two decades numerous investigations have
been carried out on the formation and propagation of adiabatic
shear bands. At high strain rates adiabatic shear localization
is a very important phenomenon that has a profound effect on
plastic deformation and fracture. This paper describes obser-
vations made of the nature of adiabatic shear bands in commer-
cially pure Ti shock loaded at a strain rate of 10^6/sec. The
experiments were carried out at controlled total elongations
of 5 to 11 %, which was achieved by varying the pedestal
height in our shock design. In all samples tested, shear bands
were observed. The quantity and shear band width increased
with increasing elongation. Above 10 % total elongation
fracture was dominant and only local strain up to fracture was
obtainable. The strains were measured from circle grids photo
etched on the outer surface of the samples. This allowed for
direct external measurement of shear band displacement relative
to the internal microscopic displacements. The local strain
between shear band segments, ie, the plateau steps on each of
the samples, irrespective of the overall elongation, had little
if any measureable strain. All local strain readings were
within the lower limit of the grid technique and did not exceed
1 %. Strains in the shear bands that were measurable did exceed
30 %.

No phase transformations in the shear band were observed, only
grain refinement and deformation. Shock hardening was observed
over the unshocked sample. However, all the post shocked
samples had essentially the same valve for all the elongations.
The microhardness values were equivalent for both matrix and
the shear bands.

For all conditions of low strain irrespective of total
elongation, the shear bands were typically characteristic of
shear bands observed at much lower strain rates. However, above
approximatly 5 % strain the shear bands had a very definite
boundary between the shear band and the matrix, and increased
in width with increasing total elongation. This increasing
boundary effect can be directly attributed to the strain heat
which is not homogeneous and is highly localized; thus, giving
rise to this boundary effect, it is similar in nature to the
heat effected zone in welds.

[43]

Adiabatic Shear Bands in One Dimension

T. W. Wright and J. W. Walter

Ballistic Research Laboratory, Aberdeen Proving Ground, MD 21005-5066, U.S.A.

ABSTRACT: This paper summarizes the progress made at the Ballistic Research Laboratory to date in analyzing and understanding the dynamical processes that cause the formation of adiabatic shear bands and the influence of various physical parameters on their formation.

A simple one dimensional model, which may be thought of as simulating a torsional Kolsky bar test on a thin walled tube, has been studied extensively by both numerical and analytical techniques. For a body in simple shear

$$x = X + u(Y,t), \quad y = Y, \quad z = Z, \tag{1}$$

the nondimensional equations of thermoviscoplasticity may be written as

$$
\begin{aligned}
\text{Momentum:} & \quad v_t = s_y/\rho, \\
\text{Energy:} & \quad \theta_t = k\theta_{yy} + s\dot{\gamma}_p, \\
\text{Elasticity:} & \quad s_t = \mu(v_y - \dot{\gamma}_p), \\
\text{Flow Law:} & \quad s = \text{sgn}(\dot{\gamma}_p)\kappa g(\theta)|\dot{\gamma}_p|^m, \\
\text{Work hardening:} & \quad \kappa_t = M(\kappa,\theta)s\dot{\gamma}_p.
\end{aligned}
\tag{2}
$$

where v is the velocity, θ is the temperature, s is the shear stress, κ is the work hardening parameter, $\dot{\gamma}_p$ is the plastic strain rate, and sgn indicates the algebraic sign of its argument.

Only insulated boundaries with constant prescribed velocity are considered. That is, $\theta_y(\pm 1, t) = 0$ and $v(\pm 1, t) = \pm 1$. The initial strain rate is assumed to be close to unity everywhere, and the initial stress is assumed to be constant. To trigger a shear band, only perturbations in the initial temperature will be considered, $\theta(y,0) = \theta_0(y)$, where θ_0 is small. Mechanical perturbations can also initiate a shear band, but for brevity we omit them here.

From a variety of analytical techniques it has been possible to understand many of the primary parametric dependences of shear band formation, at least in the quasi-static approximation. Some of the principal conclusions are that shear band formation is a

[44]

multistep process, that instability and intense localization are not coincident in time, that a fully formed shear band often behaves like a boundary layer with a well defined, calculable, spatial distribution, and that for perfectly plastic materials a theoretical "shear band susceptibility" can be identified and calculated from macroscopic laboratory measurements. The susceptibility, which appears naturally in simplified analyses, appears to be the key quantity in assessing stability, early growth rate, and minimum possible time to localization. Thermal conductivity has a substantial delaying effect on intense localization at lower applied strain rates. Elasticity has little effect until intense localization occurs. and then it may add rather elaborate structure to the late stage morphology. Work hardening, which is known to be stabilizing before localization, has a partially stabilizing effect after localization where it also adds structure to the late stage morphology. Finite element analysis indicates that inertia may also have a substantial delaying effect on severe localization, but the exact parametric dependence is not yet well understood.

Formation of Adiabatic Shear Bands by the Impact
of Wedges and Cones

S.P. Timothy[*] and I.M. Hutchings

Department of Materials Science and Metallurgy
University of Cambridge, Pembroke Street,
Cambridge CB2 3QZ, England.

Abstract

An investigation is presented of the initiation and growth of adiabatic
shear bands in a titanium alloy (Ti-6Al-4V) due to the impact of hard
wedge-ended and cone-ended projectiles. For projectiles of these shapes,
geometrical similarity of the impact deformation is maintained over the range
of velocities explored (30-300 m s^{-1}). The mean strain $\bar{\varepsilon}$ associated with the
impact indentations therefore does not vary [1] with velocity, in contrast with
the case of sphere impact examined in previous work [2-4].

Hardened tool steel projectiles, with included wedge or cone angles of 60,
90, 120 and 150° and with constant mass (0.88 g) were fired at normal incidence
at thick targets of the titanium alloy at velocities up to 300 m s^{-1}. The
impact craters were sectioned and examined metallographically to detect the
presence of adiabatic shear bands. The velocities at which shear bands were
observed varied with wedge-angle in a manner shown in Fig. 1; the relationship
for impact by cone-ended projectiles was almost the same, except that
deformation failed to localize at all for impact by 150° cones. The dynamic
hardness of the target metal was calculated from plots of the crater volume
against kinetic energy and was used in conjunction with a rigid-plastic model
to determine the mean strain rate (1 x 10^4 - 4 x 10^4 s^{-1}) as a function of the
projectile geometry and the impact velocity.

The shear band patterns were of two main types, consistent with the
"cutting" (Fig. 2a) and "radial compression" (Fig. 2b) modes of plastic
deformation observed after quasi-static indentation by cones [5,6] and
wedges [6]. The zone containing the shear band deformation was restricted
closer to the crater surface after impact by sharp cones compared to sharp
wedges [6]. particularly at low velocities (Fig. 3).

Mean strains, $\bar{\varepsilon}$, associated with quasi-static indentation of metals by
cones have been reported by Atkins and Tabor [5], who measured $\bar{\varepsilon}$ = 0.30, 0.25,
0.17 and 0.08 for indentation by 60°, 90°, 120° and 150° cones respectively.
In the present work the shear bands were found to initiate at 0.08 < $\bar{\varepsilon}$ < 0.17
in the cone impact experiments, at mean strain rates from 1 x 10^4 to 4 x 10^4 s^{-1}
This result is consistent with earlier work [2]; shear bands were found to
initiate beneath craters formed by spheres at ε = 0.12 over a similar range of
strain rate. The technique further demonstrates that a critical strain is
necessary to initiate shear bands at strain rates of about 10^4 s^{-1} where
plastic deformation is effectively adiabatic.

[*] Present address: Alcan International Ltd., Banbury Laboratories, Banbury,
Oxon. OX16 7SP.

[46]

REFERENCES

1. K.L. Johnson, J. Mech. Phys. Solids 18 (1970) 115.

2. S.P. Timothy and I.M. Hutchings, in Proc. 7th International Conference on
    High Energy Fabrication, T.Z. Blazynski (ed.), Univ. of Leeds, 1981, p.19.

3. S.P. Timothy and I.M. Hutchings, in "High Energy Rate Fabrication - 1984",
    I. Berman and J.W. Schroeder (eds.), ASME, 1984, p.31.

4. S.P. Timothy and I.M. Hutchings, in "Mechanical Properties at High Rates
    of Strain 1984", Inst. Phys. Conf. Series No. 70, 1984, p.397.

5. A.G. Atkins and D. Tabor, J. Mech. Phys. Solids 13 (1965) 149.

6. R.L. Woodward, J. Aust. Inst. Metals 19 (1974) 128.

LIST OF FIGURES

[47]

Impact velocity (m s⁻¹) vs Wedge angle (deg): shear bands formed / no shear bands

Fig. 2

(a)

0.5 mm

(b)

0.5 mm

[49]

Fig. 3

(a)

1mm

(b)

1mm

[50]

An Alternative Method to Study Rapid Crack Propagation in PE

R.M.S. Genussov and J.G.Williams

Department of Mechanical Engineering, Imperial College, London SW7 2AZ

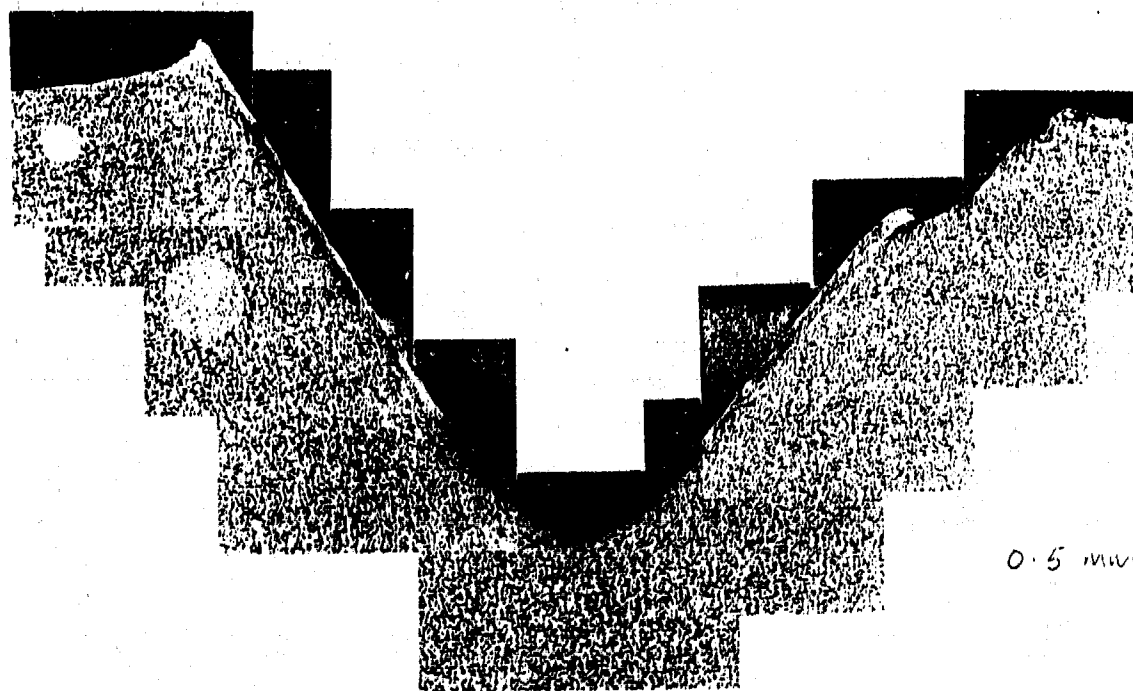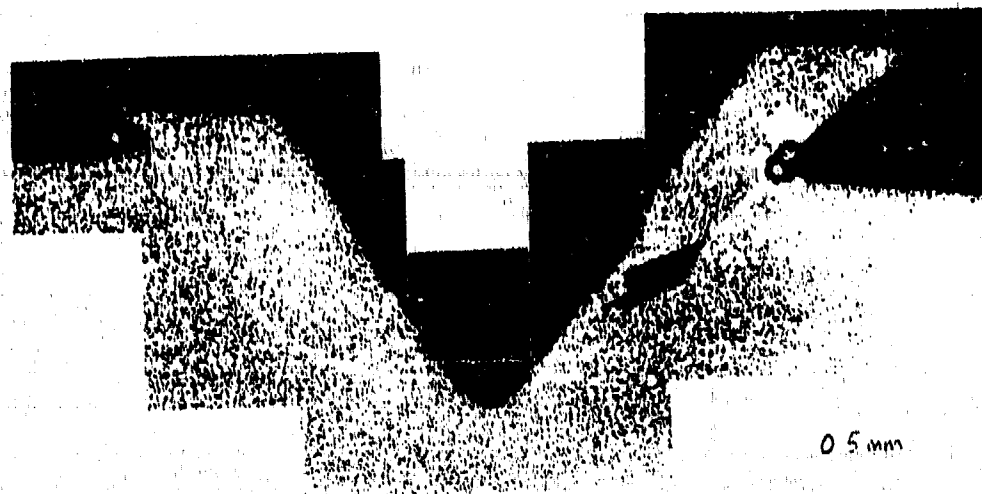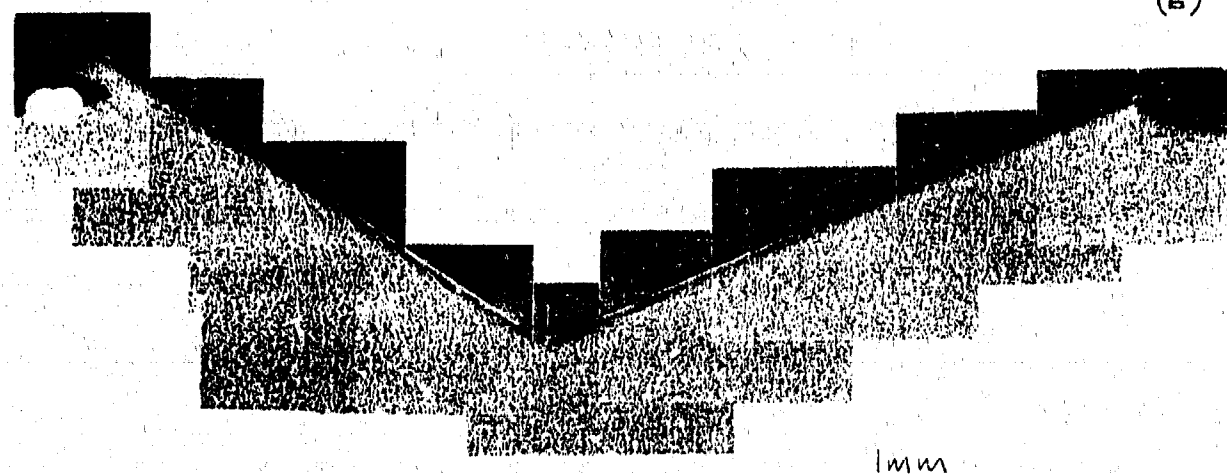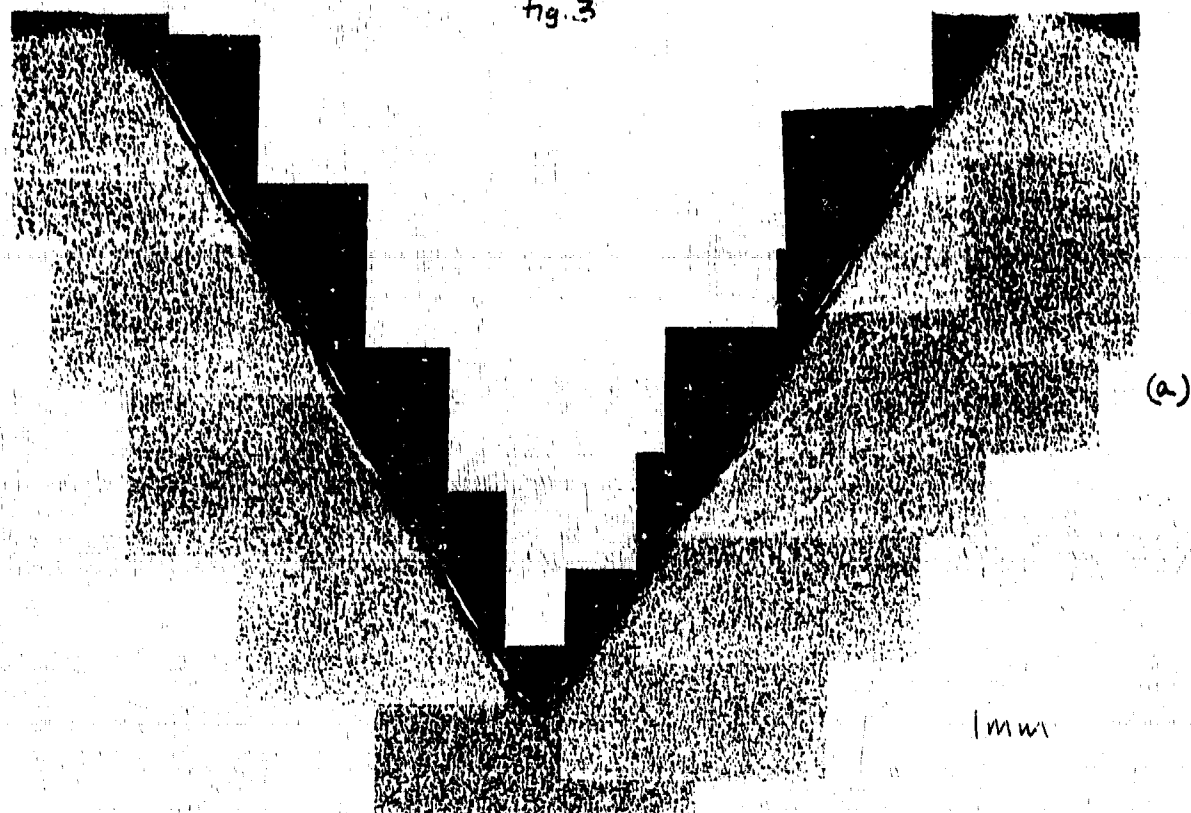Pressurised PE pipes can be prone to failure due to "Rapid Crack Propagation" (RCP). Hence, these pipes should be designed from tough PE grades whose dynamic crack resistance G_D, ensures immediate crack arrest. Quasistatic fracture calibration tests fail to generate RCP in these tough PE grades. Only impact tests successfully initiated the required mode of fast fracture in precracked PE samples. However, these tests have other drawbacks : exact monitoring of their load and crack-length traces is most complicated; their analysis hinges on sophisticated models taking into account dynamic effects; inherent transient initiation effects and gross vibrations may cause the generated G_D values to be geometry dependent and thus cannot be applied to other geometries such as pipes.

These problems pointed out the need for an alternative test which imitates the pipes' fast fracture, suppresses gross dynamic effects and is still easy to monitor and analyse. Such a test has been developed using a unique Glass-PE (G-PE) duplex sample : A polished glass slide is adhered to the crack-mouth of a razor prenotched, side-grooved PE sample (see Figure). Quasistatic tensile loading of the G-PE sample results in the glass shattering, followed by a fast and brittle fracture in the PE. Evidently, prior to glass breaking, the glass suppresses the singularity at the crack tip (which remains sharp), while large amount of elastic energy is stored in the sample. When the glass reaches its ultimate load it breaks, rapidly loading the sharp crack. A brittle crack is initiated and propelled across the entire sample by the released elastic energy.

The new technique has been successfully applied to two PE pipe-grades : BP Rigidex 002-40, and Philips TUB-71. The samples were clamped between heavy grips which were bolted to the frame of a tensile loading machine. Half of the samples were precooled to 0° C while the others were kept at ambient conditions prior to loading at room temperature. Load-displacement curves prior to RCP were plotted on the tensile machine recorder. Crack history was monitored simultaneously by an Imacon image converter camera and a digital oscilloscope connected to timing lines painted along the crack path. Both camera and oscilloscope were triggered by the breaking of a conducting line painted on the glass slide (see figure enclosed). The pictures, showing the crack history either in framing or "streak" modes, were in good agreement with the timing lines' readings. The average velocities ranged between 50 — 80 m s^{-1} at room temperature and 230 — 270 m s^{-1} in precooled samples. It should be noticed that the only effect of an increase in the remote load prior to glass-break seem to be a shorter delay between glass-break and crack initiation. After the initiation effects subsided, the crack velocity profiles seemed to maintain a constant value.

Careful SEM study of the fractured surfaces revealed the almost ideal uniform nature of the surface morphology. There was hardly any evidence of a different micromechanism at initiation or along the free surfaces, or of any changes along the crack . The relevance of

[51]

this small scale test to the real pipe problem was supported by their similar microfeatures i.e. a brittle "flaky" surface with traces of drawn-out films and fibrils.

A dynamic finite element program was employed to process the experimental data into valid crack resistance terms. The fixed boundary conditions, the glass breaking almost instantaneously with practically no energy loss, and the planar uniform crack are all easy to define in 2-D numerical terms. The 2-D elastic code simulates crack propagation by a successive gradual "release" of nodes along the crack-path and applying a decaying "holding-back" force on the last node to be released. Two node release algorithms were used : a "propagation" and a "generation" mode. In the "propagation" mode, the nodes were released as the nodal forces reached a critical value (the crack was made to propagate according to a known value of G_D). In a "generation" mode the nodes were released according to crack history data and the G_D values were calculated from the global energy balance.

The propagation mode analysis predicted that for a constant G_D material, the magnitude of the remote load at glass-break should dictate the time of initiation and crack velocity. The lower the load, the longer it should take to initiate the crack which should propagate at a lower velocity. These predictions contradicted the experimental observation of constant crack velocities with no regard to the magnitude of the remote load or initiation time. Generation mode analysis of constant crack velocity data showed G_D values to vary according to initiation time : an early initiation resulted in lower initial value of G_D which increased as the crack propagated until it reached a higher level. Late initiation resulted in a higher initial G_D value which decreased until it reached a constant low level.

These results, indicating a non-unique crack resistance - crack velocity relation, are currently being checked by conducting additional experiments and by using an improved FE viscoelastic analysis.

Schematic view of the G-PE duplex sample
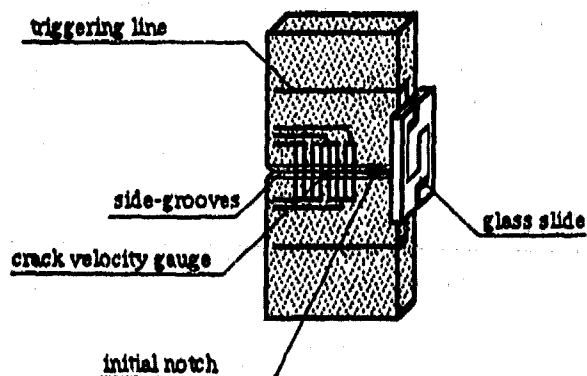
ADVANCED TESTING METHODS FOR ROTATING DISK IMPACT MACHINES

K Kussmaul, T Demler and A Klenk
Staatl. Materialpruefungsanstalt (MPA), University of
Stuttgart, Stuttgart 80, FRG

1. INTRODUCTION

Since the pioneering work of Mann resp. Manjoine and Nadai
rotating disk impact machines have essentially contributed to
the exploration of the behaviour of materials under dynamic
loading conditions, especially for strain rates between 10
1/s and 2000 1/s. Today's decreasing interest in the rotary
impact test technique is rather astonishing, as rotating disk
impact machines cover the upper range of strain rates which
are of relevance in civil applications and can be used for
tensile, compressive, bending and fracture mechanics tests.
The paper focuses on tensile and fracture mechanics tests.
Besides a standard machine (disk diameter 720 mm, maximum
rotational energy 600 kJ), MPA Stuttgart disposes of a high
energy machine with a disk diameter of 2000 mm and a maximum
rotational energy of 33 MJ at a circumferential velocity of
150 m/s. When the specified testing conditions are estab-
lished, the specimen is computer-controlled slewed into the
path of the claws by a fast acting pneumatic cylinder. The
lower bound of possible specimen dimensions is defined by the
bending stress resulting from the slewing motion. The upper
bound is established by the distance of the striking claws.
At the moment this is equivalent with a test section diameter
ranging from 6 to 20 mm for round bars and a thickness of 10
or 15 mm for compact tension (CT)-specimens.

2. TENSILE TESTS

Little attention is generally paid to the fact that an ideal
strain rate function $\dot{\varepsilon}$ = const. cannot be realized by
servohydraulic rigs or rotary impact machines. For the latter
the strain rate can only be controlled via two parameters:
- the circumferential velocity of the disk
- the load-deformation characteristic of the damper which is
  situated between claw and anvil in order to couple both via
  a semi-plastic impact.
This characteristic depends strongly on the geometry and the
material of the damper and defines at which time during the
deformation process the specified strain rate is reached and
to what extent disruptive oscillations resulting from the
acceleration of specimen and anvil are present at the load
measuring points. This represents an optimization problem, as
a long acceleration period is coupled with a reduction of the
oscillations. The formation of an upper and lower yield point
provokes a sudden increase of the strain rate exceeding the
specified value, whereas in the beginning strain hardening

[53]

range a rather constant strain rate can be found. Whilst the
elastic strain rate is dominated by the damper-character-
istic, the plastic strain rate is governed primarily by the
circumferential velocity of the disk. Materials with a
continuous transition into the plastic range, e.g. high
strength steels, do not exhibit these problems. On the other
hand, a strain rate in excess of 1000 1/s cannot be applied
to low toughness materials as fracture already initiates
during the acceleration stage.
Investigations of several fine-grained ferritic steels have
proven the applicability of the following test procedure. The
load applied is measured at the specimen itself, as load
cells or external dynamometers cannot provide reliable load-
time-graphs. Two dynamometer sections are instrumented with
two strain gages on opposite faces to compensate for bending
effects. The strain is measured via post-yield strain gages
which can be used up to a temperature of 300°C and provide
strains in excess of 20% if properly installed. In the strain
hardening range the strain can also be deduced from the
displacement of the anvil. For that purpose a bar code is
attached to one side of the anvil and a fast acting scanner
is installed.

3. FRACTURE MECHANICS APPLICATIONS

Besides double-edge notched tensile specimens CT-specimens
are suited to be tested in rotary impact machines in accor-
dance with ASTM E 399/813. This requires information about
the load and the load line displacement.
According to a proposal by Krabiell the load is measured via
strain gages which are attached in parallel to the crack path
on the top and bottom side of the specimen and which are
calibrated quasi-statically before the dynamic test. With
growing plastic deformation an increasing deviation from the
linear interdependence between the strain gage signal and the
load applied can be observed. These calibration curves can be
evaluated experimentally for static loading conditions only.
However, this is not useful, because in this case the
influence of the dynamic stress-strain-curve cannot be
modelled. Therefore the dynamic calibration curves are
calculated with the finite-element-code ABAQUS and dynamic
stress-strain-curves. The analyses made obvious that the
strain maximum is located perpendicular to the crack tip and
that other strain gage positions exhibit a linear relation
between load and strain gage output up to higher loads.
For the measurement of the crack opening displacement in the
load line clip gages or other conventional inductive or capa-
citive displacement gages cannot be used because of their low
natural frequency. Therefore the load line displacement is
measured via an opto-electronic sensor based on the scanner
principle. It offers the advantages of low additional mass,
high bandwith and low costs. According to a proposal by
Giovanola, strain gages are attached to the crack tip near
field for the detection of crack initiation. Test results on
fine-grained ferritic steels and ductile cast iron are
presented.

[54]

Automatic Analysis of Strain Rate Distribution by
High Speed Video Camera and Grid Method Using Fourier Transform

Y Morimoto, Y Seguchi and M Yamashita

Department of Mechanical Engineering, Faculty of Engineering Science,
Osaka University, Toyonaka, Osaka, 560 JAPAN

ABSTRACT: A high speed digital video camera is developed by using a
new MOS type solid state image sensor. The digital image taken by the
high speed video camera is analyzed by an image processing program on a
personal computer. In order to analyze strain rate distribution, a new
grid method using Fourier transform is developed. By using this
method, the displacement, velocity, strain and strain rate distri-
butions of an unloading wave propagating in a rubber tube are analyzed.

1. HIGH SPEED VIDEO CAMERA

A system of a high speed video camera is made with a new MOS type solid
state image sensor (Hitachi Ltd. HE98246, image size: 649x491 pixels). It
is possible to change the area size for output into any size using soft-
ware. As the selected area becomes smaller, the frame speed becomes
higher. The maximum frame speed is about 300,000 (ideal 10,000,000)
frames/sec. In this case, the frame size is only one pixel. The frame
speed or image size of this video camera is controlled by a personal
computer. The signal from the vertical output line is stored in IC
memories by using an A/D converter or stored on a video tape recorder. If
the image signal is sent to the same IC memories by cyclically rewriting,
the desired images are stored by sending a trigger after the occurrence of
the phenomenon.

2. PROGRAM OF IMAGE PROCESSING ON MICROCOMPUTER (PIMPOM)

In order to analyze the image taken by a video camera, a wide use program
on a personal computer (NEC Corp. PC-9801VX, CPU 80286) has been devel-
oped. The image size is 640x400 pixels with 16 (4 bits) of 4096 colors.
It is not necessary to use any special hardware for image processing. It
has a lot of menus such as region set, disk access, value transform, one
and two dimensional mask filtering, thinning, geometric transform, printer
output, process repeat, graphics, image input by an image scanner, Fourier
transform, Hadamard transform, histogram etc. The processing speed is
very high, because each menu is written by a machine language and these
menus are combined by a BASIC program. For example, mask and geometric
transform is processed in about 6 seconds, respectively. Value transform
is processed in about 3 seconds. This processing time is for the case
that the image size is 640x400 pixels. The processing time is in
proportion to the inverse of the area size.

3. STRAIN RATE ANALYSIS OF UNLOADING WAVE PROPAGATING IN RUBBER TUBE BY USING FOURIER TRANSFORM

This high speed video camera is applied to analysis of stress wave

1

[55]
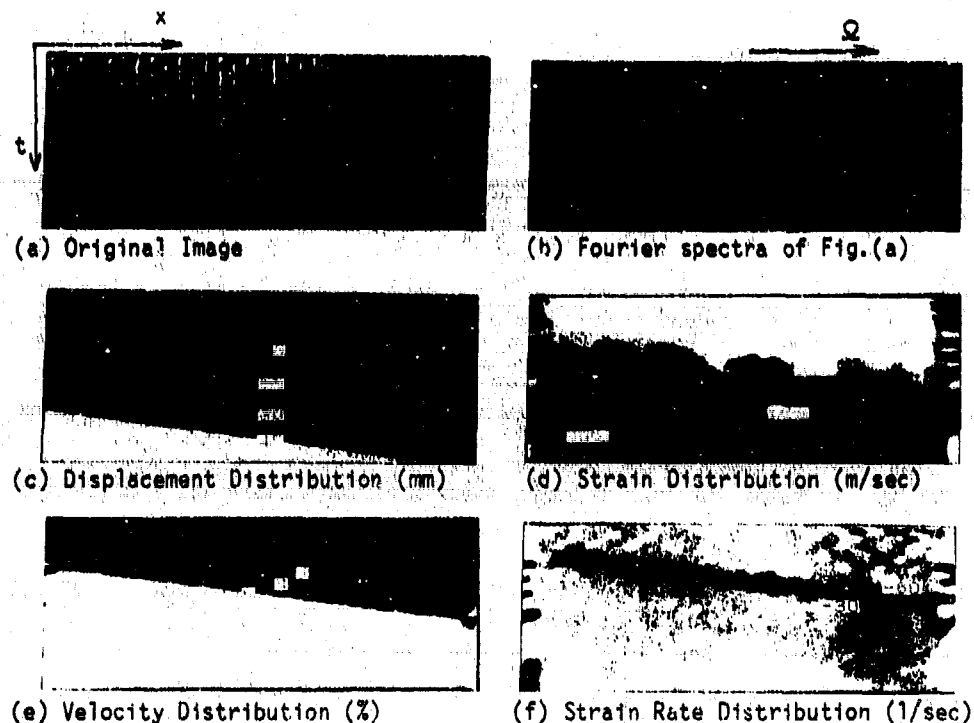
(a) Original Image

(b) Fourier spectra of Fig.(a)

(c) Displacement Distribution (mm)

(d) Strain Distribution (m/sec)

(e) Velocity Distribution (%)

(f) Strain Rate Distribution (1/sec)

Fig. 1 Analysis of Unloading Wave Propagation in Rubber Tube

propagation in a rubber tube. A grating is painted on the tube surface. When the rubber tube is stretched and cut, an unloading stress wave propagates in the tube. The one dimensional behavior of the unloading wave is imaged by the high speed video camera.

In order to analyze the displacement, strain, velocity and strain rate distributions of the tube, new moire and grid methods are developed by using the Fourier transform of the image of the deformed grating on a material. The basic procedures required in this analysis are as follows:
(1) Sampling of a deformed grating by a TV camera.(Fig. 1(a))
(2) Discrete Fourier transformation of the image.(Fig. 1(b))
(3) Extraction of the first harmonic of the spectra.
(4) Inverse discrete Fourier transformation of the first harmonic.
  (Generation of the complex grating pattern)
(5) Computation of arguments of the complex grating.
(6) Computation of displacement from the argument.(Fig. 1(c))
(7) Computation of strain by differentiating the displacement.(Fig. 1(d))
(8) Computation of velocity by differentiating the displacement(Fig. 1(e))
(9) Computation of strain rate distribution by differenciating the velocity.(Fig. 1(f))

The analysis is completely automated by digital image processing. All of the laborious and subjective procedures required in the conventional analysis such as fringe sign determination, fringe ordering and fringe interpolation are eliminated permitting objective, fast, and accurate analysis.

2

Biaxial Strain-Rate Controlled Viscoplastic Experiments on Cruciform
Specimens of AISI 316H up to 100/S

C. Albertini*, M. Mićunović** and M. Montagnani*

* CEC-JRC, Ispra Establishment, 21020 Ispra (Va) - Italy
**Svetozar Markovic University, Kragujevac - Yugoslavia

Predictions of classical and recently formulated generalized constitutive
models for metallic materials have been up to now scarcely compared with
the results of valid multiaxial experiments. We refer here to tension-
tension experiments and to their numerical simulation, realized at low and
medium strain-rate using a cruciform-specimen.
The experiments have been performed at an electromechanical biaxial
testing device with strain-rates range $[10^{-4}, 10^{-1}]s^{-1}$ as well as at a
hydropneumatic biaxial testing device with strain-rates range $[10^{-1},
10^2]s^{-1}$. A biaxial cruciform specimen has been used which was instrumented
by a photoetched fine grid with 400 cross-prints over the upper side of
the gauge field whose displacements have been recorded by perpendicular
filming during tests. From the bottom side at the centre of the gauge
field a thermocouple as well as a three-fold strain gauge rosette have
been fastened. A code used either total strain record from strain gauges
(up to 2%) or from grid measurement (from 2% up to rupture) as well as
temperature and force (i.e. stress) measurement in order to find all
components of plastic strain tensor and plastic strain rate tensor as
functions of time. As measure of directionality correctness the
experimental plastic strain rate direction in X_1, X_2 plane, i.e.:

$$tg\beta = \dot{E}_{p11}/\dot{E}_{p22}$$

has been compared with the values:

$$tg\beta_p = \frac{2T_{11}-T_{22}}{2T_{22}-T_{11}} \quad , \quad tg\beta_k = \frac{T_{11}-\nu T_{22}}{T_{22}-\nu T_{11}}$$

predicted by theories of Perzyna (with Mises yield function) and Cernocky-
Krempl, respectively, where $\dot{E}_p$ plastic strain rate tensor, T stress-
tensor, ν Poisson coefficient.
Owing to inevitable complexity of the cruciform specimen used in the
experiments a preliminary finite element stress-strain/strain-rate
analysis has been done for a number of proportional strain-rate controlled
paths using the computer code ABAQUS.
The finite elements calculations predicted a homogeneous strain
distribution over the constant thickness central part of the cruciform
specimen. These predictions, having a qualitative character due to the
rough approximation of the material models implemented in the code, have
been quantitatively confirmed by the experiments at low and medium strain
rate. The homogeneous strain distribution over the constant thickness
gauge section during the whole test already demonstrates that the applied
loading is uniformly distributed by the armfingers of the cruciform
specimen. A further direct verification of such feature has been obtained
by the strain measurements on the armfingers, which remain elastic, during
the test. The armfingers of the cruciform specimen distribute uniformly
the applied loading to the constant thickness central part of the
specimen. This fact and the homogeneous strain distribution over the
surface of the central part confirm that the constant thickness central

part of the cruciform specimen deforms in a homogeneous tensional plane stress state. Furthermore the experimental set-up permits the measurement of the components of stress and strain tensors along the principal directions. Therefore the conditions are satisfied for the correct use of an equivalence criterion for the evaluation of the material characteristics from biaxial experiments. The Huber-Mises equivalence criterion has been used for constructing the equivalent stress-strain curves which have been determined at low and medium strain-rate.
The equivalent flow curves at low strain-rate show strain hardening; the uniaxial and the equibiaxial flow curves are practically coincident up to large strain values while the equivalent flow curves corresponding to the other straining paths lies under the equibiaxial flow curves already at small strain values.
In the plane of the stress deviator, the initial yield stresses, determined both from temperature minimum and from 0.2% of equivalent plastic strain definition, practically lie on Mises circles.
Strain-rate hardening has been observed in case of equibiaxial straining at medium strain-rate.
Divergence has been observed between the straining directions determined from experiments and those predicted by some constitutive models.

Plastic Flow of a Ferritic Mild Steel and a High Strength Austenitic
Steel under Dynamic Biaxial Loading

K. Stiebler, H.-D. Kunze, E. Staskewitsch

Fraunhofer-Institut für angewandte Materialforschung, IFAM,
Lesumer Heerstr. 36, D-2820 Bremen 77, W. Germany

The increasing use of computers in the area of technical design and optimal
utilisation of materials require a better understanding of the material
behaviour at its specific loading types and in addition its mathematical
discription. Especially in the field of multiaxial loading under high rates
of deformation were only limited data available. To expand this data base
two testing rigs were designed and built to investigate materials under
these loading conditions.

With a hydraulic apparatus, thin-walled tubular specimen were simultaneous-
ly loaded by two normal stresses up to elastic strain rates in the range of
10^{-1} s^{-1}. The normal stresses were combinations of either tension/compres-
sion and internal/external pressure. Higher strain rates of 10^2 s^{-1} were
reached with a modified split Hopkinson bar which allowed simultaneous com-
bined tension and torsion stresses, to be achieved.

Both experimental set-ups were used for the quasistatic and dynamic inves-
tigation on Ck 35 ferritic mild steel. For this material, yielding is de-
fined by the lower yield point. Results of the tests with two normal stres-
ses in axial and circumferential directions show for both elastic strain
rates $\dot{\varepsilon}^e = 10^{-5}$ s^{-1} and $\dot{\varepsilon}^e = 10^{-1}$ s^{-1}, a very good agreement in the first
quadrant between the experimental yield points and the ellipses predicted
by the von Mises yield criterion, fig. 1. The results in the second quad-
rant differ somewhat from this criterion. Under combined tension and tor-
sion loading the yield points fulfill the Tresca yield criterion for both
the quasistatic ($\dot{\varepsilon}^e = 2 \cdot 10^{-5}$ s^{-1}) and the dynamic ($\dot{\varepsilon}^e = 3 \cdot 10^1$ s^{-1}) biaxial
tests, fig. 2. Consequently, the yield criterion changes with the nature
of load. The yield points of the dynamic tests showed higher stresses than
the quasistatic one.

The yield loci of the quasistatic and dynamic combined tension-torsion-
tests of an austenitic steel are described by ellipses which correspond to
different proof strain definitions of yielding, fig. 3. This figure shows,
that the size and the shape of the yield loci are functions of strain and
strain rate. For low plastic strains and plastic strain rates of
$\dot{\varepsilon}^p = 10^{-3}$ s^{-1} the yield points are in a good agreement with the von Mises
yield criterion. Whereas for large strain and strain rates ($\dot{\varepsilon}^p = 10^2$ s^{-1})
the yield loci tend towards the Tresca yield criterion.

The results of these investigations on the behaviour of materials were used in the calculations to allow realistic simulations. For the description of the quasistatic and dynamic tension-torsion behaviour of the austenitic steel, Perzyna's constitutive equation was choosen. It includes a yield criterion as a function of strain and strain rate and a function which incorporates the dependence of flow stress versus strain rate based on thermal activation. For specific measured strains and strain rates the solution of the constitutive equation results in the associated stresses. These calculated stresses are in a good agreement with the measured stresses for all uniaxial and biaxial tests.
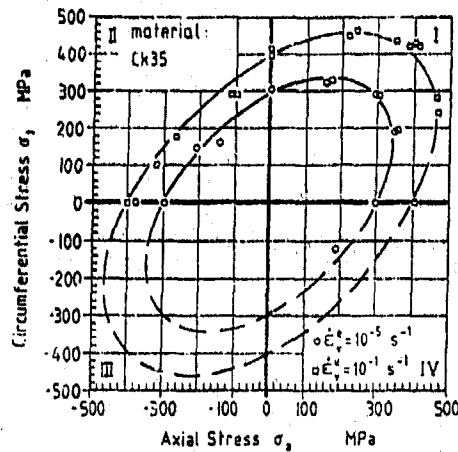

Fig. 1.
Yield loci for Ck 35 steel loaded by two direct stresses at two strain rates.
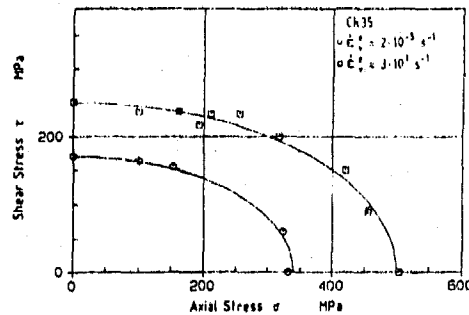

Fig. 2.
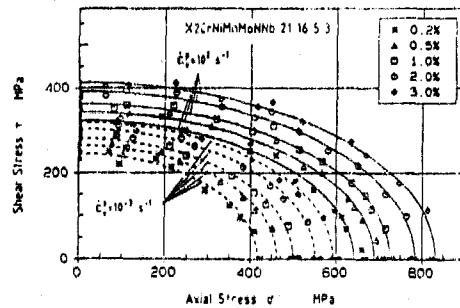Yield loci for Ck 35 steel loaded by tension-torsion at two strain rates.

Fig. 3
Yield loci of the quasistatic and dynamic combined tension-torsion-tests on austenitic steel corresponding to different proof strain definitions from $\varepsilon^p = 0.2\%$ to 0.3%.

The Use of Microscopically Based Constitutive Models in Explosive Metal
Deformation Modelling Studies

P Church
I Cullis

ABSTRACT

The numerical modelling of warheads and their terminal effects
requires an accurate description of material behaviour under the varying
load conditions associated with shock waves, and the resulting
hydrodynamic and plastic deformation. Their accuracy, however, is
limited by the constitutive relation and the ability of the equation
of state to predict the physical state variables associated with these
complex stress conditions.

There are 3 main mechanisms which affect the way a material deforms
under high strain rate explosive loading. These are work-hardening
effects, thermal softening effects and shock hardening. They are all
influenced by grain size, strain rate, phase changes, and impurity
concentrations. Ultimately, therefore, the constitutive model must
be able to describe dynamic path dependant plastic deformation over
a wide range of temperatures and material conditions.

Recent work by Follansbee on copper (1986) and Armstrong-Zerilli on
iron and copper (1986) has attempted to describe material behaviour
at high strain rate using dislocation mechanics. the Armstrong-Zerilli
model derives flow stress as a function of strain, temperature, strain
rate and grain size and distinguishes between face-centred cubic (eg
copper) and body centred cubic materials (eg iron). Account is also
taken of the influence of solute material and the original dislocation
density.

The Armstrong-Zerilli constitutve model has been in Explosively Formed
Projectile (EFP) calculations and compared with a semi-empirical
constitutive model, where high strain rate behaviour is described by
a semi-empirical work-hardening curve and a thermal softening curve.
Two EFP designs, using an Armco iron liner, based on different performance
military explosives (Octol and Composition B), have been modelled on
the DYNA2D hydrocode. The semi-empirical model and the Armstrong-
Zerilli model with the correct grain size ($25 \mu m$) give the same order
of agreement in terms of describing the experimentally observed EFP
projectile profiles. Changing the grain size to $120 \mu m$ gives better
agreement for the Armstrong-Zerilli model for both designs.

For the semi-empirical model the determination of the thermal behaviour
of the flow stress is restricted to a simple comparison with an experimental
profile. Since the EFP is crucially dependent on this thermal behaviour
of the flow stress, this represents a serious drawback if a predictive
capability is required. Therefore the semi-empirical model can only
be considered a first order material model.

The theoretical models do try and account directly for the complex material
mechanisms by dislocation mechanics, though at present no description
is provided for shock hardening, twinning or recrystallisation. The
results so far give encouragement in trying to describe the complex
internal mechanisms in EFPs. This is vital if one is trying to understand
the sensitivity of material properties in defining design envelopes.

In conclusion, therefore, the semi-empirical models are only   adequate
for first order effects (experimental profiles, velocities), whereas
the theoretical type models show great promise in also understanding
second order effects associated with the complex internal deformation
mechanisms in EFPs. More work is required in refining these theoretical
type models.

Analysis of the Strain-Rate Sensitivity at High Strain Rates in FCC and BCC Metals

Paul S. Follansbee

Los Alamos National Laboratory, Los Alamos, NM, 87545, USA

A constitutive formalism for deformation over a wide range of strain rates, temperatures, and strains has been applied to several pure fcc metals and to several fcc alloys. The formalism is based on the use of internal state variables and a phenomenological understanding of the kinetics of dislocation glide, dislocation storage, and dynamic recovery. In the mechanical threshold stress model, the applied stress (the yield stress) required for deformation in a given state is written as a combination of an athermal component, σ_a, and several thermally activated components as

$$(\sigma - \sigma_a)^r = \sum_{i}^{n} [s_i(\dot{\varepsilon},T) \ \hat{\sigma}_i]^r \ , \tag{1}$$

where $\hat{\sigma}_i$ gives the mechanical threshold stress that characterizes the interaction of dislocations with obstacle i, s_i specifies the kinetics of those interactions, n is the number of separate obstacle contributions, and r is a power that accounts for the interactions between different types of obstacles (1<r<2).

Experimental techniques have been established to measure the internal state variables and the activation energies that characterize dislocation/obstacle interactions. These techniques involve measurement of the temperature and strain-rate dependent yield stress in samples deformed according to various strain rate, strain, and temperature histories. Because we are mostly interested in the behavior at high strain rates, we restrict our yield stress measurements to room temperature and below.

In pure fcc metals, dislocation/dislocation interactions provide the only thermally activated contribution to the flow stress, in addition to the small grain boundary component, which is considered to be athermal. This simplifies the analysis in that n=1 and thus r=1 in Eq. (1). The study of fcc alloys introduces the complexity of n>1 in Eq. (1). In Ni-C alloys, for example, carbon goes to interstitial sites which yields a more rate-dependent strengthening contribution than found in pure fcc metals. In austenitic stainless steels the addition of interstitial atoms (e.g., C, N, O) and substitutional atoms (e.g., Cr, Ni, Al) leads to strongly rate-dependent deformation. Dislocation motion in a bcc lattice is opposed by a large Peierls barrier which leads to the strongly rate dependent yield stress observed in metals with this crystal structure. The generation and storage of dislocations through strain hardening then gives a second contribution to the flow stress in pure bcc metals. Thus, even pure bcc metals are complicated by n=2 in Eq. (1). The combined contribution of several strengthening mechanisms complicates the analysis. However, we

[63]

can begin by defining two classes: those contributions that evolve with strain and those that are present in the annealed condition and which are assumed to remain constant with strain. The former contribution is considered to be due to the stored dislocation density.

Strain hardening leads to an evolution of the state, through an increasing dislocation density. Evolution is treated differentially according to

$$\frac{d\hat{\sigma}}{d\epsilon} = \hat{\theta} = \theta_0(\dot{\epsilon})\left[1 - F\left[\hat{\sigma}_\epsilon/\hat{\sigma}_{\epsilon s}(\dot{\epsilon},T)\right]\right] \qquad (2)$$

where $\hat{\sigma}$ is the mechanical threshold stress that characterizes dislocation/dislocation interactions, $\hat{\sigma}_{\epsilon s}$ is the temperature and strain-rate dependent saturation value of $\hat{\sigma}_\epsilon$, and θ_0 is the Stage II hardening rate. The Stage II hardening rate had previously been considered to be a constant (of order $\mu/20$), but our work in copper (Follansbee and Kocks, 1988) led to the conclusion that when the strain rate is raised above $\approx 10^5$ s^{-1}, the Stage II hardening rate becomes strongly strain-rate dependent, which results in rapid hardening and high flow stresses. While the origin of the strain-rate dependence of θ_0 remains open, a contribution of this previous work is the observation that the behavior at high strain rates is dominated by this term, rather than by $s(\dot{\epsilon},T)$ in Eq. (1) or $\hat{\theta}_{s\epsilon}(\dot{\epsilon},T)$ in Eq. (2).

The rapid dislocation generation rates observed at high strain rates in copper and nickel may be a general phenomenon in fcc metals, although there is evidence in Nitronic 40 stainless steel that deformation twinning can offset this effect. Work in bcc metals is just beginning. Similar trends to those found in fcc metals are observed in iron and 4340 steel. In pure iron we observe that the rate of evolution is actually lower in a sample deformed dynamically than in a sample deformed slowly. Metallographic examination of these samples showed the presence of deformation twins in the former but not in the latter. The description of deformation twinning, particularly the associated kinetics, the influence on strain hardening, and the balance between deformation by twinning versus that by glide, represents a challenge for a complete deformation theory for the high strain rate regime.

REFERENCE

Follansbee, P S and Kocks U F 1988 Acta Metall 36 81

[64]

CONSTITUTIVE PROPERTIES OF COPPER AND TANTALUM
AT HIGH RATES OF TENSILE STRAIN: EXPANDING RING RESULTS*

W. H. Gourdin

University of California
Lawrence Livermore National Laboratory
Livermore, California, U.S.A.

ABSTRACT

The electromagnetic launch technique [1] has been used to study the properties of oxygen free electronic (OFE) grade copper and 99.9% tantalum rings expanded at peak strain rates of $10^4 s^{-1}$. During the free expansion phase, measurements of the ring deceleration using a velocity interferometer (VISAR) yield the flow stress, strain, and strain-rate histories. Specimen temperature is inferred from launch currents.

The results for OFE copper, processed to yield uniform grain sizes between 10 μm and 150-200 μm with minimal texture, show a sample-to-sample variation of ±20 MPa. Experiments with rolled material, for which the initial amount of cold working is uniform, indicate that approximately half of this uncertainty can be ascribed to sample-to-sample variations in the mechanical properties produced by non-uniformities in the working prior to final heat-treatment. The remainder apparently represents a limit imposed by the noise, electronic and physical, that is characteristic of measurements of the speed of the external surface of the specimen ring using the VISAR. Despite these uncertainties, however, the constitutive properties of the 10 μm and 150-200 μm materials are clearly distinguished. While the flow stress of 10 μm OFE copper increases from 280 MPa to 400 MPa for strains between 13% and 50% and strain-rates between about 8000 s^{-1} and 3000 s^{-1}, the stresses in 150-200 μm material fall 75-100 MPa lower in the same ranges of strain and strain-rate. These data agree well with Hopkinson bar data at smaller strains, confirming the apparent effect of grain size. Simple models in the literature [2,3] do not provide an adequate description of the ring data, and comparisons to more recent dislocation based models [4,5] are presented.

[61]

Tantalum specimens, because of their low electrical conductivity, must be launched with high conductivity "pusher" rings that are arrested after ring acceleration. Ring data show virtually no work hardening and limited ductility (30% natural strain to failure) for 99.9% tantalum having a grain size of approximately 100 μm. The constitutive properties obtained from ring tests are compared with the data and model of Hoge and Mukherjee [6].

1. W. H. Gourdin, submitted to Jour. Appl. Phys.; see also Proceedings of the Interational Conference on Impact Loading and Dynamic Behavior of Materials, Bremen, FRG, May, 1987.

2. D. J. Steinberg, S. G. Cochran, and M. Guinan, Jour. Appl. Phys. 51, 1498-1504 (1980).

3. G. R. Johnson and W. H. Cook, Proceedings of the 7th International Symposium on Ballistics, The Hague, Netherlands, April 1983, pp 1-7.

4. F. J. Zerilli and R. W. Armstrong, Jour. Appl. Phys. 61, 1816-1825 (1987).

5. P. S. Follansbee and U. F. Kocks, submitted to Acta Met..

6. K. G. Hoge and A. K. Mukherjee, J. Mat. Sci. 12, 1666-1672 (1977).

5494R
5/19/88

Strain rate dependence of mechanical behaviour and evaluation of the microstructure of tungsten monocrystals

L.W. Meyer, IFAM-Bremen, W.-Germany

and

C.Y. Chiem, ENSM-Nantes, Frances

Abstract

Tungsten monocrystals were compressed in $\langle 110 \rangle$-directions at three loading rates of $\dot{\varepsilon} = 10^{-4}$, 10^{0} and 10^{2} s^{-1} to investigate the strength, deformability, fracture mechanism and the micro-structure. The very early transition from elastic to plastic deformation behaviour is characteristic for the behaviour of tungsten single crystals. As a function of loading velocity this transition is reached between 20 and 100 MPa. Initially high deformation hardening is achieved up to 3 % deformation resulting in a flow stress of 1000 MPa. Increase in strength due to six orders of magnitude increase in strain rate results in a flow stress increase of about 300 MPa. With a compression strength of more than 1500 MPa at a strain rate of 10^{2} s^{-1} the level of flow stress is remarkable. This is similar to that of the sintered tungsten heavy metal alloys.

Transmission electron microscopy-discs parallel to the (011)-plane were taken in the mid of the specimen, compressed at 12 - 16 % reduction of height, to investigate the variation of the dis-location structure as a function of the strain rate. At $\dot{\varepsilon} = 10^{-4}$ s^{-1} the dislocation distribution in the (011) plane is very uniform with numerous nearly straight screw dislocations parallel to the $\langle 111 \rangle$ directions. With increased rate of strain to $\dot{\varepsilon} = 10^{0}$ s^{-1} in addition to the screw dislocations edge and mixed dislocations were observed. Also at this strain rate many of the dislocations were tangled. At $\dot{\varepsilon} = 10^{2}$ s^{-1} a cell structure is starting to form in the (011) plane, but the main orientation of the dislocations are still the $\langle 111 \rangle$ directions. Dislocation density increases with increasing strain rate. Comparing the increase of the flow stress (due to the strain rate) with the dislocation density change a logarithmic dependence is given.

. . .

[67]

In contrast to sintered tungsten alloys under dynamic loading, the monocrystals fail at 12 to 14 % reduction of height by shear failure. The shearing occurs in a planar area that is diagonal to the loading direction. It is from this orientation that the TEM specimen were taken. In the following loading, high stresses in the radial direction arise in the sheared, fractured segments. The monocrystal is not able to sustain these stresses and a cleavage crack network occurs parallel to the main crystallographic planes.

A Constitutive Description of the Deformation of Alpha Uranium Based on the Use of the Mechanical Threshold Stress as a State Variable

P. E. Armstrong, P. S. Follansbee, T. Zocco

Los Alamos National Laboratory, Los Alamos, New Mexico, 87545, USA

The deformation of isotropic, alpha uranium over a strain-rate range of 10^{-4} s^{-1} to 10^4 s^{-1}, a temperature range of 78K to 900K, and a strain range to 0.6 is modeled using a constitutive description based on the use of evolving internal state variables. The model is able to fit the experimental results and data from previous measurements, although it does not include a specific contribution from deformation twinning. The model assumes that for a given structure, the instantaneous yield stress is a function of the current temperature, T, strain rate $\dot{\varepsilon}$, and mechanical threshold stress, or

$$\frac{\sigma}{\mu} = \frac{\hat{\sigma}_a}{\mu} + \sum^{n} s_i(\dot{\varepsilon},T) \ \frac{\hat{\sigma}_i}{\mu} \qquad (1)$$

where μ is the temperature dependent polycrystalline shear modulus, $\hat{\sigma}_a$ is the mechanical threshold stress characterizing athermal dislocations interactions and $\hat{\sigma}_i$ is the mechanical threshold stress characterizing thermally activated interactions. The functions s_i describe the temperature and strain-rate dependencies of each of these thermally activated interactions. We have used the following form of the function s that has been applied to dislocation/obstacle interactions:

$$s = \left[1 - \left(\frac{kT}{g_o \mu b^3} \ln \ (\dot{\varepsilon}/\dot{\varepsilon}_o) \right)^{1/q} \right]^{1/p} \qquad (2)$$

where k is the Boltzmann constant (1.381×10^{-29} MNm/K), b is the Burgers vector, g_o is the total normalized activation energy, $\dot{\varepsilon}_o$ is a constant (typically 10^7 s$^{-1} < \dot{\varepsilon}_o < 10^{10}$ s^{-1}), and p and q are constants ($0<p<1$; $1<q<2$). To evaluate the increase in mechanical threshold stress with strain (strain hardening) we write

$$\theta = \frac{d\hat{\sigma}}{d\varepsilon} = \theta_o \left[1 - F \left(\frac{\hat{\sigma}}{\hat{\sigma}_s(T,\dot{\varepsilon})} \right) \right] \qquad (3)$$

where θ is the differential increase in the mechanical threshold stress, θ_o is the initial (or Stage II) strain-hardening rate, and $\hat{\sigma}_s$ is the saturation value of the mechanical threshold stress. The Stage II hardening rate is usually a constant, roughly equal to $\mu/20$. The Voce law is obeyed when $F=1$ in Eq. (3). Key to Eq. (3) is the concept of a saturation state, represented by $\hat{\sigma}_s$, which is the temperature and strain-rate dependent maximum threshold stress reached at large strains. Because the initial dislocation density was observed to be very low, we separate the mechanical threshold stress into three components,

[69]

$$\hat{\theta} = \hat{\theta}_a + \hat{\theta}_I + \hat{\theta}_\epsilon \quad , \tag{4}$$

where $\hat{\theta}_I$ is the initial value ($\hat{\theta}_I \approx 600$ MPa), presumably due to the Peierls barrier, and $\hat{\theta}_\epsilon$ is the contribution due to the dislocation density which is evolving. Equation (1) therefore becomes

$$\frac{\sigma}{\mu} = \frac{\hat{\theta}_a}{\mu} + s(\dot{\epsilon},T) \, [\hat{\theta}_I + \hat{\theta}_\epsilon] \quad , \tag{5}$$

where s is again given by Eq. (2). In Eq. (4) and (5) only the $\hat{\theta}_\epsilon$ term needs to be described using Eq. (3). An integrated form of Eq. (3) was used with the further assumption of Voce law behavior (F=1), giving

$$\epsilon = \frac{\hat{\theta}_{\epsilon s}}{\theta_o} \ln\left(\frac{\hat{\theta}_{\epsilon s}}{\hat{\theta}_{\epsilon s} \cdot \hat{\theta}_\epsilon}\right) \quad , \tag{6}$$

The temperature and strain-rate dependencies of $\hat{\theta}_{\epsilon s}$ and θ_o were described with an equation that had been used previously in fcc metals to describe the temperature and strain-rate dependency of $\hat{\theta}_{\epsilon s}$,

$$\ln (\hat{\theta}_{\epsilon s}) = \ln (\hat{\theta}_{so}) + \frac{kT}{A} \ln (\frac{\dot{\epsilon}}{\dot{\epsilon}_s}) \quad , \tag{7}$$

where $\dot{\epsilon}_s$, A and $\hat{\theta}_{so}$ are constants. This equation has a physical interpretation in describing $\hat{\theta}_{\epsilon s}$ but its application to θ_o, as in

$$\ln (\theta_o) = \ln (\theta_{os}) + \frac{kT}{B} \ln (\frac{\dot{\epsilon}}{\dot{\epsilon}_s}) \tag{8}$$

is purely empirical.

The parameters in the above equations were determined from a fit to 200 experimental results (yield stress as a function of temperature and strain rate on samples prestrained according to various strain-rate, strain, and temperature histories). Although the model can be made to agree with the experimental data, its physical basis in uranium, where twinning is an important deformation mechanism, is questioned.

Deformation microstructures are characterized using optical and transmission electron microscopy. The general observation is that deformation initially occurs primarily by deformation twinning, but that with increasing strain there is a transition to deformation primarily by slip. The effect of this transition on the proposed constitutive formulation is discussed and compared with the results of the analysis.

Localization Analysis under Dynamic Loading

Y. Leroy* and M. Ortiz

Brown University, Providence, RI 02912 USA.

A finite element method proposed by Ortiz et al. (1987) is used to study shear
band formation in rate independent and rate dependent pressure sensitive solids
under dynamic loading.

This new method is characterized by the addition to the strain interpolation of
an extra mode of deformation carrying a suitable strain discontinuity. This
added mode of deformation permits to alleviate the overly stiff response of
isoparametric elements observed in problems involving strain localization.

Results concerning localization criteria are first reviewed. These conditions are
pertinent to the set up of the added modes in the finite element method used here
as well as to the design of crossed triangular meshes.
For a rate independent solid, the analysis is based on the acoustic tensor defined
for Hill's comparison solid (1958). Localization is possible as soon as a wave
velocity is found to vanish along some direction which defines the normal to the
incipient discontinuity. The wave polarisation vector determines the mode of
localization. For rate dependent materials wave velocities always remain real.
Nevertheless, localization is observed for such material in the form of unstable
growth of, for example, shearing mode of deformation, Marchand and Duffy
(1987).
Using a linearized instability analysis, Molinari (1987), Leroy and Ortiz (1989)
have determined necessary conditions for the earliest possible localization
instabilities. The main outcome of such analysis is that the first possible
instabilities, i.e. those which grow infinitely slowly, can be recovered by
considering the inviscid limit of the constitutive model.

As a first example a single element problem is presented in order to motivate the
necessity of a specialized element when dealing with localization. Delay in the
localization process when rate sensivity of the solid is increased is also observed.
Next we turn our attention to the dynamic response of frictional solids. The
constitutive description adopted in the calculations is of the Drucker-Prager
type with a monotonic hardening law on the friction angle up to a saturation
level. The dilatancy angle is taken to be null throughout the analysis, rendering
the plastic response non-associative. We consider a rectangular sample of
material constrained to undergo plane strain compression. Velocities are
prescribed on its upper surface following a ramp variation in time. The final
impact velocity is of the order of 1/1000 of the elastic longitudinal wave speed.

*   Presently at Koninklijke/Shell Exploratie en Produktie Laboratorium, The
Netherlands.

Several tests are conducted for a rate independent model and a rate dependent model based on a linear overstress viscous law. These results are compared with the static and quasi-static analysis.

The most striking difference between the quasi-static and the dynamic solutions concern the geometry of the shear band. Whereas under quasi-static loading a single shear band emerges in each quarter of the specimen, a network of bands is seen to arise under dynamic loading. Shown in fig. 1 is the distribution of effective platic strain for the dynamic rate independent case. The introduction of rate sensivity has several effects on the solution. Substantial delay in the localization time is observed as well as a broadening of the shear band away from its nucleus.

A noteworthy outcome of these computations is the fact that the geometry of shear bands, both as regards their thickness and spatial distribution is quite sensitive to rate dependence and inertia effects. These results raise questions on the prospects for describing the thickness of shear band by means of a single parameter, a feature common to many non-local and generalized continuum theories.

References:

Hill R., 1958, J. Mech. Phys. Solids, 6, pp 236-249.
Leroy Y. and M. Ortiz, 1989, Int. J. Num. Anal. Meth. Geomech., in press.
Marchand A. and Duffy J, 1988, J. Mech. Phys. Solids, 36, pp 251-283.
Molinari A., 1987, Proc. Int. CNRS coll. on Non-linear Phenomena in Materials Sciences, Aussois.
Ortiz M., Leroy Y. and Needleman A., 1987, Comp. Meth. Appl. Engr., 61, pp 189-214.
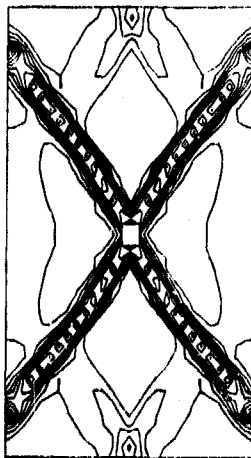
Fig. 1: distribution of effective plastic strain for the rate independent dynamic test.

Simulation of High Strain Rate Effects
With Micro-Computers

Dr. Steven Segletes
Dr. J. A. Zukas

Computational Mechanics Consultants, Inc.
8600 La Salle Road
Suite 614, Oxford Building
Towson, Maryland 21204

This paper describes the development and application of a computer program
for the study of materials response to short-duration loading, i.e.,
situations where wave motion in the material due to impact, explosive
loading or energy deposition must be accurately tracked.

Wave propagation codes were originally developed to solve problems charac-
terized by:

a. the presence of shock waves (alternatively, steep stress or velocity
gradients)

b. Localized materials response (i.e., situations where the overall geo-
metric configuration of a structure is of secondary importance compared to
the constitution and characteristics of the material in the vicinity of
the applied load)

c. loading and response times in the submillisecond regime.

Characteristics of computer codes to solve these problems have been dis-
cussed by Zukas (1982, 1987) among others. Excellent results have been
obtained with wave codes involving many different materials in engineering
designs with very complex shapes. Good accuracy has been achieved, in
comparison to exact solutions or with experimental results when the
materials involved are very well known and characterized. When this is
not done, when the codes are used as black boxes with engineering mat-
erials which are not well understood or characterized, it is not uncommon
to obtain qualitatively incorrect solutions, i.e., garbage in, garbage out.
The greatest limitations on accuracy in wave propagation calculations are
the material descriptions embodied in the constitutive equations, particu-
larly with material failure. Equally important is the requirement that
the material data (the various coefficients of the constitutive description)
must be appropriate to the characteristic time scale of the problem studied.

The ZeuS code is a 2-D explicit Lagrangian finite element code originally
designed to operate in the PC or MS-DOS environment. Because of its ex-
plicit integration scheme, it is best suited for high velocity impact
situations although nothing in the physics of the formulation inhibits its
use for low velocity impacts. As a general rule, though, problems which
fall into the structural dynamics category - situations where the response
is measured in a time frame of milliseconds to seconds and where both the
geometry of the structure as well as the material constitution must be
considered - are best addressed with codes employing implicit integration
schemes. A ZeuS simulation can model objects involving up to ten isotropic
inert and five explosive materials simultaneously. The expandable material
library maintained by the ZeuS interactive pre-processor permits material
characteristics to be stored for a virtually limitless number of materials.
Within the 640 kbyte environment of MS-DOS, ZeuS permits simulations in-
volving 2500 nodes and 4500 elements. The node and element state variables
are contained completely in RAM memory, thereby eliminating the need to
engage in time consuming, inefficient, disk-swapping of data. Pre- and
post-processing modules are a standard part of the ZeuS package, and make
the tasks of defining a simulation and graphically displaying results
straightforward. The post processor supports graphical display on the
standard IBM (and compatible) graphics adapters: the CGA, EGA and VGA.

The normalized speed of computation varies with several factors, including
the type of PC machine, the amount of contact processing required by the
simulation, and the size of the data bus anticipated by the compiled ZeuS
code (e.g., 8, 16, or 32 bit code). At the low end, a 4.77 MHz IBM-PC/XT
(8 bit code) runs at a normalized speed of processing inherent in the
computation. On the other hand, ZeuS, when compiled for 32 bit 80386
machines, and running at 20 MHz processor speeds, can achieve normalized
speeds under .003 sec/(cycle note). Such computational speeds for codes
of this variety are typically found only on mainframe computers. Addition-
ally, when employing the PC's 16 or 32 bit protected modes of operation,
RAM storage of state variables may exceed 640 kbytes, thereby allowing
simulations to be run which use much more than 2500 nodes and 4500 elements.

Results of calculations are presented for hypervelocity impact, perforation
of finite plates by long rod projectiles at ordnance velocities and Taylor
anvil impact situations. Good agreement is shown with experimental data,
where available.

[74]

Stability Conditions for Simple Shearing

A. S. Douglas
H. Tz. Chen and
R. Malek-Madani

Since few physical events lead to simple shearing with homogeneous fields, it is important to investigate the stability of shearing motions which are *inhomogeneous*. Experiments which examine shear localization using torsion of thin cylindrical specimens usually have thick sections adjacent to the thin test section in order to grip the specimen. These thick sections act as large thermal masses, causing significant heat transfer from the test section into the thicker section. This cooling of the edges prevents localization at the interface but it also ensures a nonuniform temperature field and (because of the nature of the material constitutive law) velocity field.

The problem considered here is that of the shearing of a thermo-viscoplastic material in which the effects of heat conduction and material inertia are included explicitly. Just as in experiments, the inhomogeneous fields arise because heat is conducted from the boundaries giving rise to a nonuniform thermal field, which dictates a non-uniform velocity distribution.

A perturbation method is used to examine the stability of the steady solutions to the governing equations. Since the resulting set of partial differential equations have spatially dependent coefficients, an integral method is used to establish criteria for the existence of steady solutions. Three different materials laws are examined and conditions for stable steady motions are obtained.

MICROSTRUCTURE TRANSFORMATIONS IN PURE POLYCRISTALLINE α-TITANIUM UNDER STATIC AND DYNAMIC LOADING.

S. LECLERCQ. C. NGUY. P. BENSUSSAN
ETABLISSEMENT TECHNIQUE CENTRAL DE L'ARMEMENT
16,BIS AVENUE PRIEUR DE LA COTE D'OR
94114 ARCUEIL CEDEX FRANCE

To understand the mechanism of deformation in metals of hexagonal crystal structure, compression tests have been performed at strain rates in the range from 10^{-4} to 10^{3} s^{-1} in commercially pure titanium annealed one hour at 700°C. Two deformation modes have been observed to be active: slip and twinning. The object of this study is to analyse the effect of strain rate and specimen orientation on slip and twinning occurence. Transmission electron and optical microscopy observations have been performed in order to establish a relationship between macroscopic and microscopic phenomena.

MECHANICAL PROPERTIES

The stress-strain curves are similar under static and dynamic conditions. Nevertheless, the flow stress required to obtain a given deformation is lower under static conditions than under dynamic ones.

The specimen orientation appears to have an influence on the mechanical properties under dynamic as well as static conditions. Compressions along ST and LT directions lead to the same flow stress; flow stress is lower when the loading axis is parallel to the L direction.

MICROSTRUCTURAL CHARACTERIZATION

The microstructural study reveals that twinning is an important deformation mode even at room temperature. Fraction of twinned grains increases with deformation and strain rate. The number of twins in a given grain increases also with strain rate.

Transmission electron microscopy allows to analyse the dislocation network. For both static and dynamic specimens, dislocations are arranged in bands. The mean distance between two walls is about 4 μm.

CONCLUSION

The flow stress increase with strain rate can be explained by a change in the mechanism which controls dislocations motion; twinning can also have an influence but its participation to the deformation is not yet well understood.

Active twinning or slip modes is not the same for all the specimen orientations. Easy glide are predicted to be predominantly prismatic in L specimens, basal and pyramidal in the LT and ST specimens. This can explain the different mechanical behaviour of the L specimens.

SEQUENCE OF THE DEVELOPMENT OF DEFORMATION STRUCTURE OF Al AND Cu SINGLE CRYSTALS UNDER 0.5 MBar and 1 MBar SHOCK LOADING

M.A.Mogilevsky, L.S.Bushnev
Lavrentyev Institute of Hyarodynamics
Siberian Division of the USSR Academy of Sciences
Novosibirsk 630090 USSR

1. The plastic deformation under shock loading may take place
at the compression front on exposure in the state of peak compressi-
on and unloading. Some peculiarities of shock deformation were reve-
aled earlier |1| by examining the twinning structure (compression and
unloading systems, sequential activation of different systems, a full
time of compression at the front). The dislocation structure develop-
ment has not been investigated systematically.

2. The shock loading of single crystals of Cu under 1 MBar and
Al under 0.1 to 0.5 MBar at 77° with a 1 to 2 % residual deformation
has been realized.

3. As far as the dislocation density is concerned, the well-
known results on oscillographic shock front width in Al under 40 GPa
and in Cu under 100 GPa |2|, being about 1 to 3 ns, allowed estimating
the density of moving dislocations at the front. It is in a signifi-
cant excess of a full density of dislocations in the recovered speci-
mens, that is indicative of the pronounced rearrangement of the struc-
ture.

4. The polygonal structure formation in Al at the final compres-
sion stage and during exposure is attended with dislocation reactions
and decrease in dislocation density. The role of interaction between
dislocations of different systems is also confirmed by the analysis
of the dislocation structure of Cu under 5 GPa and by a computer si-
mulation of the behaviour of the crystalline lattice under a high
one-dimensional deformation |3|.

5. In the shock-loaded Al and Cu, there were revealed specific
defects, such as long (up to hundreds of microns) strips of defor-
mation formed during rarefaction, where an intense deformation was
attended with disorientation). A lower microhardness of Cu in the strip
and lower dislocation density make it possible to interpret them as
adiabatic shears, which were not previously observed in copper.

|1| Mogilevsky M.A. , Physics Reports,1983, v.97, No. 6, 357.
|2| Chhabildas L.C., Asay J.R., J.Appl.Phys., 1979, v.50,, p.2749.
|3| Mogilevsky M.A.,In: Proc. Int. Conf. on Impact Loading and Dynamic
Behaviour of Materials, Bremen, 1987.

MECHANISMS OF DISLOCATION MOTION IN 7075-T73 ALUMINIUM ALLOY AT STRAIN RATES AROUND 10^5s^{-1}.

C G BURSTOW, M C LOVELL AND A L RODGERS

The Royal Military College of Science (Cranfield), Shrivenham, SWINDON, Wiltshire, England.

The testing of aluminium alloys at strain rates below 10^3s^{-1} has led to the consensus that the dominant deformation mechanism is thermal activation of dislocation movement. While at higher strain rates there is some indication of viscous drag effects. Our results on 7075-T73 do not fit this picture.

Results for this alloy at strain rates around 10^4s^{-1} were reported by us at Bremen in May 1987. These were obtained using a Direct Impact Hopkinson Bar (DIHB). The DIHB is however limited at high strain rates by its time resolution of about 1μs. To extend our results to higher strain rates we have constructed a Plate Impact Facility (PIF). Using a compressed gas gun and quartz piezoelectric stress transducers a time resolution of 12ns has been achieved.

To obtain as much information as possible from each shot the following arrangement is used. A loading plate strikes a specimen of the aluminium with a quartz gauge mounted on its rear surface. The stress wave, induced by the impact, is measured by the gauge after a single transit across the specimen. The separation of the elastic and plastic wavefronts during this transit allows the Hugoniot Elastic Limited (HEL) to be observed.

Measurements of the HEL for 7075-T73 have been made over the strain rate range 6.6 x 10^4s^{-1} to 4.9 x 10^5s^{-1} at ambient temperature. The results correlate closely with our earlier DIHB data and continue to show no significant strain rate dependence. It is concluded that for strain rates up to 5 x 10^5s^{-1} and temperatures of 20°C or above the limiting factor controlling dislocation motion is not thermal activation but the athermal back stress.

EFFECTS OF GRAIN SIZE AND STRAIN RATE
ON THE MECHANICAL RESPONSE OF COPPER

David H. Lassila
University of California
Lawrence Livermore National Laboratory
Livermore, CA 94550

ABSTRACT

The flow stress of copper is known to increase with decrease in grain size and this behavior can be described reasonably well by the Hall-Petch expression;

$$\sigma(\varepsilon) = \sigma_0(\varepsilon) + k(\varepsilon)d^{-1/2} \tag{1}$$

where $\sigma(\varepsilon)$ is the tensile flow stress, $\sigma_0(\varepsilon)$ is a constant (sometimes referred to as frictional stress), $k(\varepsilon)$ is the Hall-Petch constant, and d is the average grain diameter. The Hall-Petch relationship is empirical, however, some authors have suggested various mechanisms to explain the dependence of the constants on material chemistry and microstructure as well as loading conditions. Thus far all work in this area has indicated that the constant $k(\varepsilon)$ should be, as a first order approximation, independent of deformation rate.

In this study the effects of grain size and deformation rate on the flow stress of OFE copper were examined. Testing was performed in compression at ambient conditions at strain rates from 10^{-3} s^{-1} to 5×10^3 s^{-1}. Testing at different strain rates allowed the dependence of the Hall-Petch parameters on strain rate to be examined. The effect of various crystolographic textures on mechanical behavior was also examined. The findings of the study are as follows:

•   Decrease in the grain size caused an increase in flow stress. The observed dependence of flow stress on grain size was found to be consistent with the Hall-Petch relationship. The Hall-Petch Parameter $k(\varepsilon)$ was found to be independent of strain up to a strain level of 20%.

•   Results of the study suggest that strain rate does not have an influence on the proportional relationship between flow stress and grain size, i.e., the Hall-Petch parameter $k(\varepsilon)$ is not strain rate dependent.

•   Crystallographic texture had no discernable effect on stress-strain response.

Effects of Grain Size and Temperature on the Mechanical Properties of OFHC Copper

D J Parry and A G Walker

Department of Physics, Loughborough University of Technology, Loughborough, Leicestershire, LE11 3TU. UK

Abstract: A comprehensive investigation has been undertaken of the dynamic mechanical properties of OFHC copper over a strain rate range of about $2 \times 10^{-3}s^{-1}$ to $6 \times 10^3 s^{-1}$ with testing temperatures of 20°C to 600°C and grain sizes from 20μm to 240μm. The low strain rate region was studied using an Instron screw machine, while at the higher rates compressive (to $6 \times 10^3 s^{-1}$) and tensile (to $1.5 \times 10^3 s^{-1}$) split Hopkinson pressure bar systems were employed.

The results can be divided into two distinct regions according to the strain rate. For rates below about $10^3 s^{-1}$ the flow stress increases slowly with strain rate in a manner consistent with a thermally activated mechanism. The strain-rate sensitivity $\lambda = \partial\sigma/\partial\log\dot{\varepsilon}$ (at constant strain) is found to be independent of strain rate and grain size but increases with strain and temperature. There is a progressive reduction in the flow stress with increasing grain size and temperature, until at 600°C the differences in flow stress for all the grain sizes becomes insignificant.

At strain rates in excess of approximately $10^3 s^{-1}$ the flow stress increases much more rapidly with strain rate for all grain sizes and temperatures. The room temperature results are in agreement with a linear viscous-drag type of relationship. At elevated temperatures there are insufficient results to allow any difinite conclusions to be made regarding the form of the strain rate dependence.

The validity of the Hall-Petch relationship has also been investigated by plotting flow stress as a function of the reciprocal of the square root of the grain diameter for five grains sizes over the wide range of strain rate and temperature indicated above. The linear dependence predicted by the relationship was found to be valid for most combinations of strain-rate and temperature. However, at 20°C and the low strain rate of $2 \times 10^{-3}s^{-1}$, the results show evidence of a bilinear relationship for strain above 1%, with a transition grain size of 32μm.

[81]

Dynamic Fracture of Ceramics and Ceramic Composites

J. Duffy and S. Suresh
Division of Engineering, Brown University, Providence, RI 02912, U.S.A.

The potential advantages of ceramic matrix composites (CMC) are well-known; CMC's, for instance, are the only material of reasonable cost able to withstand very high temperatures. Their great disadvantage at present is their brittleness. Tests must be devised to evaluate their fracture behavior when subjected to impact loading. Our results indicate that this is feasible if the specimen is first properly fatigue-precracked and carefully loaded.

Experiments are described in which stress-wave loading is employed to fracture a notched CMC specimen with a prefatigued crack at the root of the notch. Tests are performed both in Mode I and Mode III, with specimens of a fine polycrystalline Al_2O_3 and with an Al_2O_3 containing $25^v/o$ SiC whiskers. Quasi-static tests are also performed and we are thus able to measure the fracture toughness values both statically and under truly dynamic conditions and for two fracture modes. The critical advance comes in specimen preparation: our development of techniques making possible the growth of fatigue cracks in CMC's by cyclic compressive loading. In the dynamic fracture test, the stress wave is initiated explosively. The geometry and loading insure plane strain conditions at the crack tip. A full finite element analysis is available confirming the accuracy of results. Values of K_{Id} can be calculated. In addition, the experimental method has been adapted to dynamic Mode III fracture. The present experimental results for Al_2O_3 reveal that the fracture initiation toughness values are about 50% higher under dynamic loading in Mode I than quasi-statically. The corresponding ratio is 30% for Mode III. In Al_2O_3 · SiC_w, these ratios decrease to about 30% in Mode I and only about 5% in Mode III. Scanning electron microscopy reveals that Mode I fracture initiation occurs predominantly by an intergranular failure mode irrespective of whether the loading is quasi-static or dynamic. Dynamically, however, there is evidence of a relatively greater percentage of transgranular failure. In distinct contrast with the macroscopically flat fracture surfaces observed under tensile loading, a highly tortuous and rough fracture surface was observed for Mode III fracture in both the quasi-static and dynamic tests.

Microcracks running dynamically in a brittle solid influence both the elastic moduli and strength. If such a material contains a population of microcracks, the velocity of the microcracks and the conditions for microcrack coalescence in front of the macro-crack tip will determine the measured values of tensile fracture toughness. A model is proposed which determines an estimate of the stiffness loss caused by a dilute population of microcracks aligned in a direction normal to the far-field tensile stress axis. This solution is then used to calculate the stiffness loss in brittle polycrystalline solids. The dynamic to static fracture toughness ratio is predicted as a function of microcrack velocity and elastic properties. Experimentally measured values of dynamic to static fracture toughness ratio in Al_2O_3 and Al_2O_3 with SiC_w fall within the bounds predicted by the analysis.

Structure - Property Characterization of a Shock-Loaded Boron Carbide-Aluminum Cermet

W.R. Blumenthal and G.T. Gray III

Materials Science And Technology Division, Los Alamos National Laboratory, Los Alamos, New Mexico 87545 USA

ABSTRACT

The propagation of shock waves through metals and alloys is known to induce metallurgical changes such as the formation of dislocations, deformation twins, point defects, and phase transformation products in the microstructure. Consequently, the mechanical properties of metals and alloys (i.e. hardness and yield strength) are highly dependent on their shock histories, in particular, the shock pressure and shock duration. Under quasi-static compression loading most ceramics and cermets initially respond elastically and subsequently fail at a critical stress with little or no macroscopic yielding. The mechanical response is controlled by the elastic properties of the material followed by the intervention of one or more microstructural flaws. Microstructural studies on shock-recovered minerals (quartz, anorthite, and periclase) have revealed planar features, "shock lamallae", implying inhomogeneous local plastic flow above the Hugoniot elastic limit (HEL) as suggested by Grady (1977). Also grain boundary flaws and microcracks can lead to fragmentation of poly-crystalline ceramics at compressive shock pressures below the HEL. Hence, the development of high fracture toughness cermets is of interest since fragmentation is a serious limitation to impact performance.

Shock-recovery experiments on a 65 vol% boron carbide-35 vol% aluminum cermet supplied by the University of Washington were performed as a function of shock pressure. The purpose was to: a) develop shock-recovery techniques for cermets and ceramics which reduce the destruction of the microstructure by accompanying tensile stress waves enabling intact recovery of the shock-loaded samples and b) investigate changes in the microstructure and mechanical properties of a high fracture toughness aluminum-boron carbide cermet as a function of peak shock pressure. The investigation also compares quasi-static and dynamic (Hopkinson Bar) uniaxial compression results. The objective in this case was to determine the effect of moderate strain rate loading on the mechanical properties (modulus and compressive strength) and failure behavior of the cermet.

The material was made by infiltrating pure liquid aluminum into a pre-sintered porous boron carbide skeleton resulting in a finely inter-connected microstructure with an average B_4C phase size of 7 microns and a porosity level below 1.5%. TEM characterization of the as-received material revealed the substructure of the cermet to consist of pre-dominantly defect-free B_4C grains interspersed with the aluminum regions.

[83]

Shock-loading experiments were performed on the cermet as a function of shock pressure. Samples were recovered largely intact due to the use of confinement and "soft-recovery" techniques (Gray 1988). Post-shock examination by optical and transmission electron microscopy (TEM) showed the B_4C structure to be unchanged up to 5 GPa, while the Al phase exhibited a high density of randomly distributed dislocations. After a shock of 10.6 GPa some of the B_4C grains displayed dislocation debris, but the majority showed no evidence of plastic deformation. Uniaxial compression testing of the unshocked cermet was performed at two nominal strain rates, 10^{-3} s^{-1} and 10^3 s^{-1} (Figure 1). Dynamically, the material showed limited yielding after about 1.5% elastic strain and subsequently accumulated about 1% inelastic strain (2.5% total strain) prior to failure. Quasi-statically, the cermet began yielding at about 1% strain and only accumulated between 0.5%-0.9% inelastic strain (1.5%-1.9% total strain) prior to failure. The unshocked cermet showed a 9%-24% increase in strength when the strain rate was increased from 10^{-3} s^{-1} (1.94 GPa) to 10^3 s^{-1} (from 2.1 GPa to 2.4 GPa) .

In summary: 1) momentum trapping, confinement, and "soft" arrest techniques are critical to successful shock recovery and subsequent microstructural analysis. 2) The predominant response of the cermet to both the 5 and 10.6 GPa shocks is elastic, although the aluminum phase behaved plastically. 3) No localized damage was observed at shock pressures of either 5 GPa or 10.6 GPa. 4) Inelastic deformation and strength improve with strain rate under uniaxial compressive loading.

REFERENCES

Grady D E 1977 *High Pressure Research* ed M H Manghnani and S Akimoto (New York: Academic Press) pp 389-435
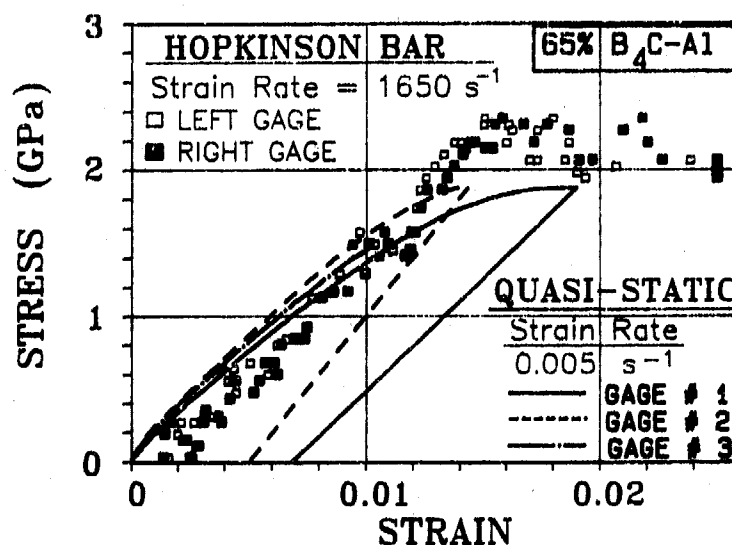Gray G T III, Follansbee P S, and Frantz C E 1988 *Mat. Sci. & Engin.* in press

Figure 1: Stress-strain plot for both quasi-static and Hopkinson bar compression loading of a 65% B_4C - Al cermet.

Impact Strength of Ceramics at High Temperatures

T. Nojima and K. Ogawa

Department of Aeronautical Engineering, Kyoto University, Kyoto, 606 Japan

Introduction

This report aims to present an outlook of mechanical properties of some engi-
neering ceramics under slow impact load and their testing methods.   Three
kinds of popular ceramics (alumina, SiC and TTZ) are chosen for characteri-
zation of impact properties up to 1200°C.   Conventional low rate tests were
also performed to assess the rate effect.   The present work consists of (1)
the strength-data are characterized at RT through three point bend, Brazilian
and tensile tests.   The bending strength σ_b is assessed and compared with
tensile data by the use of Weibull's failure probability theory.   Brazilian
test data are also compared with these data and (2) high temperature strength
of these ceramics is characterized by three point bend tests.   Character-
istics of fracture pattern are also reported in conjunction with deformation
rate and temperature.

Specimen

Tested ceramics are 99.5% purity alumina, 95% purity SiC and TTZ (transforma-
tion toughened ZrO_2).   Bend specimens are 5x5mm square cross-sectional bar
(span length is 25.4~25.8).   Brazilian specimens are $10^\phi \times 5t$.   Tensile
specimens of alumina are $3.2^\psi \times 30$mm.

Experimental Method and Data

Three kinds of Hopkinson bar type impact tests were carried out; three point
bend test (Figure 1), Brazilian test (Figure 2) and tensile test (Figure 3).
The strength-data through these tests are shown in Table I and Figure 4.
The ratio between three point bend and tensile strength at RT, σ_b/σ_t, is 1.6
for impact test and 2.0 in low rate test.   On the other hand, the strength
ratio through Weibull failure probability theory is 1.68~1.75 for the modu-
lus $m=9\sim10$ (the m-value is from bending data in low rate tests at RT.)
(σ_t; the tensile strength in tensile test, $(\sigma_t)_B$; the tensile strength by
Brazilian test.)
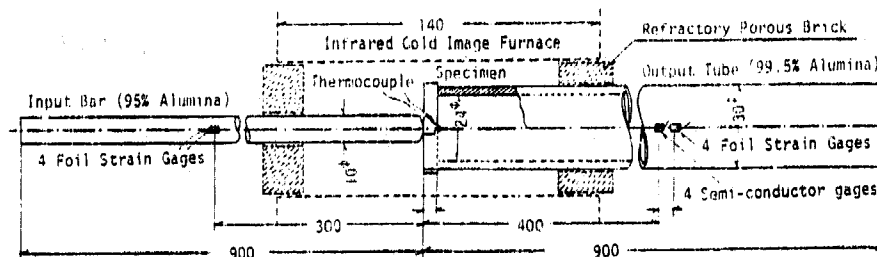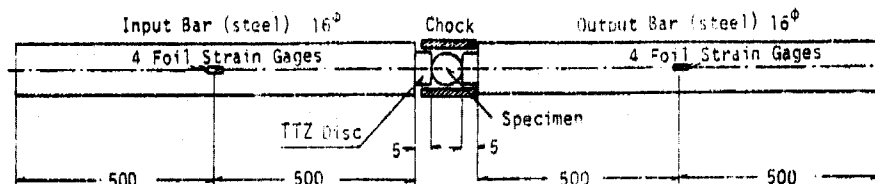

Figure 1   Experimental set-up of bend test

Figure 2   Experimental set-up of Brazilian test

Bend test

$$\sigma_b = \frac{(P_m l_B/4)}{(H^2 \cdot W/6)}$$

Brazilian test

$$(\sigma_t)_B = \frac{2P_m}{(\pi D t)}$$

$H=W=5\text{mm}$

l_B; span length

P_m; maximum load

D; diameter

t; thickness

Weibull theory

$$\frac{\sigma_b}{\sigma_t} = \left\{ \frac{V_t}{V_b} \cdot 2(m+1)^2 \right\}^{\frac{1}{m}}$$
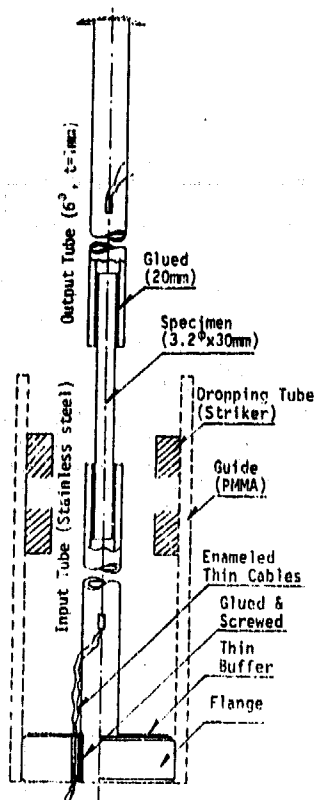
V_b, V_t; effective volume $(\sigma>0)$

Figure 3 Set-up of tensile test

Table I Strength-data (average value)

Bend test (RT~1200°C)

	Temp.	Impact test	Low rate test
Alumina	RT	σ_b=408MPa	σ_b=308MPa
	800C	‑‑	291
	1000C	361	310
	1200C	329	236
SiC	RT	σ_b=383MPa	σ_b=413MPa
	800C	416	445
	1200C	403	440
TTZ	RT	σ_b=1304MPa	σ_b=1053MPa
	500C	‑‑	873
	800C	962	687
	1200C	435	434

Brazilian test

		Impact test	Low rate test
Alumina	RT	$(\sigma_t)_B$=199MPa	$(\sigma_t)_B$=143MPa
SiC		188	196
TTZ		351	292

Tensile test

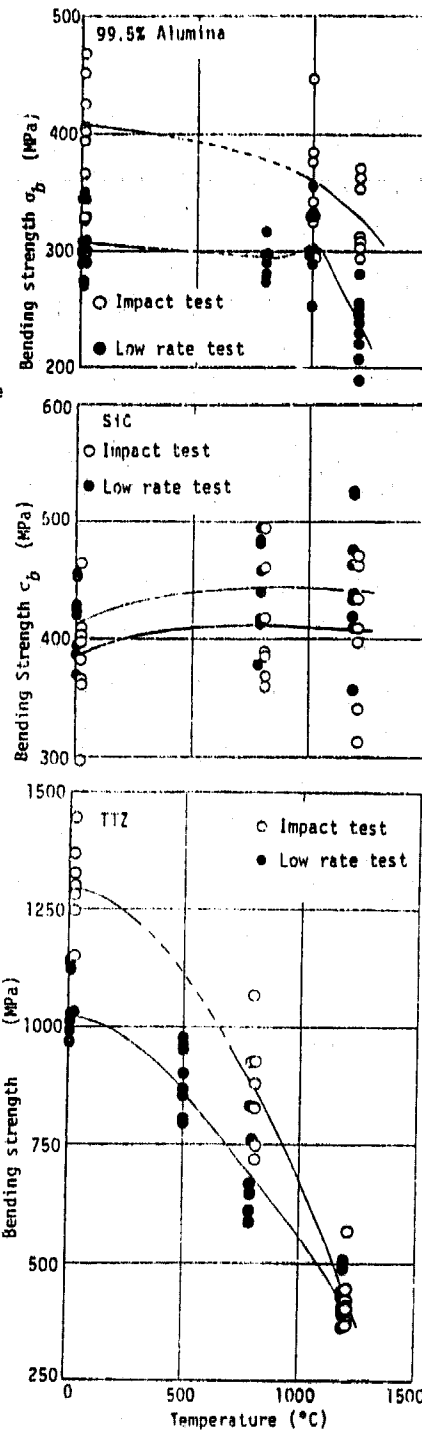|		Impact test	Low rate test
Alumina	RT	σ_t=258MPa	σ_t=151MPa

Figure 4 Temperature dependence of bending stress

[82]

ON THE DYNAMIC SHEAR STRENGTH OF SHOCK LOADED TWO PHASE CERAMICS

Y. Yeshurun, Z. Rosenberg, D.G. Brandon*
RAFAEL A.D.A. P.O.Box 2250, Haifa 31021, Israel
*Dept. of Materials Engineering, Technion, Haifa 3200, ISRAEL

ABSTRACT

The dynamic properties of monolithic ceramics are usually altered by the presence of a second phase. Impedance mismatch is the primary factor responsible for microstructural damage in the region of the phase boundaries. Planar shock recovery experiments have shown that microcracks in the alumina/glass interface are generally initiated at a stress level below the observeved Hugoniot Elastic Limit (HEL).

It turns that the spall strength decreases with increasing of the impact pressure. These studies also showed that the onset of the loss of spall strength is almost the same as the microcracks initiation stress level. This indicates that spall strength is associated with microstructural damage in two phase ceramics.

In this paper we also calculate the threshold shear stress at which microcracks are initiated using simple arguments relating to the different shock properties of the two phases. Thus we assume that the mismatch in particle velocity between the two phases is the cause to the interfacial shear stresses at the phase boundaries. From our calculation we conclude that the shear threshold stress for microcracks formation depends on grain size, the Hugoniot mismatch and the impact pressure. These calculations are also in good agreement with the average shear stresses in the shocked specimen as determined with longitudinal and Transvers Manganin gauges.

BALLISTIC IMPACT OF CERAMICS
J.E.Field, Q.Sun*, D.Townsend**

University of Cambridge, Department of Physics,
Cavendish Laboratory, Madingley Road,
Cambridge, CB3 OHE, U.K.

* Permanent Address: The Institute of Mechanics,
Chinese Academy of Science, Beijing, China.
** Now at British Aerospace, Filton, Bristol, U.K.

In recent years, there has been a growing interest in the response of ceramics to ballistic impact. This paper describes a study of the impact behaviour of a range of ceramics when impacted by steel spheres. High speed photography with a Hadland 790 IMACON camera was used to observe the modes of failure of the ceramics, damage to the projectile and to obtain quantitative data on the kinetics of impact. The projectiles were accelerated by a single stage gas gun of the double-diaphragm type. The velocity range covered was 30 to 1000m s^{-1}.

A large number of ceramic types and projectile materials have been investigated. It is only possible to present a few examples in the paper and Table 1 gives information on their relevant physical properties. The projectiles were 5mm diameter hardened steel spheres in all cases except where stated. The ceramics were in the form of 50mm x 50mm tile specimens with thicknesses in the range 3 to 20mm.

Table 1. Material properties of target and projectile materials

Material	Density $\rho/10^3$kg m^{-3}	Hardness H_v/GPA	Fracture Toughness K_{Ic}/MN m$^{-3/2}$	Shear Modulus G/GPa	Bulk Modulus K/GPa	Young Modulus E/GPa	Poissons Ratio υ
Soda-lime glass	2.50	4.5 ± 0.4	0.75 ± 0.03	27.6 ± 0.8	42.5 ± 2.7	79.2 ± 3.0	0.19 ±0.02
Glass ceramic A	2.47	9.2 ± 0.5	1.77 ± 0.12	34.8 ± 0.9	45.5 ± 3.4	83.3 ± 4.0	0.20 ± 0.03
Glass ceramic B	2.59	8.2 ± 1.1	0.42 ± 0.05	34.3 ± 0.9	59.0 ± 2.6	92.0 ± 4.0	0.24 ± 0.01
Alumina	3.69	11.9± 1.6	2.99 ± 0.17	108 ± 4	147 ± 10	260 ± 10	0.21 ± 0.03
Hardened steel	7.80	10.0± 0.5		77.4	163.7	201	0.30

(a) Impacts on alumina

In this case, the hardness of the target is greater than that of the projectile (see Table 1). For impact velocities up to ~180m s^{-1} the sphere rebounds from the target. The high pressures generated, due to the high hardness of the alumina, result in extensive plastic deformation of the projectile and the formation of a flat. If the impact velocity is increased, fracture of the projectile occurs.

The impact of a hardened steel sphere on an alumina tile specimen produces a Hertzian-type cone failure over the velocity range investigated (50 to 900m s^{-1}). For impact velocities greater than ~220m s^{-1}, the cone crack propagates completely through an 8.6mm thick specimen resulting in a conical fragment. The semi-apex angle of the cone, θ, is less than that obtained by static loading. As the velocity of impact increases, θ increases reaching a value of ~57^0 at the highest velocities. The cone has a smooth upper region and a lower roughened region. The roughened region is caused by the interaction of the propagating

cone crack with the reflected tensile wave from the rear face of the specimen. The change of angle for the lower part of the cone can also be explained by considering the stress wave interaction.

(b) Impacts on glass ceramic type A

In this case, the hardness of the target is less than that of the projectile (see Table 1), and very little damage of the sphere results even at the highest velocities. Impacts of ~40m s^{-1} generated Hertzian-type ring cracks in this material. Above 55m s^{-1}, the cone cracks reach the rear of 10mm thick specimens producing a conical fragment. As the velocity of impact increases the semi-apex angle, θ, decreases. Lateral cracks produced from the deformed zone at the impact site form at impact velocities greater than 80m s^{-1}. Spall failure was evident in this glass ceramic, for 10mm thick specimens, at velocities above ~120m s^{-1}. At impact velocities >300m s^{-1}, a second cone crack was formed in the material with a much larger semi-apex angle than the initial cone crack. The radial cracks which are formed by bending are evident at velocities above ~60m s^{-1}. The number of radial cracks increases with impact velocity. Penetration of 10mm thick specimens takes place at velocities above ~450m s^{-1}.

(c) Impacts on soda-lime glass

The damage modes with soda-lime glass are similar to those in the glass ceramic though they take place at lower velocities. For example, the Hertzian cone crack ejects at velocities above ~30m s^{-1}. The hardness of soda-lime glass is much less than that of hardened steel (see Table 1) and negligible damage is suffered by the projectile. At high velocities, failure modes such as the Hertzian cone, lateral and median cracking and (with thin plates) radial fracture which can all be obtained by quasi-static loading are increasingly dominated by stress wave controlled fracture.

(d) Discussion

The relative hardnesses of projectile and specimen are of great importance. In the one category, are soda-lime glass and the glass ceramics with lower hardnesses than that of the projectile and which do not deform the projectile. In the second category, are aluminas, boron carbide etc... with higher hardnesses. They deform, break up and eventually shatter the hardened steel projectile. This different behaviour has a great affect on the energetics of impact. The toughnesses of the materials have a relatively small effect on the behaviour.

Impacts onto ceramics which are harder than the projectile show that at 300m s^{-1} about 80% of the impact energy is consumed in plastic deformation of the projectile and about 15% is taken by the rebounding fragments. Only a small amount of energy is needed to produce the fractures in the specimen and the conical fragment which ejects at only about 4m s^{-1}. Impacts with brittle specimens which are softer than the projectile do not deform it. Again little energy is consumed in fracturing the specimen. A large amount of energy is left in the projectile and the fragments which eject from the rear of the ceramic.

High speed photography has proved of great value in identifying the different modes of failure of both the specimen and the projectile during the ballistic impact of ceramics. A camera such as the IMACON with its ease of synchronisation, ability to record at modest light levels and production onto polaroid film has allowed each experiment to be photographed routinely. Combined with accurate impact velocity measurement and the results from the momentum balance we now have a great deal of data on a wide range of ceramics.

[89]

LOW AND HIGH STRAIN RATE EXPERIMENTS ON MODEL KEVLAR-EPOXY MICROCOMPOSITES

I. Gilath, S. Eliezer, Y. Gazit, N. Barnea

Soreq Nuclear Research Center, Yavne 70600, Israel

and

H.D. Wagner

Weizmann Institute of Science, Rehovoth, Israel

ABSTRACT:

Two new experimental methods were used to investigate model microcomposites for quasistatic and dynamic fracture behaviour.

Fracture modes at low and very high strain rate impact experiments were studied using model unidirectional composites. The model microcomposites consist of a set of single fibers embedded in an epoxy film such that the interfiber distance, number of fibers, interface and resin properties can be controlled. Microcomposite monolayers can demonstrate basic failure modes of reinforced composites.

The preparation of controlled geometry model composites was possible due to a new method developed by Wagner et al. [1,2,3].

The quasistatic deformation and fracture modes were tested using a specially designed custom-made miniature tensile testing machine [2]. The sequences of the fracture events were recorded using a colour video camera fitted to a polarised light stereo zoom microscope. The results of tensile testing are summarized in table no. 1

The dynamic tests at ultra high strain rate were performed using short pulsed laser induced shock waves. This new method developed by Gilath et al. [4-8] for metal foils, was applied to study the fracture mode of thin tapes of model microcomposites. To avoid laser ablation of the thin samples, the shock wave was delivered through a thin aluminum foil. Due to the small diameter of the laser beam, high shock wave pressure and very fast energy deposition, short pulsed laser experiments are the most suitable to study dynamic fracture for small samples such as microcomposites.

The second advantage of laser induced shock wave experiments is the possibility to obtain very close energy density steps at the amplifier stages of the laser system thereby enabling the intermittent monitoring of the various failure modes in the sample.

The following values were measured, see table no. 2:

a) The energy density necessary to lift the epoxy film from the aluminum support.
b) The energy density necessary to induce damage in epoxy film when reinforcement is undamaged.
c) The energy density for complete rupture of epoxy and fibers in microcomposite.

Material	Young Modulus E(GPa)	Failure strain %	Strength [MPa]
Kevlar 29	58.9	4.0	2640
CY223/HY956	2.0	3.0	31
8 fiber monolayer	2.8	3.2	65

Table 1. Mechanical properties of single fiber, matrix and microcomposite.

Experiment	Energy density delivered, J/cm^2	Pressure in aluminum at interphase, Kbar (simulation)	Pressure transmitted to epoxy, kbar
A	75±10	9	3.5
B	206±10	15	5.7
C	300±10	20	7.6

Table no. 2. Energy densities and pressures obtained in pulsed laser experiments.

REFERENCES

1. H.D. Wagner, "Statistical Concepts in the study of fracture properties of fibres and composites", In Application of Fracture Mechanics to Composite Materials" (ed. R.B. Pipes and K. Friedrich), Elsevier Science Publishers B.V., to appear (1988).
2. H.D. Wagner and L.W. Steenbakkers, "Microdamage analysis of Fibrous Composite monolayers under tensile stress" (submitted 1988).
3. L.W. Steenbakkers, H.D. Wagner, Polymeric Composites Lab; Materials Research Dept., The Weizmann Institute of Science Report PCL-88-02 (1988).
4. I. Gilath, D. Salzmann, M. Givon, M.P. Dariel, L. Kornblith, T. Bar Noy, "Spallation as an effect of laser induced shock waves", J. of Materials Science, 23, 1825 (1988).
5. I. Gilath, S. Eliezer, M.P. Dariel, L. Kornblith, "Total elongation at fracture at ultra-high strain rates", J. of Mat. Science Letters, 7, 915 (1988).
6. I. Gilath, S. Eliezer, M.P. Dariel, L. Kornblith, "Brittle-to-ductile transition in laser induced spall at ultra high strain rate in the 6061-T6 aluminum alloy", Appl. Phys. Letters, 52, 1207 (1988).
7. D. Salzmann, I. Gilath, B. Arad, "Experimental measurements of the conditions for the planarity of laser-driven shock waves", Appl. Phys. Lett., 52, 1128 (1988).
8. S. Eliezer, I. Gilath, T. Bar Noy, "Laser induced spall in metals, phenomenological model, experiment and simulation" (submitted 1988).

CHARACTERISATION OF THE IMPACT STRENGTH OF WOVEN CARBON/EPOXY LAMINATES

J. Harding, Y. Li*, K. Saka** and M. E. C. Taylor
Department of Engineering Science
University of Oxford, U.K.

As part of a wider programme to study the impact response of hybrid woven reinforced carbon/glass laminates it has been necessary to make an estimate of the effect of strain rate on the failure strengths of the individual reinforcing plies in tension and compression and of the interlaminar shear strength on the planes between neighbouring plies. This requires tests to be performed at a quasi-static and an impact rate on non-hybrid specimens reinforced with woven layers of either carbon or glass. The present paper describes the experimental techniques and specimen designs used at both rates of loading in tests on the carbon reinforced specimens.

For loading in both tension and compression the same design of specimen, a thin strip waisted in the thickness direction, see Fig.1, was used at both rates of strain. The quasi-static tests were performed on a standard screw-driven Instron testing machine while the impact tests used a modified split Hopkinson's pressure bar apparatus. Typical stress-strain curves obtained are shown in Fig.2. A marked increase in the failure strength and some increase in both elastic modulus and failure strain
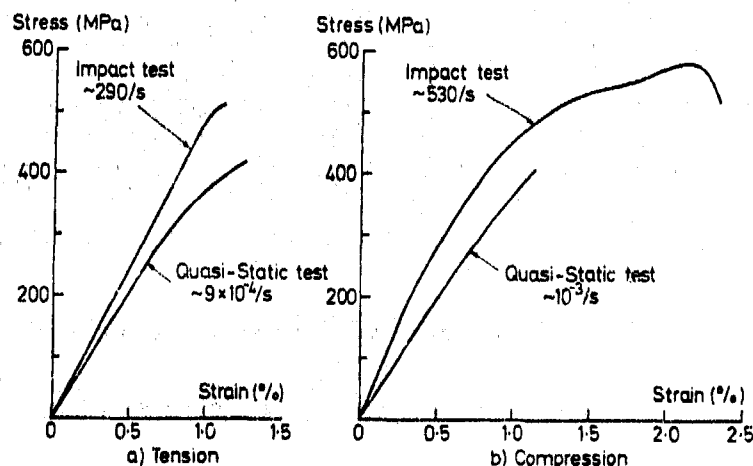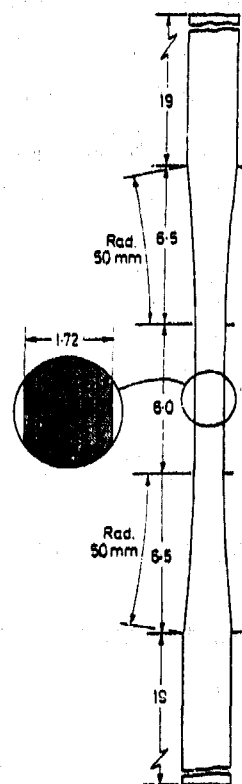

Fig.1 Tension/Compression Specimen
(all dimensions in mm)

Fig.2 Effect of Strain Rate on Stress-Strain Curves
in tension and compression

---

*On leave from the Northwestern Polytechnical University, Xian, China

**Now at Stockport College of Technology, Wellington Road South, Stockport

with strain rate is apparent for loading along a principal direction of reinforcement in both tension and compression.

For the interlaminar shear tests several specimen designs have been invest- igated, for all of which the shear strain along the failure surface was found to be highly non-uniform. The specimen design chosen, see Fig. 3, was relatively simple to manufacture and test, again using the Hopkinson's bar at the impact rate, and a clear interlaminar failure was obtained, see Fig.4. A significant increase in the applied load at which this failure occurs was observed at the higher rate of straining.
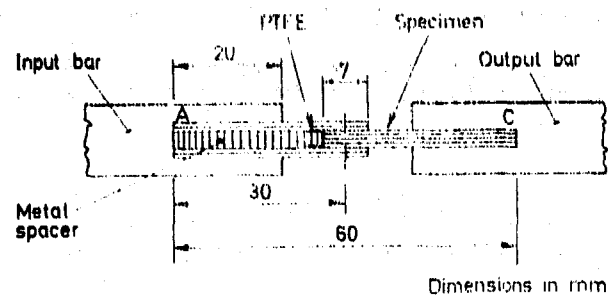
Fig.3 Design of Interlaminar Shear Specimen
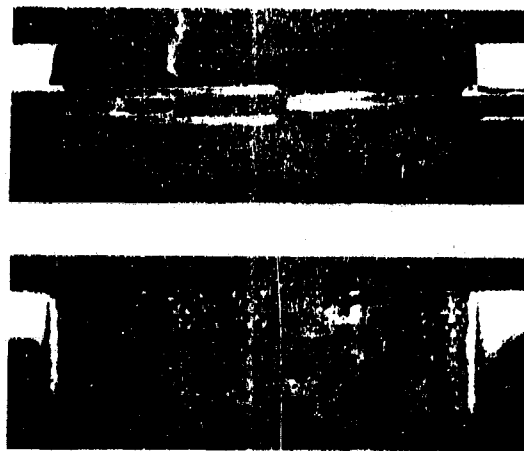
Fig.4 Fracture Surfaces for Impacted Shear Specimen

THE IMPACT ON A COMPOSITE PLATE :
A BOTH THEORETICAL AND EXPERIMENTAL APPROACH
OF THE IN-PLANE AND TRANSVERSE EFFECTS.

N. BEAUMONT, L. PENAZZI
Etablissement Technique Central de l'Armement
16 bis Avenue Prieur de la Côte d'Or 94114 ARCUEIL CEDEX

INTRODUCTION

The impact of a sphere on a carbon fiber reinforced plastic plate (CFRP) may be considered as an impactor's kinetic energy transfer to the plate. This energy separates into various types of energy, the relative importance of which depends on various parameters such as the initial velocity of the indenter and the energy release rate of the material.

The evaluation of the relevance of each type of energy has been previously performed by several in-situ and post-mortem observations. The fact that post-mortem analyses only shows final states of the impacted plates and not the chronological evolution due to the various mechanisms has already been stressed [Beaumont N. 1988a].

EXPERIMENTS

The impact experiments where performed using a gas gun. The spherical indenter (d : 6.35 mm) is made of steel. A high speed camera and strain gages where used to perform in-situ observations. After the impact, several post-mortem observations were performed using US-SCAN and optic microscopy. All those methods have been developped in another paper.

MODELISATION

A complete model has been established in the frame of non-equilibrium thermodynamics. The sphere-plate system is assumed to be fully described by a number of external and internal variables and by two thermodynamical potentials.(fig. 1)
Experiments results have led to impose the following model-hypotheses :

- The indenter penetrates into the plates. That is to say that the Hertzian contact energy can be neglected [Shivakumar 1985]

- The plate has an elastic-brittle behaviour. That is to say that the plasticity of the matrix is neglected and the energy release rate remains constant during the whole delamination.

- The delamination of the plate is fully governed by the kinematic of the impact and spreads at the indentation spreading velocity noted U.

- The preferential delamination direction is correlated with the flexion moduli of the plate.

- The inertia effects are neglected

CONCLUSION

Several in-situ observation systems have been developped in order to have more information on the behaviour of a CFRP plate impacted by a spherical steel indenter. The physical understanding of the phenomenon lead to the construction of a model established in the frame of non-equilibrium thermodynamics.
Thanks to this model, it is possible to predict the residual speed of a spherical indenter impacting a CFRP plate with a quasi-isotropic lay-up in the case of an elastic-brittle-behaviour of the plate. In the case of strongly anisotropic layers, another model has to be considered taking into account the lay-up effects.
For any lay-up and any material, as long as delamination takes place during impact and has not reached saturation, it is possible to predict the shape and surface of the delaminated zone
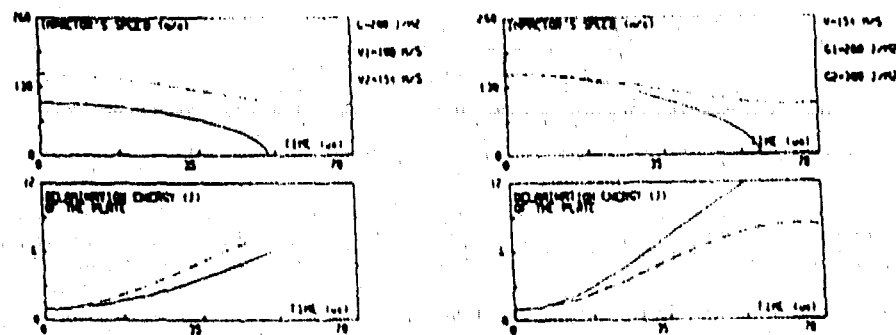
Fig. 1 Predictions of the indenter's velocity and of the delamination energy
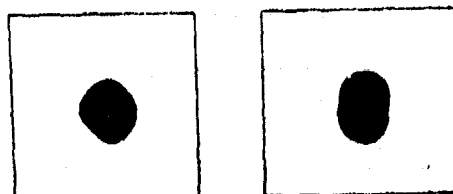

Fig. 2 Prediction of the shape and of the surface of the delaminated area

LAMB WAVE PROPAGATION IN AS4/3501-6 COMPOSITE PLATES EXHIBITING MICROSTRUCTURE

J.S. Epstein, Assistant Professor
The Center for the Advancement of Computational Mechanics
The Georgia Institute of Technology, Atlanta, GA., 30332, USA

H. Murakami, Associate Professor
The Applied Mechanics and Engineering Science Department
The Univ. of California at San Diego, La Jolla, CA., 92093, USA

Dr. M. Abdallah
The Advanced Methods Group
The Hercules Aerospace Corporation
Magna, UT., 84044, USA

Mr. V.A. Deason
The Applied Optics Group
The Idaho National Engineering Laboratory
Idaho Falls, ID., 83415, USA

ABSTRACT

We wish to discuss the phenomena of low velocity elastic impact in AS4/3501-6 graphite/epoxy composite plates. To accomplish this objective an investigation combining computational, experimental and precise manufacturing methods was developed. Computationally, a finite element - mixture theory formulation is employed to capture microstructural detail at the composite interface. Experimentally, dynamic moire interferometry is developed and employed to study transient microstructural displacement fields on the composite free edge under impact.
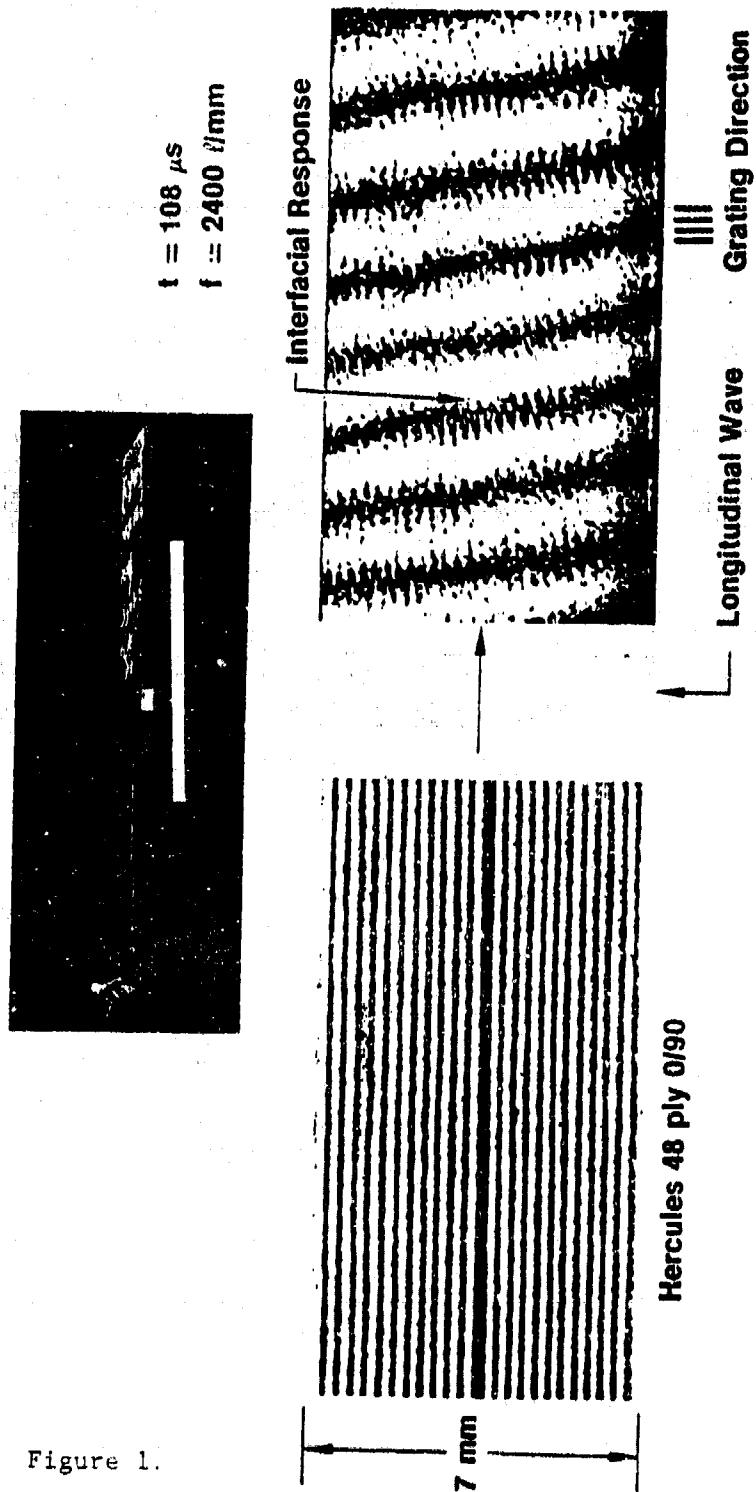
Four types of composite plates were manufactured using the AS4/3501-6 fibers. The specimens consisted of alternating layers of 0 and 90 degree fiber orientations with constant plate dimensions equaling 50 mm wide, 7 mm thick and 250 mm in length. The layup sequence was varied in the plates. Specifically, the first series of plates consisted of pure 90 degree fibers; the second sequence consisted of $[0_{16}/90_{16}/0_{16}]$; the third sequence was $[0_2/90_2]_s$ for 24 plies and the final sequence was $[0/90]_s$ for 48 plies.

The impact process occurred by a striker bar impacting the composite plate parallel to the layer direction at 11 m/s. Moire interferometry displacement fields of the pulse propagation on the composite free edge were obtained using a 20 ns. pulsed ruby laser. These displacement fields are obtained both near and far field from impact. Figure 1 details the longitudinal displacement field far field from impact. The bulk fringes are the result of the bulk lamb wave propagation. The reticulation or microstructure within the bulk fringes correspond to the layering of the composite. Figure 2, shows that this microstructure is the result of the differing wave velocities in the 0 and 90 degree fiber orientations, 8 and 3 km/s respectively. Under stronger elastic impacts the interface shear of figure 1 would grow developing into a delamination. Similar displacement fields exhibiting microstructure are found on the plate free edge for the 24 and 3 ply specimens. Uniform displacement fields are found on the pure 90 degree specimens. Finally displacement fields for a natural delamination occurring at the interface in the 3 ply specimen will be presented. This lecture will compare the non-delaminated displacement fields to the finite element - mixture theory formulation to asses a broader understanding of the complete parameters causing interface delamination under low velocity impact.
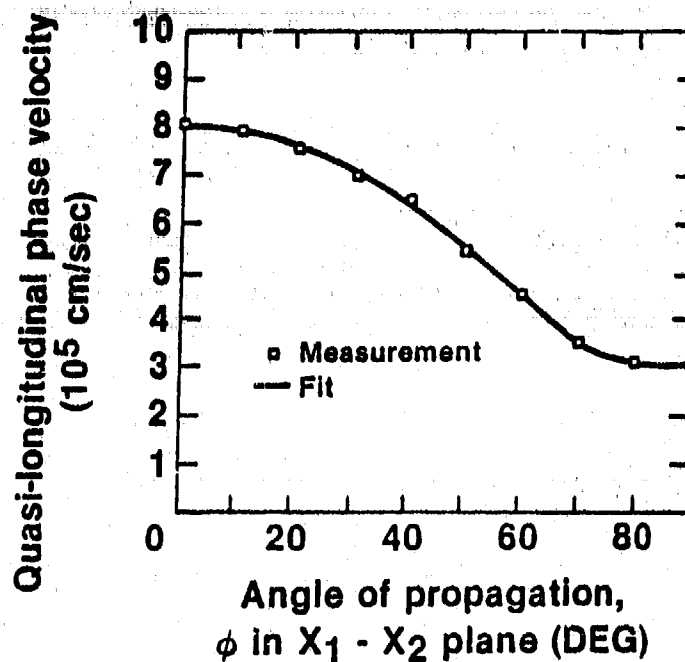
Dynamic Moire Interferometry
G/E Composite Stress Wave Behavior

t = 108 μs
f = 2400 ℓ/mm

Interfacial Response

Longitudinal Wave

Grating Direction

Hercules 48 ply 0/90

7 mm

Figure 1.

Quasi-Longitudinal Phase Velocity Data Versus Angle of Propagation, ϕ in the X_1 - X_2 Plane for a Unidirectional Composite Laminate* (AS4/3501-6) (100 x 304 x 8.3mm)

*L. Pearson, B. Murri, D. Gardiner Hercules Aerospace

7-1087

Figure 2, the phase velocity verses angle of propagation relationship for AS4/3501-6 graphite epoxy prepreg (courtesy B. Murri and D. Gardiner Hercules Aerospace).

[978]

Dynamic indentation of two dimensional ring systems

T Y Reddy, A S Kaddour and S R Reid
Department of Mechanical Engineering, UMIST,
PO Box 88, Manchester, England

ABSTRACT

Dynamic crushing of single rings (Reid and Reddy (1979)), ring chains (Reid and Reddy (1983) and Reid and Bell (1984)) as well as that of two dimensional ring systems (Stronge and Shim (1987,1988)) have been studied. This paper is concerned with dynamic indentation of hexagonally close packed systems made of rings (19.05 mm diameter and 12.7 mm length) under impact conditions, to extend the understanding of the energy absorbing characteristics of such systems as well as those of cellular structures and solids. Typical systems were 286 mm (15 rings) wide and 267 mm (16 rows) deep and were enclosed in a rigid frame with a central opening of 95.5 mm wide on one side.

A rigid mass of 0.16 kg (95.25 mm wide and 12.7 mm height) was propelled along a guided track by a cartridge gun to impact the ring systems centrally at velocities in the range of 36 ms^{-1} to 72 ms^{-1}. Deformation process was recorded by using a high speed camera with a film speed of about 6000 frames per second.

Two different deformation patterns depending on the ratio of the energy absorbing capacity of the struck rings to the kinetic energy of the striker defined as the Q factor by Stronge and Shim (1987) were observed. At low values of Q the deformation started with an initial crushing mode, in which the rings were directly crushed (with little lateral expansion) as if they were constrained at the sides. This was followed by a shear type of deformation in which the rings were crushed to deform at an oblique angle to the direction of impact. There was considerable lateral expansion of the rings crushed in the shear mode. The shear bands started at the corners of the striker and formed a wedge shape. Continuing deformation resulted in the growth (widening) of these shear bands. Such behaviour was also observed in quasi-static indentation tests on similar systems. At higher impact velocities, i.e. for high Q values, the crushing mode dominated in causing deformation. The deformation front was cylindrical. Rings adjacent to the side walls and distal end support were found to deform due to the reflection at these supports stress waves produced during impact.

In all the systems tested the initial decelerations were found to be higher than the average decelerations, the ratio of these two values being higher for higher values of Q. Considering the strain rate effects and using the quasistatic failure mode of rings, an elementary energy balance procedure is adapted to predict the variation of the striker velocity. Considering the simplicity of the analysis the predictions compare reasonably well with experimental observations.

References

S R Reid and W W Bell (1984), *Mechanical Behaviour at High Rates of Strain* Ed. J Harding. Institute of Physics, Conf. Series 70, 471-478.

S R Reid and T Y Reddy (1979), *Mechanical Behaviour at High Rates of Strain* Ed. J Harding, Institute of Physics Conf. Series 47,

S R Reid and T Y Reddy (1983), *Int. J. Impact Engg*, 1., 85-106

W J Stronge and V P W Shim (1987), *Int. J. Mech. Sci.*, 29, 381-406.

W J Stronge and V P W Shim (1988), *J.Engg.Mat.Tech. (Trans ASME)* 110, 185-190

A DESIGN GUIDELINE FOR PREDICTING MAXIMUM CENTRAL DEFLECTIONS OF IMPULSIVELY LOADED PLATES

G N Nurick - Applied Mechanics Research Unit,
University of Cape Town.

An extension of Johnson's (1) damage number is refined for use as a design guideline for predicting the maximum central deflection of plates subjected to impulsive loads. This prediction compares favourably with experimental evidence. In addition, using the experimental results an upper bound on the loading conditions may be determined, i.e. the maximum deflection before tearing of the plate material takes place. This is illustrated for circular and rectangular plates of varying dimension and loading conditions.

1.   Johnson W 1972 Impact Strength of Materials p.303. Edward Arnold.

On the Effects of Materials and Radius to Thickness Ratio in Dynamic
Plastic Buckling of Circular Tubes under Axial Impact

K Kawata, S Matsumoto and E Yoshimizu

Science University of Tokyo, Noda, Chiba-ken 278 Japan

ABSTRACT: In dynamic plastic buckling of circular tubes under axial
impact, the effect of materials in the mean plastic buckling load
(MPBL) vs. loading velocity relation for bcc and fcc metals and the
effect of radius to thickness ratio in MPBL are clarified, using a
new precise dynamic properties characterization system based upon
the KHKK one bar method. Experimental values are fairly explained
by a theoretical expression derived by the authors, composed of three
mechanisms of bending, rolling and toroidal deformation.

INTRODUCTION

In designing the crashworthiness of structural elements such as circular
tube under axial impact, the effect of materials in the MPBL vs. loading
velocity relation and the effect of radius to thickness ratio in MPBL
should be known, basing upon the precise experimental result. The precise
curve of dynamic plastic buckling load vs. displacement seems not be hither-
to satisfactorily determined. Such data acquisition could not be carried
out until precise high velocity mechanical properties characterization
system with no reflected wave disturbance, such as the KHKK one bar method
(Kawata et al 1979) appeared. These experimental data are compared with
the theoretical expression newly derived by Kawata et al (1988).

CONCLUSIONS

1) A new theory of dynamic plastic buckling of circular tube with wide
range of R/t under axial impact, is derived basing upon a model with
bending, rolling and toroidal deformation mechanisms. The theoretical
values well coincides with experimental ones for specimens of R/t ranging
from about 20 to 120 and of various metals, tested here.
2) Dynamic plastic buckling load vs. displacement relation can be satis-
factorily determined by the new precise dynamic property characterzation
system basing upon the KHKK one bar method without reflected stress wave
disturbance.
3) Dynamic MPBL can be calculated for various loading velocity by con-
sidering the dynamic mechanical properties of the materials, giving fair
coincidence with experiment.
4) The effect of materials in the MPBL vs. loading velocity relation is
clarified for both of fcc and bcc metallic materials.
5) The effect of R/t ratio in MPBL is clarified experimentally and is
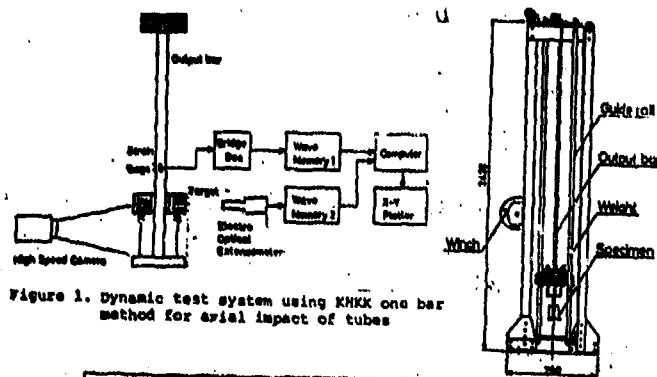fairly explained by the above mentioned theory.

[100]

Figure 1. Dynamic test system using KHKK one bar method for axial impact of tubes
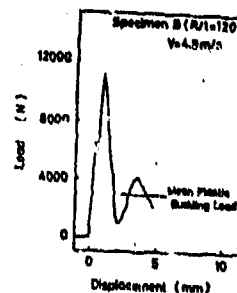

Figure 2.
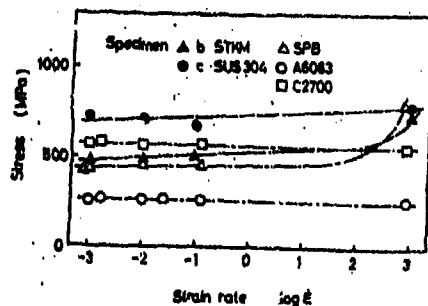A dynamic load vs. displacement record in dynamic buckling

Figure 3.
Flow stress vs. strain rate for five materials

Table 1. Test materials
A Tinplate
B Aluminium
C Brass
D Stainless steel
E Carbon steel for general mechanical structures

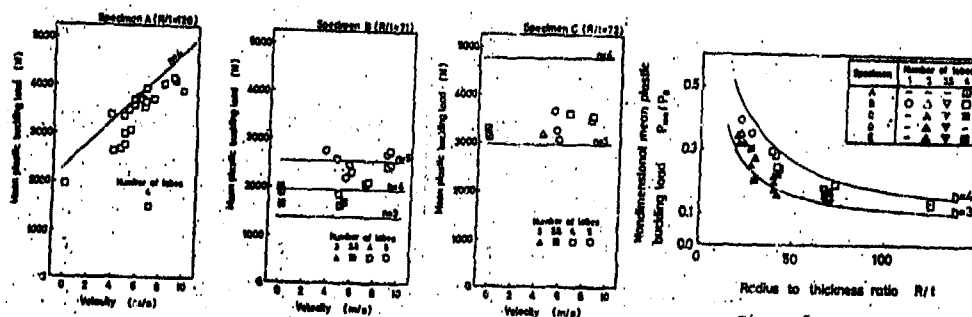| Specimen	A	B	C	D	E
Material	SPB	A6063	C2700	SUS304	STKM
Length	110		195		
Radius	26.55		31.25 – 32.30	30.15 – 30.35	
Thickness	0.22		0.30 – 1.00		
R/t	120		30 – 72		

Figure 4. Experimental results on mean plastic buckling load vs. loading velocity compared with theory

Figure 5.
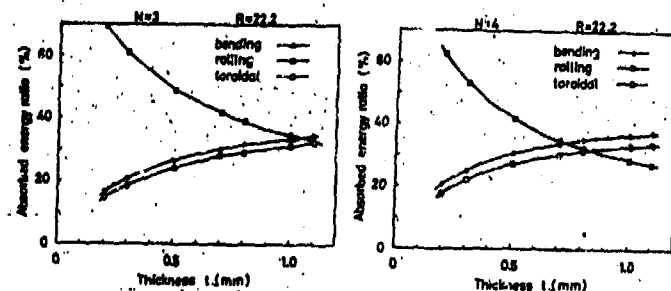Experimetal results on nondimensional MPBL vs. radius to thickness ratio compared with theory

Figure 11. Proportion of absorbed energy by three deformation mechanisms R=22.2, N=3 and 4

Dynamic Coupling of Plastic Deformations in Multi-Component Structures

W J Stronge and D Shu
Department of Engineering
University of Cambridge

ABSTRACT

The distribution of energy dissipation in multi-component structures that are deformed by impact depends on the structural arrangement, the relative compliances and the distribution of mass in the components. A collision against a rigid-perfectly plastic, multi-component structure results in at least two distinct stages of deformation; a transient followed by a modal stage of deformation. Deformation during the transient stage is characterised by travelling hinges or hinge lines while the modal stage has a time-independent velocity distribution. The total impact kinetic energy is disbursed throughout the structure during these stages of deformation. In general the fraction of the total energy dissipated in each component depends primarily on the structural arrangement and the relative compliance; the mass of the component is of secondary importance. The structural arrangement can be classified as either a parallel or series system in analogy with electric circuits. The distinction between these systems is based on displacement constraints that define the connectivity between elements.

In the parallel arrangement, all components have the same displacement at the impact point; the dynamic load is imparted to all components simultaneously. In a multi-component structure with this arrangement, the fraction of the total energy absorbed in a component during the transient phase increases with the relative compliance and decreases with the relative mass ratio. During the modal stage of deformation, the fraction of the total energy dissipated increases in proportion with the relative compliance. The deformation of a component is independent of the relative mass ratio provided the mode of deformation is not changed when the mass ratio changes. To conclude, the heavier and stronger components of a structure absorb a larger part of the initial kinetic energy in a parallel structural arrangement.

In the series arrangement, only the dynamic forces that have passed through an element are transmitted to successive elements. With this arrangement the fracture of the energy absorbed in a component during the transient stage increases with relative mass and decreases with relative compliance. Again the stronger components absorb a larger fraction of the initial energy imparted to the structure.

Applications of these results to the analysis of ship structures composed of frames covered by plates will be discussed.

The Use of Simulation Techniques to Study Perforation Mechanisms in Laminated Metallic Composites

I.G.Crouch(*) and R.L.Woodward

Materials Research Laboratory, Defence Science and Technology Organisation, Ascot Vale, Victoria 3032, Australia

EXTENDED ABSTRACT

As a class of composites, metallic laminates offer recognised benefits in terms of structural properties, especially enhanced toughness (Kaufman, 1967; Taylor et al, 1976; Throop et al, 1979) and improved fatigue performance (Taylor et al, 1976; Vogelsang, 1966). This is particularly true with the weakly-bonded systems, such as the adhesively-bonded, aluminium laminates. The addition of low-density, polymeric fibres to reinforce the weak interlayer, as in the case of ARALL, a hybrid laminate currently being marketed commercially by Alcoa, increases the specific strength values whilst enhancing fatigue crack tolerance even further. These attractive specific properties have led to a number of full-scale trials within aircraft structures (Vogelsang, 1986), for which weight savings of about 30% are claimed possible. Unfortunately, little is reported of the through-thickness properties of these laminates, especially under impact conditions, for it is these properties which need investigating before such structural laminates could be considered as suitable materials for containment applications or in situations where perforation, at high rates of strain, is a possibility.

The energy-absorbing capacity of metallic laminates has recently been highlighted by Crouch (1988) who compared the perforation characteristics of adhesively-bonded, aluminium laminates with medium-strength, monolithic, aluminium alloy plates. It was shown that such laminates suppress failure by the through-thickness shearing mechanism known as plugging and consequently, under certain conditions, can absorb more kinetic energy. The perforation of metallic laminates by blunt objects is, however, a complex terminal ballistic event and attempts to mathematically model the process have proved extremely difficult because little is known about the plastic flow and yield criteria associated with metallic laminates. A solution for simple, unbonded, two-layer laminates, which treats both the plug acceleration and dishing failure aspects of the process, has been developed (Woodward et al, 1988) by examining the deformation of the two component layers separately. For a multi-layered configuration a continuum approach is required, necessitating either a better understanding of composite behaviour or, alternatively, approaches which sample properties in a form similar to the actual stress state in a ballistic experiment.

The object of this work was to establish such a set of quasi-static, mechanical test procedures which would accurately simulate part of the complex perforation process. Data and derived parameters from these tests can then be used as realistic input data in mathematical models of laminate perforation.

(*) Current address: Royal Armaments Research and Development Establishment, Chobham Lane, Chertsey, Surrey, KT16 OEE, U.K.

The perforation mechanisms of weakly-bonded metallic laminates are compared with the failure mode of monolithic aluminium plates when impacted with blunt-nosed projectiles. Figures 1a and 1b illustrate the comparative damage features associated with both the monolithic and laminated materials: (A) compression, (B) shearing, (C) tensile stretching and (D) delamination. A family of quasi-static simulation tests have been developed for laminates which generate relevant and meaningful mechanical property data in a form suitable as input data for mathematical modelling of the perforation process. Figures 2a and 2b show how constrained compression tests have been used to simulate the compression stage in the perforation of both classes of materials by blunt-nosed projectiles.

Figure 1a

Figure 1b

Figure 2a

Figure 2b
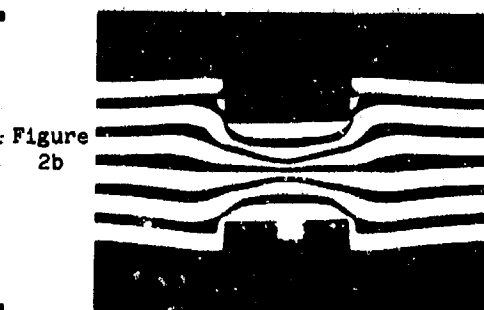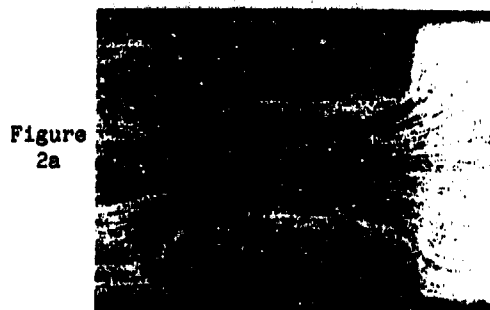
The properties described in this work are currently being utilised in a simple sequential model which treats plug acceleration and target delamination as two basic stages in the perforation of laminated metallic composites. Using data derived from these simulation tests, good estimates of critical ballistic impact velocities are being obtained and the effects of parameter changes on performance are being correctly described.

Crouch I G 1988 Proc.of MECH'88 Conf.on New Materials and Processes for Mechanical Design, Brisbane, pp.21-26.
Kaufman J G 1967 Trans ASME, pp.503-507
Taylor L G and Ryder D A 1976 Composites, pp.27-33
Throop J F and Fujozak R R 1979, ASTM-STP-651, pp.246-266
Vogelsang L B and Gunnick J W 1986 Mats.and Design, Vol.7(6), pp.287-300
Woodward R L and Crouch I G 1988, MRL-TR-1111, DSTO(Melbourne)
Woodward R L and De Morton M E 1976, Int.J.Mech.Sci., Vol.18, pp.119-127

Instabilities at High Strain Rate of AISI 316 Damaged by Creep, Fatigue and Irradiation. Discussion of Adiabatic Temperature Oscillations.

C. Albertini, A.M. Eleiche* and M. Montagnani

CEC-JRC, Ispra Establishment, 21020 Ispra (Va) - Italy
*Visiting scientist at JRC-Ispra, on leave from the Cairo University

Nuclear reactor components are submitted, in the case of a hypothetical severe accident, to dynamic loading generating strain rates of up to 1000 s^{-1}. The structural behaviour during severe accidents can be assessed provided that the mecnanical properties of the material at the time of the accident can be predicted by constitutive equations. Therefore, the tensile mechanical properties of the nuclear grade austenitic stainless steel AISI 316H were measured at strain rates ranging from 10^{-3} to 10^3 s^{-1}, which steel was previously submitted to increasing amounts of pre-damage by creep, low cycle fatigue and irradiation at a temperature of 550°C.

The following programme of pre-damage treatments was performed on the as-received AISI 316H stainless steel.
- irradiation to 2 dpa (E > 0.1 MeV) in the High Flux Reactor in Petten, in sodium at 550°C;
- low cycle fatigue at 550°C (performed by P.N.C. Tokyo at the University of Tckyo), cycle strain range 0.6% and 1%, cycle ratio n/NF of 0.2, 0.4 and 0.6;
- Low cycle fatigue as above with superposition of irradiation to 2 dpa;
- creep at 550°C, 300 MPa (performed at JRC-Ispra), at the fractions of 0.2, 0.4 and 0.6 of the 2000 h life-time.

From the typical flow curves regarding creep, low cycle fatigue, low cycle fatigue and irradiation damaged materials, respectively, we observe that the single damage process (creep alone, low cycle fatigue alone, irradiation alone) is a hardening process which provokes an increase in the flow stress at a given strain and a reduction of ductility with respect to the as-received material. We observe also that up to large strain values the strain rate increase causes a flow stress increase at a given strain in each of the material conditions considered alone. Dynamic strain ageing serrations are observed along the low strain rate curves of as-received and damaged materials, while at high strain rate, larger instabilities of the stress-strain curve of the damaged materials are present. Furthermore, we observe that the superposition of irradiation and low cycle fatigue enhances the effect of flow stress increase at a given strain and that of ductility reduction with respect to the as-received material, and introduces a trend to strain rate softening.

In an attempt to find a correlation between the mechanical response of the damaged materials and the amount of damage, two parameters were defined. One parameter (0.2% yield stress ratio of damaged to as-received material) measures the increase of flow stress with respect to the as-received material. The other parameter (fracture strain ratio of damaged to as-received material) measures the reduction of ductility with respect to the as-received material. The numerical values of these two parameters show a correlation which is worth further verification because its consistency would permit a simplified implementation of the effects of different damage processes in the constitutive equations. Nevertheless, a more complete theoretical modelling of the damaged material properties for structural calculations must take into account also the instabilities

[105]

which modulate the averaged mechanical response of the damaged materials with oscillations of the flow curves. The amplitude, frequency and nature of these oscillations depend on strain rate, temperature and stress state. The low strain rate flow curve of the creep-subjected material shows the serrations of dynamic strain ageing. Some informations about the nature of dynamic strain ageing can be deduced by observing the records of the stress-time and of the temperature increase of the specimen-time which show osscillations at corresponding times. This fact means that dynamic strain ageing is a thermally activated phenomenon.
The medium strain rate flow curve of the creep-subjected material is smooth without oscillations; also the stress-time and the temperature increase of the specimen-time curves are smooth without oscillations.
The high strain rate flow curve of the creep-subjected material shows an initial upper and lower yield point followed by large oscillations due to instabilities. Both the stress-time and the temperature increase-time curves at high strain rate show also oscillations at the same time. The oscillations of the high strain rate flow curve are assisted by thermal activation. The constraint to slip due to the short time and the consequent dislocation locking are responsible for the remarkably high strain rate hardening with superimposed large instabilities.
These facts could mean that the straining modes at grain level, developed during the creep and tensile tests at low strain rate, are of a similar nature, mainly by micro-flow along grain boundaries, while they develop new mechanisms at high strain rate, characterized by slip (or twinning) inside the grains. The same phenomenon is also confirmed by the experimental evidence that the monotonic tensile curves at low and high strain rate coincide with the correspondintg flow curves of the interrupted test performed at the same strain rate. Also the strain rate softening and the higher ductility reduction at low strain rate, shown by the pre-fatigued and irradiated material, can be explained as being due to different mechanisms of deformation at low and high strain rate.
A first attempt to establish an equation, based on atomistic models, able to predict the onset of serrated yielding, taking into account the strain and strain rate histories, was made by Eleiche et al. (1987).
Nevertheless, this approach does not take into account the directionality dependence introduced by the stress state. In fact, recent experiments on the same AISI 316H tested in tension at 550°C, showed the disappearance of the dynamic strain ageing instability along the flow curves determined under torsional stress state. In the same experiments campaign it was stated that under torsional stress state by increasing the damage through sequential reverse prestraining, the yield stress decreases and the residual ductility increases.. These results in torsion are compared with those obtained in tension and here reported, from which they differ substantially.

A numerical study of dynamic shear failure in reinforced concrete beams

T. Yokoyama and K. Kishida

Dept. of Precision Engineering, Faculty of Engineering
Osaka University, Suita, Osaka 565, Japan

Extended Abstract

The present paper attempts to investigate direct shear failure in the
roof slabs of shallow-buried RC box-type structures (Figure 1) under
impulsive pressure loading. Since direct shear failure is governed by the
buildup of the transverse shear force at the roof support, an elastic
Timoshenko beam model is adopted for the RC roof slab. The finite element
equations of motion for the Timoshenko beam are derived from Hamilton's
principle and solved using a step-by-step integration method.

The finite element procedure was applied to obtain the dynamic response
of the RC slabs or beams under distributed impulsive pressures. The
experimental data used for the analysis come from a series of the dynamic
tests on the shallow-buried RC box-type structures conducted by Kiger and
Slawson (1984). Each test structure was covered with a shallow layer of
soil and was loaded with a high-explosive induced blast pressure $q(t)$,
which was approximated by a triangular pulse with a zero rise time. The
main characteristics of the example RC beam are summarized in Table 1.
Because of symmetry, only half of the RC beam was considered.

Figures 2(b) and 2(c) show plots of normalized support shear (V/V_u) and
normalized support moment (M/M_u) versus time for two different peak
pressures for the example RC beam with fixed ends. The present results
agree reasonably well with the normal mode solutions. It should be
remarked that the curves in Figure 2 are theoretical because, as soon as
either ratio V/V_u or M/M_u exceeds a value of one, the RC beam is presumed
to have reached its strength capacity and is no longer elastic. The time
at which $V/V_u = 1$ is denoted as t_s, and the time at which $M/M_u = 1$ is
denoted as t_m. The occurrence of failure in either direct shear or
flexure depends on whether the failure threshold (V/V_u and $M/M_u = 1$)
intersects these curves at an early or a later time, respectively.

The transition from a predicted direct shear failure to no shear failure
occurs when $t_s = t_m$. If this transition for different combinations of
peak pressure P_0 and rise time t_r is plotted in the P_0-t_r domain, a
series of points produces a "failure curve." Typical failure curves
determined for two beam-end conditions are given in Figure 3. Points that
lie in the region above a failure curve define a loading condition for
which analysis indicates a direct shear failure, while points that lie in
the region below the failure curve describe loading parameter
combinations which will cause either a flexural failure or no failure in
the RC beam. Parametric studies demonstrate that the failure curves are
sensitive to loading parameters (P_0 and t_r) and structural parameters (
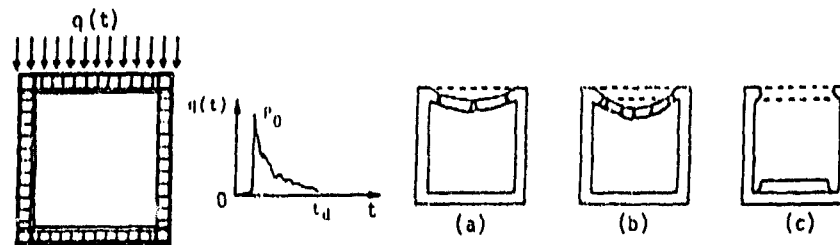R, Ω and L/d), but are not significantly affected by load duration t_d.

Figure 1: Failure modes of RC box-type structures subjected to transverse, uniformly distributed, impulsive loads: (a) flexural damage; (b) combined flexural and shear damage; (c) collapse under direct shear
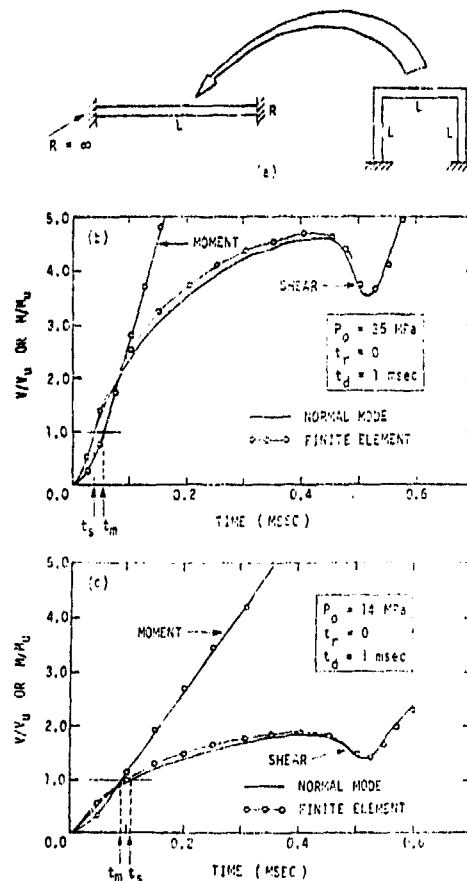

Table 1: Main characteristics of example RC beam

Parameter	value
Beam length (L)	1.14 m
Beam width (b)	0.0254 m
Beam depth (h)	0.184 m
Effective beam depth (d)	0.162 m
Young's modulus (E)	33.1 GPa
Poisson's ratio (ν)	0.2
Shear coefficient (k')	0.822
Mass density (ρ)	2,400 kg/m^3
Ultimate shear capacity (V_u)	6,140 kg
Ultimate moment capacity (M_u)	370 kg-m
Strength enhancement factor (Ω)	1.6

Figure 2: Normalized support shear and moment versus time for example RC beam : (a) fixed ends; (b) peak pressure P_0 = 35 MPa; (c) peak pressure P_0 = 14 MPa
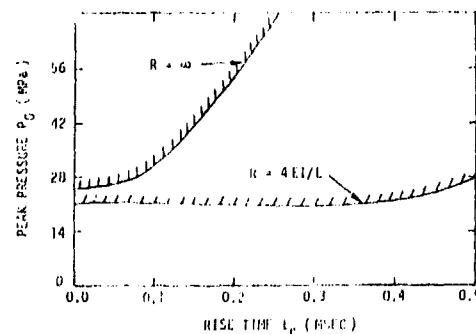
Figure 3: Effect of beam-end restraint on failure curve

[108]

Dynamic properties of construction materials using
a large diameter Kolsky bar

D. R. Morris and A. J. Watson

Department of Civil and Structural Engineering
The University of Sheffield.

ABSTRACT

High strain rate testing at the University of Sheffield's Dynamics Testing
Laboratory, near Buxton, Derbyshire, has been developed using 38mm diameter
maraging steel pressure bars and a small explosive charge to produce the
the stress pulse. The large diameter pressure bars are of particular
interest to engineers because they admit the use of thicker discs of
specimen in the test, on the basis of Davies and Hunter's (1963) geometric
criterion.

The diameter of the pressure bar was chosen as 38mm for the purpose of
testing construction materials with particle sizes up to 2mm. The pressure
bars were aligned vertically and supported in a steel frame. The dynamic
strains produced in the input and output pressure bars were measured using
four 1mm electrical resistance strain gauges (ERSG) connected to a
Wheatstone bridge, and the amplified output was captured on a Gould OS 4050
digital storage oscilloscope (see fig 1) and subsequently transferred to an
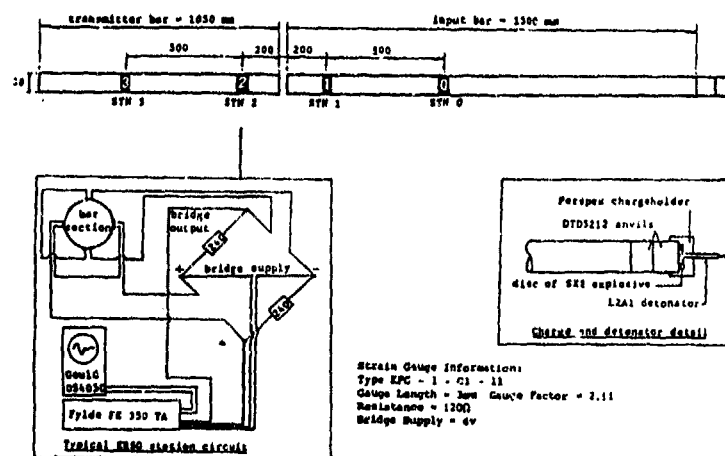Olivetti M24 personal computer.

fig 1 : Details of the 38mm diameter DTD5212 Kolsky bar apparatus

The recorded stress pulses were corrected for dispersion using an FFT with
Bancrofts data. The correction gave very good agreement with experimental
data.

The rod velocity of specimens was found using dynamic photoelasticity to
observe the progress of a stress pulse through the specimen (See fig 2).
The camera used was the Barr and Stroud CP5 rotating mirror camera, which
can operate at 2,000,000 frames per second.
This method gave a useful visual check on the progress of a stress pulse
through a specimen but the experiment required a camera setting which gave
an interframe time of 1.9 microseconds. The accuracy of the rod velocity
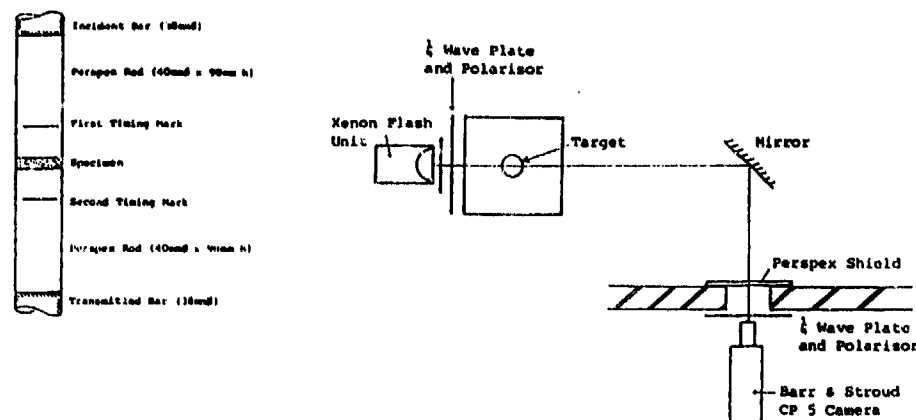found using this method was limited by the camera speed.

[109]

fig 2 : Photoelastic method for finding the rod velocity of specimens

Stress / strain in the specimens was found using Lindhom and Yeakleys method. Initial tests were carried out on Perspex discs, (38mm diamter) of different height. The yield stress and yield strain for different heights of Perspex were plotted together, and it can be seen (fig 3) that a marked change of behaviour of the specimen occurs between the 12.5mm and 15mm specimen heights. The critical height of the specimen marks the transition between two modes of specimen behaviour as a result of the influence of boundary conditions. The smaller specimens failed at greater stress and strain values, because the friction coefficient of the Perspex cylinder ends was more significant than radial inertia. Using the correct height of specimen (14.5mm) the error due to friction was of the order of +5% yield stress. As the height of the specimen was increased beyond 14.5mm, the inertia term due to radial strain acceleration for the specimen increased, reducing yield stress
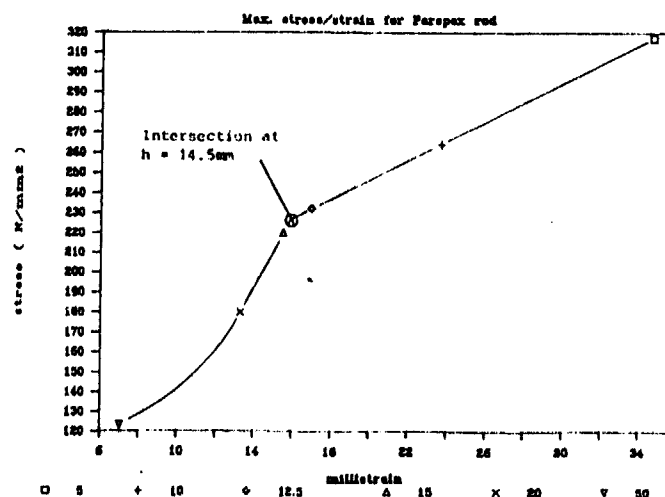

fig 3 : Yield stress and yield strain calculated from Kolsky
bar data for specimens of different height.

A number of construction materials were tested in the Kolsky Bar, and two sets of results are presented in the paper : a high quality brick pavior, and sand/cement mortar.

ULTIMATE STRENGTH OF BOX COLUMNS
SUBJECTED TO IMPACT LOADING

by
Tomasz Wierzbicki
Department of Ocean Engineering
Massachusetts Institute of Technology
Cambridge, MA 02139
and
Leonhard Recke
BMW, Research and Development Center
8000 Munich 40

Abstract

Buckling of plates and shells under dynamic loading have been studied in the literature
for several decades. A comprehensive literature review on this subject was published,
among others by Singer (1981), Lindberg and Florence (1986) and Jones (1989). It was
found that the dynamic buckling load increases with the rate of loading and is always
greater than the corresponding static buckling load. In the case of plates subjected to a
mass impact the rise in the plate stiffness was found to be attributed to the transverse
inertia of the plate.

A related problem of the ultimate strength of plates under longitudinal impact does not
appear to have been studied in the literature. It is expected though that the trend will
be similar to the case of a buckling load. The problem of the determination of the
maximum strength of compression members under impact loading is of great
importance in many industrial applications, most notably in the impact energy
absorption and collision protection of vehicles. For example, thin-walled box columns
loaded statically exhibits a sharp peak load followed by subsequent lower peaks
corresponding to folding and crushing of the column's walls. The magnitude of the
peak load (often referred in the literature as ultimate or crippling load) depends on the
cross-sectional dimensions of the column, elastic constants and the yield stress of the
material. The peak load of the same column loaded dynamically is larger.

The objective of this communication is to present a simplified method of predicting the
ultimate strength of prismatic multi-cornered columns subjected to impact loading. The
impact velocities considered in this paper are relatively low and correspond to typical
collision velocities of automobiles and airplanes. The impacting mass is assumed to be
larger than the total mass of the column.

The analysis consists of two parts. First, a new two-degree-of-freedom deformation
model of a single corner element of the multi-cornered column is developed and the

post-buckling stiffness and ultimate load is evaluated. This is derived in a closed form from the first yield criterion. The calculated strength of a perfect plate agrees within 15 % with the exact solution (Rhodes 1985). The accuracy is further increased by taking into account the effect of initial imperfections.

In the second part of the analysis, the lateral inertia of the column walls is incorporated into the governing equation. The axial inertia is neglected for the considered class of problems (large mass, low velocity). The formulation is based on the concept of the growth of initial imperfection with time. The resulting initial value problem for a system of ordinary differential equations is solved numerically. It is shown that the dynamic ultimate strength depends on the magnitude of the striking mass as well as on the impact velocity. A correlation of the predicted strain-time diagrams are made with the test results reported by Singer (1981).

The present results will help interpret the drop tower test on box columns performed in many laboratories around the world. In this type of experiment, the force-time history at the mass/column interface is determined from the reading of the accelerometers. The readings are usually affected by the inaccuracies in differenciating the displacements to get accelerations and by the superposed elastic vibrations of the system. Therefore, the experimentally determined peak load is not uniquelly defined and/or is affected by the filtering frequency. Our analysis provide a much needed insight into the physics of the impact problem.

At the present stage we have studied the inertia effect only. The peak load is also influenced by the strain rate effect and the delayed yield phenomenon (Campbell 1957). Consideration of the above factors is left to a future continuation of this research.

References

J.D. Campbell et. al. (1957), Delayed Yield and other Dynamic Loading Phenomena in a Medium Carbon Steel, Proc. Conferences on Properties of Materials at High Rates of Strain, April 20 - May 2, 1957, Institution of Mechanical Engineers, London.

N. Jones, (1989), Structural Impact, Cambridge Unversity Press.

Lindberg and A.L. Florence, (1986), "Dynamic Buckling", Stanford Research Institute.

J. Rodes, (1983), Effective Width in Plate Buckling, in "Developments in Thin-Walled Structures", Vol. I, Elsevere Applied Science Series, 1983.

J. Singer (1981), Dynamic Buckling of Plates under Longitudiual Impact Impact. TAE No., 430, Isreel Institute of Technology.
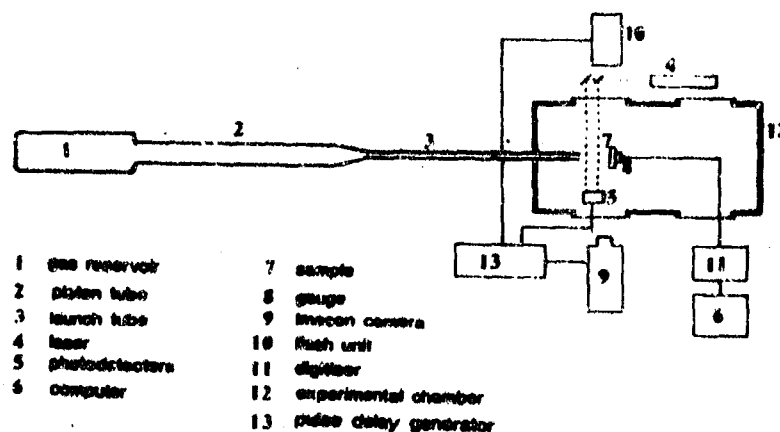
Pages 113 + 114
Omitted

Hypervelocity Impact Research in British Aerospace

D.G. Dixon and D. Townsend
British Aerospace PLC, Sowerby Research Centre,
FPC 266, PO Box 5 Filton, Bristol BS12 2QW.

ABSTRACT

A new experimental facility is described. This comprises a two stage
light gas gun and associated diagnostics which will be used to carry out
impact experiments and measure high strain rate properties of materials.
The gas gun launch tube has an 8mm bore, firing into an evacuated
experimental chamber and, to date, the maximum recorded velocity is 3.2
km/s using a one gram projectile. Diagnostic equipment includes high
speed photography, impact pressure measurement with piezoelectric gauges
connected to a fast digitizer and projectile velocity measurement.

Areas of research include debris distribution and fragmentation of
targets and projectiles, accuracy and applicability of existing high
strain rate data and microstructural effects in dynamic fracture. A
schematic of the gun is shown below.

1 gas reservoir
2 piston tube
3 launch tube
4 laser
5 photodetectors
6 computer
7 sample
8 gauge
9 imacon camera
10 flash unit
11 digitizer
12 experimental chamber
13 pulse delay generator

ABSTRACT

Hydraulic Shock-Structure Interaction

by

G.A.O. Davies, J.M.R. Graham, R. Hillier and D. Hitchings

This paper addresses the problem of constructing a numerical model of the entire hydraulic shock and damage sequence of events. This embraces the penetration of a supersonic missile fragment into a thin-walled structure, followed by the deceleration of the projectile in the fluid. The cavitation is modelled and the consequent pressure rise due to fluid compression. The constitutive law is discussed. Finally the fluid pressure is applied to the structure (or a pressure alleviation device) and the consequent response modelled.

The numerical and financial consequences of modelling an entire three-dimensional wing-box are stated, together with a cheaper alternative.

Finally the sparsity of data is outlined for representing the composite matrix toughness and its dependence on strain rate. The evidence indicates a rapid deterioration in resistance to interlaminar shear failure with strain rates in excess of 100 per second.

AN ANALYTICAL MODEL TO DESIGN COMPOSITE MATERIAL ARMOURS

B. Parga Landa

E.T.S.Arquitectura. Universidad Politécnica de Madrid. Ciudad Universitaria s/n 28040 MADRID (SPAIN)

ABSTRACT: This paper presents a simple analytical model for predicting the impact behaviour of Composite Material armours. It can be used to calculate the armour ballistic curve and other data up to the time of penetration, the total force retarding the projectile, the tension in each layer, the displacements and velocities of the plate and projectile, the strain rate supported by each layer, and the stresses and strains in the plate .

1. TECHNIQUE

1.1 Behaviour of single yarns under transverse impact

The problem considered is as follows: a rigid projectile of mass m and velocity v impacts a plate of lengh L, width W and thickness H and made of n layers of fabric.

The stress analysis is based on the general assumption that the fibre behaviour is linear elastic up to the fracture (Harding, 1987).

When the projectile reaches the n+1 layer the equation system is (Parga,B., 1988):

$$v_n = v_{n-1} - a_n(t_n - t_{n-1})$$

$$a_n = \frac{2}{m} \sum T_i \ \frac{(n-1+1) \ h}{c \ (t_n - t_{i-1})}$$

$$T_i = \frac{2Sc}{t} (t_n - t_{n-1} - 2t_{i-1}) \ E \left[\frac{1}{2} \left(\frac{(n-i+1) \ h}{c \ (t_n - t_{n-1})} \right)^2 - \frac{1}{8} \left(\frac{(n-i+1) \ h}{c \ (t_n - t_{n-1})} \right)^4 \right]$$

$$h = v_{n-1} \ (t_n - t_{n-1}) - \frac{1}{2} a_n \ (t_n - t_{n-1})^2$$

which is a system of n+3 equations and n+3 unknowns: v_n, a_n, t_n and T_i, i = 1,..,n

The fracture criterion adopted has been that of maximum strain.

In the case of Composite Material armours it is assumed that as soon as the projectile strikes the impregnated yarn, fibre debonding is produced. So two deformation waves will propagate one through the yarn and the other through the resin. When yarns are impregnated with a matrix content below the critical content, the resultant wave speed proposed is:

[117]

$$c = c_m + \frac{c_f - c_m}{K}(V_f + K - 1)$$

where: V_f 1-K, c_m is the matrix wave velocity, c_f is the fibre wave velocity, K is the critical resin content per unit, V_f is the fibre volume fraction per unit.

1.2 Behaviour of fabrics under transverse impact

If the only mechanism operating between the primary and the secondary yarns is friction, the relation between the primary yarn tension supporting the projectile T_1 and the tension T supported by the same yarn after n secondary yarns are passed is: $T = T_1 e^{-\mu \beta n}$ where: μ is the friction coefficient between primary and secondary yarns, β is the contact angle between primary and secondary yarns, n is the number of secondary yarns considered. This fact modificates the total area affected by the impact.

2. RESULTS

To take experimental scatter into account in determining the dynamic modulus, simulations were performed using two different values. Ballistic limit curves were obtained, looking for the lowest velocity that perforates an armour plate for a given surface density. Then the surface density of the armour was increased by half a unit and the process repeated.
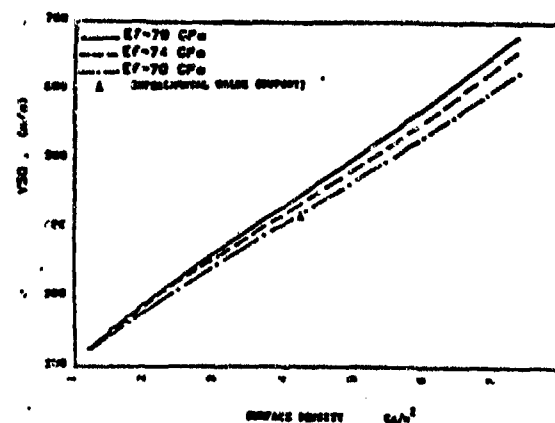

Fig. Ballistic curves vs- surface density for a Kevlar 29 soft armour plate when impacted by a 9mm Parabellum projectile. Triangles are the experimental values of V50 (Dupont 1983b).

3. CONCLUSIONS

1. The impact behaviour of soft armour plates is simulated by a unidimensional model

2. The model permits the simulation of the penetration process into Composite Materials with much shorter computer times than with conventional impact codes.

3. Predicted ballistic curves match experimental values fairly well.

Response to impact of layered structures

Y. Xia

C. Ruiz

University of Oxford
Department of Engineering Science
Parks Road
Oxford OX1 3PJ

Structures consisting of two or more layers joined by rivets or
adhesively bonded are common in aeroengines and airframes. Under normal
service conditions the shear stresses between adjoining layers are usually
considerably lower than the tensile or compressive stresses carried by the
layers themselves and the only mode of failure that needs to be considered
by designers is the one associated with direct stresses. Impact loading on
the other hand is capable of inducing relatively high shear stresses that
may cause the layers to separate with a consequent reduction of residual
strength after the impact. In this report, the problem is illustrated by
means of dynamic photoelasticity, using a two-layer contilever beam that is
analysed by solving the stress wave equations directly and by the ABAQUS
computer code. It is shown that the ratio of shear stress to tensile stress
can be about four times higher under dynamic conditions than under static
conditions. Frictional effects are also shown to be important in
dissipating some of the kinetic energy of the impactor. The effects of
these findings on the design of dual layered shields are finally discussed.

[119]

UPPER-SHELF DYNAMIC FRACTURE TOUGHNESS OF HIGH-TOUGHNESS

MATERIALS USING SMALL SPECIMENS

H. COUQUE, R.J. DEXTER, S.J. HUDAK, Jr. and U.S. LINDHOLM

Division of Engineering and Materials Sciences,
Southwest Research Institute,
6220 Culebra, P.O. Drawer 28510, San Antonio, TX 78284

Abstract - An experimental method involving coupled pressure bars (CPBs) [1], preloaded in tension, has been used to measure dynamic fracture initiation, propagation and arrest properties of A533B pressure vessel steel at temperatures up to 50°C (77°C above the Nil Ductility Temperature). Two compact specimens are simultaneously loaded by releasing the energy stored in the pressure bars by the controlled fracture of a brittle notched specimen. Loading characteristics and crack opening displacements are deduced by analyzing strain histories measured on one pressure bar, as well as by using eddy current displacement transducers. The dynamic crack initiation event is characterized by a stress intensity rate ($\dot{K}_1$) of 3×10^6 MPa $\sqrt{m}$ s^{-1}. The crack then rapidly propagates under a constant crack opening displacement rate inducing crack velocities ranging from 200 to 600 m/s. A precise analysis of the experiment has been performed using a dynamic viscoplastic finite element computer program. The resolution of the procedure has been investigated by obtaining replicate measurements of three quantities versus time-specifically, crack opening displacement, at two locations, and crack growth. The well-defined displacement boundary conditions in the experiment, along with the analysis procedure, enable accurate evaluation of dynamic crack initiation and propagation toughness of high toughness material using small specimens.

[1] H. COUQUE, S.J. HUDAK, JR. and U.S. LINDHOLM, J. Phys., Colloque C3, Sup. n°9, T49, C3-347, 1988.

[120]/121

THERMAL EFFECTS IN ADIABATIC SHEAR BAND LOCALIZATION FAILURE

Piotr PERZYNA

Institute of Fundamental Technological Research
Polish Academy of Sciences, Warsaw, Poland

Abstract. The paper aims at the description of the influence of thermal effects on shear band localization failure.

In technological dynamical processes failure can arise as a result of an adiabatic shear band localization generally attributed to a plastic instability generated by thermal softening during plastic deformations. Recent experimental observations /cf. H.H.Grebe, H.-R.Pak and M.A.Meyers, Metall.Trans., 16A,761-775, 1985; K.A.Hartley, J.Duffy and R.H.Hawley, J.Mech.Phys.Solids, 35, 283-301,1987/ have shown that the shear band procreates in a region of a body deformed where the resistance to plastic deformation is lower and the predisposition for band formation is higher. Shear bands nucleate due to the presence of a local inhomogeneity or defects causing enhanced local deformation and local heating. The shear band once procreated behaves differently than matrix global body.

. Basing on available experimental observation results an analysis of important phenomena for proper description of the final failure during dynamic deformation processes have been investigated. It has been found that such phenomena as the inelastic flow process, the instability of flow process along localized shear bands, the micro-damage process which consists of the nucleation,growth and coalescence of microcracks and the final mechanism of failure are very much influence by thermal effects.

This conclusion suggests to consider thermomechanical coupling and to treat the dynamic deformation process as adiabatic. It has been postulated that the response of a material within shear band region is different than in adjacent zones. Within shear band region the deformation process is characterized by very large strain rates and very serious temperature changes.

During the first stage of the flow process a thermo-elastic-plastic model of a material with internal micro-damage effects is applied. A criterion for localization of the plastic defor-

mation within shear bands is examined. Particular attention is focussed on the investigation of thermal effects and induced anisotropy on localization phenomenon.

Postcritical behaviour within shear bands is modelled by a thermo-elastic-viscoplastic response of a material with advanced micro-damage process.

Both models are developed within the framework of thermodynamic theory of the rate type with internal state variables. The main role in these models is played by a set of the internal state variables. This set cosists of the isotropic hardening-softening parameter α, the residual stress tensor $\underset{\sim}{\alpha}$ and the porosity ξ.

A set of the evolution equations proposed for the shear band region is temperature and rate dependent.

Both models introduced are consistent with the requirement that the thermo-elastic-plastic response of a porous solid can be obtained as a limit case for quasi-static processes of the thermo--elastic-viscoplastic behaviour.

The dynamic failure criterion within shear bands is proposed.

The anisotropic softening of the material implied by thermal effects and the micro-damage process is described. A simple micro-mechanical model of final failure with influence of thermal and anisotropic effects is proposed. Discussion of the mechanical results is given.

EXPERIMENTAL AND NUMERICAL STUDIES OF THE BEHAVIOUR
AND THE RUPTURE OF 35 NCD16 STEEL UNDER
DYNAMIC LOADING

Ph. BENSUSSAN , L. PENAZZI

Etablissement Technique Central de l'Armement
16 bis avenue Prieur de la Cote d'Or
94114 ARCUEIL Cedex ; FRANCE

The plastic constitutive and damage laws, as well as the fracture toughness of a 35 NCD16 steel (0.378 C - 0.39 Si - 0.16 Mn - 0.003 S - 0.008 P - 4 ~11 Ni - 1.82 Cr - 0.44 Mo - in W%) heat treated to 3 different yield strength to ductility ratios, have been studied under tensile dynamic loading . Tests have been performed on a dynamic tensile apparatus, the principle of which is based on that of split Hopkinson bars . Smooth, notched and fatigue precracked axisymmetrical specimen have been used . Both the load at the specimen ends and the notch opening displacement or the specimen elongation have been experimentally recorded .

Dynamic elasto-plastic finite element analyses of the specimens have been performed . It is shown how the plastic constitutive laws have been determined by comparing finite element simulations and experimental results, in spite of stress and strain gradients that occur in smooth bars under dynamic loading . The results are compared to those obtained under dynamic compression and under static sollicitation both in tension and compression .

The stress and strain distribution in the round notched bars under dynamic loading have been obtained by finite element calculations as a function of time for 3 notch geometries leading to different stress triaxility ratio distributions . From these numerical results and experimental results, multiaxial damage laws similar to Rice and Tracey's ductile growth of voids model, have been shown to applicable . Rupture criteria, based on critical void growths, have also been determined . Differences between experimental and predicted loads and mean diametrical strains at rupture have been interpreted in terms of the existence of a critical threshold plastic strain for void initiation wich has not been taken into account in the model .

The experimental procedures followed to determine the fracture toughness from tests performed on axisymmetrically cracked specimens have been justified on the basis of the finite element simulations . Experimental and calculated variations with time of the load in the reduced section and the crack mouth opening displacement have been shown to be in good agreement . Fracture toughness have been found to be well predicted by integrating the damage low identified on notched bars, and by assuming that cracks initiate as soon as the rupture criterion is reached over a critical microstructural distance from the crack tip . The model can explain the increase of fracture toughness with loading rate in 35 NCD16 steel for which an increase of the flow stress with strain rate is observed, and for which dynamic rupture appears to proceed by ductile void growth mechanisms and not by cleavage .

[124]

DYNAMIC UNIAXIAL CRUSHING AND PENETRATION OF WOOD

S R Reid, C Peng and T Y Reddy
Department of Mechanical Engineering, UMIST, Manchester M60 1QD.

In recent years considerable attention has been focussed on to the behaviour of cellular materials. Materials with a regular honeycomb structure have been studied under conditions of transverse loading (e.g. Klintworth and Stronge (1988) and Gibson et al (1982)) and various features of their modes of deformation have been discussed in detail. In particular the tendency of such materials to fail locally at well defined stress levels has been identified as a major characteristic. Similar behaviour is to be found in many other man-made (e.g. polymeric foams) and naturally occurring (e.g. wood) cellular materials. When cylindrical specimens of cellular materials are crushed, the deformation results from the growth of these localized failure zones, the deformation taking place at a constant or gradually increasing stress (the crushing stress). For a constrained or low density material, this continues until the length of the specimen has been engulfed by the deformation fronts at which point rapid hardening occurs as the crushed cells are themselves compressed in a consolidation phase. For an unconstrained higher density specimen the deformation ceases when the specimen fractures. Fig. 1 shows typical load-deformation behaviour for samples of Yellow Pine and Oak tested parallel to the grain and perpendicular to it.

The characteristic shape of the load/displacement (stress/mean strain) curves makes cellular materials attractive as potential materials for use in impact energy absorption. This has been discussed by Gibson and Ashby (1988) in their interesting new text on the topic of cellular materials. Wood has traditionally been used for energy absorption and containment and applications can be found ranging from old wooden warships (Johnson 1986a,b) to present day designs for nuclear transport flasks. The use of wood in such dynamic loading applications and more especially the need to model impact events involving wood presupposes a quantitative understanding of the response of wood under high rate loading conditions. To the author's knowledge no systematic examination of the dynamic behaviour of wood has appeared in the literature.

Fig.1 Quasi-static load-deflection curves for cylindrical wood specimens 45 mm dia. x 18 mm thick.

A sample of the data for two woods, Yellow Pine and American Oak, produced in an extensive set of impact (Peng 1987) and penetration tests will be presented. The first set of tests involves an apparatus in which cylindrical specimens of wood were attached to an aluminium backing disc and push rod and fired from a cartridge gun against the end of a load cell
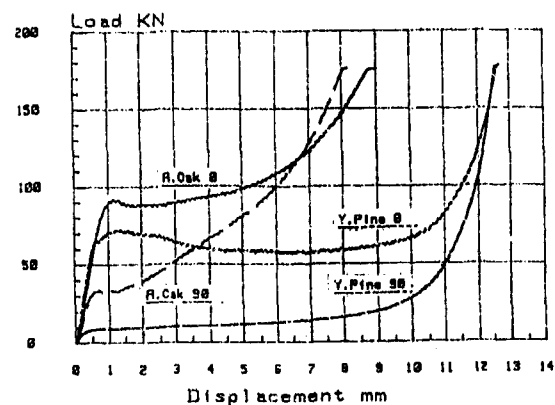
at velocities of around 100 ms^{-1}. The behaviours of specimens loaded parallel to the grain and across the grain were investigated. The deformation of some of the specimens was filmed and the initial localised nature of the deformation observed. The impact loads were measured using a long, strain-gauged load cell which measures force pulses in the same way as in a Hopkinson bar apparatus. Enhancement of the initial crush stress by factors of up to 2.5 for loading parallel to the grain and 5.0 for loading across the grain were observed.

The penetration of flat ended cylindrical projectiles fired normally into a block of wood produces distinctive deformation patterns which depend primarily on the orientation of the grain. The extremes are sketched in Fig. 2. This shows a localized, heavily crushed plug beneath the indenter when the grain is parallel to the direction of penetration and a more extensive frustum-shaped cavity behind a region in which the fibres have been crushed transversely and bent when the loading is across the grain. As well as describing the change in the nature of deformed region as the impact velocity is increased, penetration force traces are presented which were acquired by installing an accelerometer in the cylindrical projectile. At impact velocities of approximately 50 m/s the initial penetration stress increases by a factor of four or more compared with the quasi-static value for a short period following contact before falling to a lower plateau which is about twice the quasi-static penetration force.

In both types of test the localised nature of the deformation process is evident and will be discussed.

Fig.2 Deformation modes for Yellow Pine following cylindrical penetration (a) along the grains (b) perpendicular to the grains.

References

Gibson, L.J. and Ashby, M.F., 1988, *Cellular Solids* (Pergamon).

Gibson, L.J., Ashby, M.F., Schajer, G.S. and Robertson,C.I., 1982, *Proc.Roy.Soc. London*,A382, 25.

Johnson, W., 1986a, *Int.J.Impact Engg.* 4, 161.

Johnson, W., 1986b, *Int.J.Impact Engg.* 4, 175.

Klintworth, J.W. and Stronge, W.J.,1988, *Int.J.Mech.Sci.*, 30, 273.

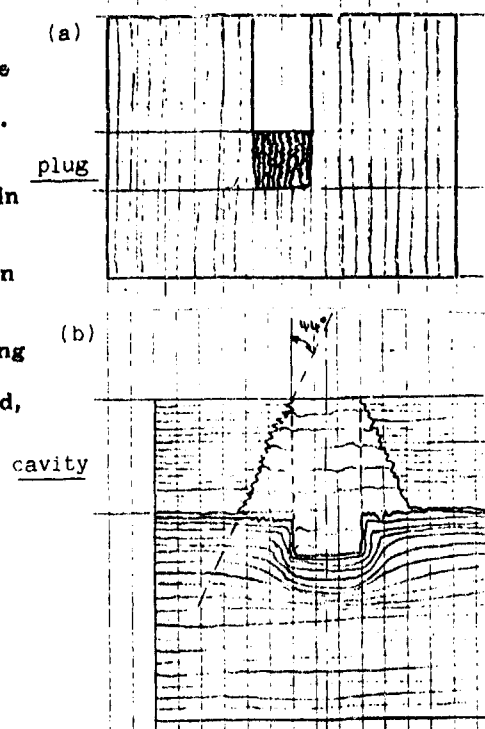Peng, C., 1987, *Crushing of Wood under Static and Impact Conditions*, MSc thesis, UMIST.

[126]

QUASI-STATIC VERSUS DYNAMIC FRACTURE PROPERTIES

OF CERAMIC FIBER REINFORCED MATERIALS

J. LANKFORD and H. COUQUE

Division of Engineering and Materials Sciences,
Southwest Research Institute,
6220 Culebra, P.O. Drawer 28510, San Antonio, TX 78284

Abstract - A major advance in the toughening of ceramics has been achieved by means of ceramic fiber reinforcement. The principal mechanism by which benefit is realized is through pullout of fibers, whose frictional resistance creates sufficient crack closure to significantly raise the fracture toughness. However, all studies to date have involved relatively slow rates of loading; there is some question as to whether this mechanism w'll obtain at rapid, or impact, loading rates. This paper reports on the results of tests aimed at evaluating the dynamic versus static fracture behavior of SiC-fiber reinforced glass-ceramic composite.

The dynamic fracture tests have been performed using an adaptation to brittle materials of a recently developed dynamic fracture experiment [1]. Hopkinson pressure bars preloaded in tension are utilized to load simultaneously two compact type specimens with notch of different radius. The experiment is characterized by well-defined specimen boundary loading conditions, and by stress intensity rates $(\dot{K}_1)$ on the order of 10^6 MPa$\sqrt{\text{m}}$ s^{-1}. Crack velocities are measured by using a crack gage technique.

Static fracture stresses are compared with the stresses required for dynamic crack initiation, and results are interpreted in terms of fracture mode. It will be shown that even under dynamic loading conditions, the influence of the weak axially-oriented fiber-matrix interfaces manifest themselves in the fracture path. Furthermore, the observed multiple fracture locations appear to be related to the loading mode involved in the compact type specimen geometry.

[1] H. COUQUE, S.J. HUDAK, JR. and U.S. LINDHOLM, J. Phys., Colloque C3, Sup. n°9, T49, C3-347, 1988.